

**Analysis of the *Arabidopsis* Nudix hydrolase
NUDT7 as a modulator of plant immunity
and cell death**

Inaugural-Dissertation
zur
Erlangung des Doktorgrades
der Mathematisch-Naturwissenschaftlichen Fakultät
der Universität zu Köln

vorgelegt von

Marco Straus

aus Bürstadt

Köln, März 2009

Die vorliegende Arbeit wurde am Max-Planck-Institut für Züchtungsforschung in Köln in der Abteilung für Molekulare Phytopathologie (Direktor: Prof. Dr. P. Schulze-Lefert) angefertigt.



MAX-PLANCK-GESELLSCHAFT



Berichterstatter: Prof. Dr. Paul Schulze-Lefert
Prof. Dr. Ulf-Ingo Flügge

Prüfungsvorsitzender: Prof. Dr. Martin Hülskamp

Tag der Disputation: 13. Mai 2009

Abstract

Plants are exposed to diverse biotic and abiotic stresses and have evolved sophisticated protective mechanisms. A major outstanding question is how plants respond effectively to a stress stimulus but limit their reaction to save energy for growth and reproduction. *EDS1* (*ENHANCED DISEASE SUSCEPTIBILITY 1*) encodes a nucleo-cytoplasmic regulator of plant basal defence against host-adapted virulent pathogens and race-specific resistance to avirulent pathogens mediated by TIR (Toll-Interleukin)-type NBS-LRR (Nucleotide Binding Site-Leucine Rich Repeats) Resistance (R) proteins. *EDS1* also functions in reactive oxygen species (ROS)-induced signalling during photo-oxidative stress. R protein activation of *EDS1* signalling typically results in accumulation of the phenolic stress hormone salicylic acid (SA), generation of ROS, localized programmed cell death (PCD) (the hypersensitive response (HR)) and restriction of pathogen growth. *Arabidopsis* nudix hydrolase *NUDT7* was identified as a negative component of the *EDS1* defence and cell death pathway. *Nudt7* null mutants display enhanced basal resistance, elevated levels of SA, retarded growth and spontaneous initiation, but not spread, of leaf cell death. Genetic epistasis analysis showed that all of the *nud7* defects require *EDS1*. The work presented here characterizes further the genetic relationship between *NUDT7* and *EDS1* and molecular functions of *NUDT7* in *EDS1* stress signalling. *EDS1* and *NUDT7* genes are responsive to multitude of abiotic and biotic stresses. Inspection of *NUDT7* protein revealed a cytosolic localization in healthy and stress-induced leaf tissue. While the *nudt7* mutation enhances *EDS1* transcript accumulation, *EDS1* acts principally at the level of *NUDT7* protein accumulation although a direct interaction between *EDS1* and *NUDT7* was not observed. Others have reported that *nudt7* constitutive disease resistance is due to increased responsiveness to MAMPs (Microbe-Associated Molecular Patterns). In this work it was established using multiple MAMP-triggered read-outs that neither *nudt7* nor *eds1* mutants exhibit an altered MAMP response. Results are consistent with activities of *EDS1* and *NUDT7* in fine regulation defence and cell death to invasive pathogens. Induction of oxidative stress resulted in severe growth retardation, cell death induction and ROS accumulation in *nudt7* that was *EDS1*-dependent. Oxidative stress-induced cell death in *nudt7* was independent of SA while the superoxide-generating NADPH oxidase AtRbohD was required for cell death initiation and ROS (H₂O₂) accumulation. Gene

expression microarray analysis revealed that SA likely regulates ROS homeostasis in *nudt7*. Together, these data suggest a central role of the EDS1 pathway in modulating chloroplastic ROS signals that promote retardation of growth retardation and cell death initiation.

Zusammenfassung

Pflanzen sind diversen biotischen und abiotischen Stressen ausgesetzt was zur Entwicklung ausgeklügelter Schutzmechanismen geführt hat. Eine herausragende, offene Frage ist wie Pflanzen effektiv auf Stress Stimuli reagieren aber gleichzeitig die Reaktion regulieren um Ressourcen für Wachstum und Reproduktion zu wahren. *EDS1* (*ENHANCED DISEASE SUSCEPTIBILITY 1*) kodiert einen nucleocytoplasmatischen Regulator basaler Abwehrmechanismen gegen an den Wirt angepasste Pathogene und rassen-spezifische Resistenz gegen avirulente Pathogene vermittelt durch TIR (Toll-Interleukin) NBS-LRR (Nucleotide Binding Site-Leucine Rich Repeats) Resistenz (R) Proteine. *EDS1* ist auch an der Übermittlung von Sauerstoffradikal (reactive oxygen species (ROS))-induzierten Signalen beteiligt, die durch photo-oxidativen Stress generiert werden. R ProteinAktivierung des *EDS1* Signallweges resultiert typischerweise in der Akkumulation des phenolischen Stresshormons Salicylsäure (SA), Produktion von ROS, lokalem, programmierten Zelltod (PCD) (hypersensitive response (HR)) und Begrenzung der Pathogenausbreitung. Die *Arabidopsis* Nudix Hydrolase *NUDT7* wurde als negative Komponente des *EDS1* Signalweges identifiziert. *Nudt7* Null Mutanten zeigen erhöhte basale Resistenz, erhöhte SA Konzentrationen, unterdrücktes Wachstum und spontane Initiierung von Zelltod der sich aber nicht ausbreitet.

Genetische Epistasis Experimente haben gezeigt, dass alle *nudt7* Defekte *EDS1* benötigen. Die hier vorliegende Studie charakterisiert die genetische Beziehung von *NUDT7* zu *EDS1* and die molekulare Funktion von *NUDT7* im *EDS1* Signalweg. Die *EDS1* und *NUDT7* Gene reagieren beide auf eine Vielzahl biotischer und abiotischer Stresse. Eine genauere Betrachtung des *NUDT7* Proteins konnte eine cytosolische Lokalisation in gesundem und gestresstem Blattgewebe aufzeigen. Während die *nudt7* Mutation zu erhöhten *EDS1* Transkriptlevel führt, beeinflusst *EDS1* prinzipiell *NUDT7* Protein Akumulation obwohl keine direkte Interaktion beider Proteine gefunden werden konnte. Andere Studien haben berichtet, dass konstitutive Resistenz in *nudt7* auf eine erhöhte Empfindlichkeit gegenüber MAMPs (Microbe-Associated Molecular Patterns) zurückgeht. Mittels verschiedener MAMP-getriggertter Read-outs konnte in dieser Studie gezeigt werden, dass weder *nudt7* noch *eds1* eine veränderte MAMP-Antwort zeigen. Die Resultate stehen in Einklang mit den Aktivitäten von

EDS1 und NUDT7 bei der Fein-Regulation von Abwehrmechanismen und Zelltodinduktion gegenüber invasiven Pathogenen. Induktion von oxidativem Stress resultierte in *EDS1*-abhängiger Reduktion des Pflanzenwachstums, Initiierung von Zelltod und Akkumulation von ROS in *nudt7*. Oxidativer Stress-induzierter Zelltod in *nudt7* war unabhängig von SA während die Superoxid-generierende NADPH oxidase AtRbohD für Zelltodinitiierung und ROS (H₂O₂) Akkumulation benötigt wurde. Microarray Gen Expressionsanalyse legte nahe, dass SA an der Regulierung der Redox Homeostase in *nudt7* beteiligt ist. Zusammenfassend legen die hier präsentierten Daten eine zentrale Rolle des EDS1 Signallweges in der Modulierung chloroplastischer ROS Signale nahe, welche zu Wachstumsstörungen und zur Initiierung von Zelltod führt.

Table of contents

ABSTRACT	I
ZUSAMMENFASSUNG	III
TABLE OF CONTENTS	V
TABLE OF ABBREVIATIONS	X
1. INTRODUCTION	1
1.1. PLANT INNATE IMMUNITY - A MULTI-LAYERED DEFENCE SYSTEM	2
1.1.1. Non-host resistance and PAMP-triggered immunity (PTI)	2
1.1.2. Pathogen effectors and effector-triggered immunity (ETI)	4
1.2. REACTIVE OXYGEN SPECIES – A COMPLEX NETWORK OF PRODUCTION, SCAVENGING AND SIGNALLING	7
1.2.1. Generation of ROS	7
1.2.2. ROS scavenging	9
1.2.3. ROS signalling	10
1.2.4. ROS and cell death.....	11
1.3. EDS1 – A REGULATORY NODE FOR IMMUNE AND OXIDATIVE STRESS RESPONSES	13
1.3.1. EDS1 and plant innate immunity	13
1.3.2. EDS1 and ROS signalling.....	14
1.4. SALICYLIC ACID	15
1.4.1. SA synthesis and its role in plant disease resistance.....	15
1.4.2. SA, ROS and cell death	16
1.5. THE NUDIX HYDROLASE NUDT7 – A NEGATIVE REGULATOR OF EDS1	17
1.5.1. Nudix hydrolases	18
1.5.2. NUDT7 in plant defence and oxidative stress signalling.....	18
1.6. AIMS OF THE THESIS	19

2. MATERIALS AND METHODS	21
2.1. MATERIALS.....	21
2.1.1. Plant materials.....	21
2.1.2. Pathogens	22
2.1.2.1. <i>Hyaloperonospora parasitica</i>	22
2.1.2.2. <i>Pseudomonas syringae</i> pv. <i>tomato</i>	22
2.1.3. Oligonucleotides	22
2.1.4. Enzymes.....	23
2.1.4.1. Restriction endonucleases.....	23
2.1.4.2. Nucleic acid modifying enzymes.....	24
2.1.5. Chemicals.....	24
2.1.6. Antibiotics.....	24
2.1.7. Media	24
2.1.8. Antibodies.....	26
2.1.9. Buffers and solutions	26
2.2. METHODS.....	28
2.2.1. Maintenance and cultivation of <i>Arabidopsis</i> plant material	28
2.2.2. Generation of <i>Arabidopsis</i> F ₁ and F ₂ progeny.....	29
2.2.3. <i>Arabidopsis</i> seed sterilization	29
2.2.4. Inoculation and maintenance of <i>Hyaloperonospora parasitica</i>	29
2.2.5. Quantification of <i>H. parasitica</i> sporulation.....	30
2.2.6. DAB staining	30
2.2.7. Lactophenol trypan blue staining.....	31
2.2.8. Quantification of cell death.....	31
2.2.9. Maintenance of <i>P. syringae</i> pv. <i>tomato</i> cultures	31
2.2.10. <i>P. syringae</i> pv. <i>tomato</i> inoculations for time course experiments and growth assays	31
2.2.11. Fresh weight analysis of soil-grown plants.....	32
2.2.12. Sterile growth.....	33
2.2.13. Flg22 growth assay	33
2.2.14. Oxidative stress analysis	33
2.2.15. Biochemical methods.....	33
2.2.15.1. <i>Arabidopsis</i> total protein extraction for immunoblot analysis.....	33

2.2.15.2. Protein purification using StrepII affinity purification	34
2.2.15.3. Nuclear fractionation for immunoblot analysis	35
2.2.15.4. Isolation of microsomal membranes	36
2.2.15.5. Denaturing SDS-polyacrylamide gel electrophoresis (SDS-PAGE).....	36
2.2.15.6. Immunoblot analysis.....	37
2.2.15.7. In-gel MAP kinase assay	38
2.2.15.8. Ethylene Measurements	39
2.2.16. Antibody production and purification.....	40
2.2.16.1. Protein expression in <i>E. coli</i>	40
2.2.16.2. Antibody purification.....	40
2.2.17. Molecular biological methods.....	41
2.2.17.1. Isolation of genomic DNA from <i>Arabidopsis</i> (Quick prep for PCR).....	41
2.2.17.2. Isolation of total RNA from <i>Arabidopsis</i>	41
2.2.17.3. Reverse transcription-polymerase chain reaction (RT-PCR)	42
2.2.17.4. Polymerase chain reaction (PCR)	42
2.2.17.5. Quantitative real time (qRT) PCR	43
2.2.17.6. Agarose gel electrophoresis of DNA	43
2.2.18. Microarray analysis.....	43
2.2.18.1. Sample preparation	43
2.2.18.2. Data analysis	44
3. RESULTS	47
3.1. GENERATION OF NUDT7 ANTIBODY AND TRANSGENIC LINES OVER EXPRESSING NUDT7	47
3.1.1. Generation of antisera recognizing NUDT7 protein.....	47
3.1.2. Complementation analysis of epitope-tagged NUDT7 over expresser lines	47
3.2. ANALYSIS OF <i>NUDT7</i> TRANSCRIPT AND PROTEIN EXPRESSION.....	50
3.2.1. Co-regulation of <i>EDS1</i> and <i>NUDT7</i> in response to stress	50
3.2.2. <i>NUDT7</i> transcript and protein are upregulated in response to avirulent bacteria.....	54

3.2.3.	NUDT7 localization is not altered upon pathogen challenge	56
3.3.	IMPACT OF DEFENCE-RELATED MUTANTS ON THE <i>nudt7-1</i>	
	PHENOTYPE	57
3.3.1.	EDS1 triggers an SA-antagonized defence pathway	57
3.3.2.	The <i>nudt7-1</i> phenotype is influenced by other defence mutations	59
3.4.	THE ROLES OF <i>EDS1</i> AND <i>NUDT7</i> IN BASAL RESISTANCE AND	
	OXIDATIVE STRESS RESPONSES	61
3.4.1.	<i>nudt7-1</i> growth retardation is abolished under sterile conditions	61
3.4.2.	<i>nudt7-1</i> mutant plants are not hyper-responsive to the MAMP flg22	61
3.4.3.	<i>nudt7-1</i> plants are rendered hyper susceptible towards oxidative stress by EDS1-mediated signals	65
3.4.4.	SA promotes H ₂ O ₂ accumulation but has no effect on the induction of cell death in response to paraquat application	69
3.4.5.	<i>Nudt7-1/rbohD</i> displays an <i>eds1-2</i> like phenotype after paraquat treatment	71
3.5.	A GENE EXPRESSION MICROARRAY TO IDENTIFY GENES IN	
	<i>nudt7-1</i> AND <i>nudt7-1/sid2-1</i> THAT ARE REGULATED IN AN EDS1-	
	DEPENDENT MANNER	72
4.	DISCUSSION	81
4.1.	EDS1 AND NUDT7 ARE PART OF A PLANT STRESS-INDUCIBLE	
	GENETIC PROGRAMME	82
4.2.	EDS1 IS NOT IMPORTANT FOR MAMP-TRIGGERED IMMUNITY	85
4.3.	RELATIONSHIP OF EDS1 AND NUDT7 TO ROS ACCUMULATION	
	AND SIGNALLING	86
4.4.	SA LIMITS EDS1-DEPENDENT CELL DEATH INITIATION	
	IN <i>nudt7-1</i>	88
4.5.	H₂O₂ IS AN IMPORTANT COMPONENT OF PARAQUAT INDUCED	
	INITIATION OF CELL DEATH	89
4.6.	TRANSCRIPTOMICS REVEAL ALTERED REDOX HOMEOSTASIS AND	
	CONSTITUTIVE DEFENCE SIGNALLING IN <i>nudt7-1</i> AND <i>nudt7-1/sid2-1</i>	90
4.7.	POSITIONING NUDT7 IN THE EDS1 PATHWAY	91
4.8.	SUMMARY AND PERSPECTIVES	94

5. REFERENCES.....	95
SUPPLEMENTAL DATA	111
DANKSAGUNG.....	123
ERKLÄRUNG.....	125
LEBENS LAUF	127

Table of abbreviations

::	fused to (in context of gene fusion constructs)
°C	degree Celsius
<i>avr</i>	avirulence
C	carboxy-terminal
<i>CaMV</i>	cauliflower mosaic virus
CC	coil-coiled
cfu	colony forming units
DAB	3,3'-Diaminobenzidine
dATP	deoxyadenosinetriphosphate
dCTP	deoxycytidinetriphosphate
dGTP	deoxyguanosinetriphosphate
dH ₂ O	deionised water
DMSO	dimethylsulfoxide
DNA	deoxyribonucleic acid
dNTP	deoxynucleosidetriphosphate
DTT	dithiothreitol
dTTP	deoxythymidinetriphosphate
EDS1	Enhanced Disease Susceptibility 1
EDTA	ethylenediaminetetraacetic acid
EEE	excess excitation energy
EtOH	ethanol
flg	flagellin
FLS2	Flagellin Sensing 2
FMO1	Flavin-dependent Monooxygenase 1
g	gram
<i>g</i>	gravity constant (9.81 ms ⁻¹)
h	hour
H ₂ O ₂	hydrogen peroxide
HO [•]	hydroxyl radical
HRP	horseradish peroxidase
IP	immunoprecipitation
JA	jasmonic acid
KDa	Kilo Dalton(s)
l	litre
LRR	leucine-rich repeats
LSD1	Lesions Simulating Disease 1
μ	micro
m	milli
M	molar (mol/l)
MAMP	microbe-associated molecular pattern
MAP	mitogen activated protein kinase

min	minute(s)
ml	millilitre
μM	micromolar
mM	millimolar
MPK	MAP Kinase
mRNA	messenger ribonucleic acid
N	amino-terminal
NADPH	Nicotinamide adenine dinucleotide phosphate
NBS	nucleotide binding site
NUDIX	n ucleoside d iphosphates linked to other moieties X
NUDT7	nudix-type motif 7
$^1\text{O}_2$	singlet oxygen
O_2	oxygen
$\text{O}_2^{\bullet-}$	superoxide
OD	optical density
<i>OE</i>	over expresser
PAD4	Phytoalexin Deficient 4
PAGE	polyacrylamide gel-electrophoresis
PAMP	pathogen-associated molecular pattern
PCD	programmed cell death
PCR	polymerase chain reaction
pH	negative decimal logarithm of the H^+ concentration
pi	post inoculation
<i>PR</i>	pathogenesis related
PS	photosystem
<i>Pst</i>	<i>Pseudomonas syringae</i> pv. <i>tomato</i>
PTI	PAMP-triggered immunity
pv.	pathovar
qRT-PCR	quantitative real time polymerase chain reaction
R	resistance
AtRbohD	Arabidopsis thaliana Respiratory burst oxidase homologue D
RCD	runaway cell death
ROS	reactive oxygen species
rpm	rounds per minute
RPM	resistance to <i>Pseudomonas syringae</i> pv. <i>maculicola</i>
<i>RPP</i>	resistance to <i>Peronospora parasitica</i>
<i>RPS</i>	resistance to <i>Pseudomonas syringae</i>
RT	room temperature
RT-PCR	reverse transcription-polymerase chain reaction
SA	salicylic acid
SAR	systemic acquired resistance
SDS	sodium dodecyl sulphate
sec	second(s)

SID2	Salicylic Acid Induction–Deficient 2
StrepII	Streptomycin II
TBS	Tris buffered saline
T-DNA	Transfer DNA
TIR	Drosophila Toll and mammalian Interleukin-1 Receptor
Tris	Tris-(hydroxymethyl)-aminomethane
U	unit
UV	ultraviolet
V	Volt
<i>vir</i>	virulence
w/v	weight per volume
WT	wild type

1. Introduction

The ability to synthesize sugars by photosynthesis renders plants valuable nutrient sources for multiple pathogens and pests such as bacteria, fungi, oomycetes and insects. In response to constant attempts of pathogenic colonization plants evolved robust and effective defence barriers (Dangl and Jones, 2006). Unlike animals that possess an innate immune system and an adaptive immune system relying on specialized cells and antigen-specific receptors (Janeway et al., 2001), plants have evolved an innate immune system by which cells are autonomously capable of sensing pathogens and mounting an immune response (Nürnberger et al., 2004).

Pathogens attacking plants have to overcome constitutive defence barriers such as wax cuticles and cell walls before facing a sophisticated multi-layered induced defence system that allows plants to detect and combat pathogens in the extracellular space (apoplast) as well as intracellularly (Dangl and Jones, 2001). In spite of the large number of pathogens disease is exceptional (Hammond-Kosack and Parker, 2003). However, some pathogens evolved mechanisms to suppress plant immunity and cause disease on particular hosts. In crop plants, disease causing pathogens can lead to large yield losses with a great economic impact (Fletcher et al., 2006).

Although research over the past decades has made enormous progress in understanding the molecular basis of plant innate immunity important questions are still not solved. There is still a big gap in understanding how signals from different plant immunity layers are integrated and how downstream signalling events after recognition of a pathogen are transduced into an adequate immune response. It is also unclear how plants control their immune response machinery so as not to overreact to pathogen stress stimuli that would remove energy for growth and reproduction. Unravelling the molecular basis of plant innate immunity could help to develop strategies of practical disease control measures that confer durable resistance in e.g. crop plants.

1.1. Plant innate immunity - a multi-layered defence system

1.1.1. Non-host resistance and PAMP-triggered immunity (PTI)

Non-host resistance describes the disease resistance of an entire plant species to all genetic variants of a non-adapted pathogen species and is probably the most common form of plant resistance. Preformed physical (wax cuticles, cell walls), chemical (toxic secondary metabolites) and enzymatic (anti-microbial enzymes) barriers as well as inducible defence responses contribute to non-host resistance although the precise mechanisms of defence remain elusive (Heath, 2000). However, pathogen-triggered cell wall remodelling and cell polarisation suggest an important role of cell wall integrity in non-host resistance and point to a surveillance system that is able to sense changes in the cell wall (Kobayashi et al., 1997; McLusky et al., 1999; Schulze-Lefert, 2004).

Progress in understanding inducible non-host resistance at the pre-invasive level was made by characterising the penetration mutants *pen1*, *pen2* and *pen3* that are required for resistance in *Arabidopsis thaliana* (hereafter called *Arabidopsis*) to non-adapted powdery mildew fungi such as *Blumeria graminis* or *Erysiphe pisi*. *PEN1* encodes a plasma membrane-anchored syntaxin with a SNARE (soluble N-ethylmaleimide-sensitive factor attachment protein receptor) domain (Collins et al., 2003) and was shown to form pathogen-induced ternary complex together with SNAP33 (SNARE synaptosomal-associated protein 33) and two VAMPs (vesicle-associated membrane proteins) VAMP721 and VAMP722 that may mediate vesicle fusion at the site of fungal penetration thereby delivering cell wall material or antimicrobial compounds (Kwon et al., 2008). The importance of this work is given by the fact that requirement and recruitment of this SNARE complex along the site of fungal penetration provides evidence for pathogen-induced cellular re-distribution and shows mechanistic similarities to the formation of the immunological synapse in vertebrates. *PEN2*, encoding a family 1 glycoside hydrolase (Lipka et al., 2005) and *PEN3*, a drug resistance ATP binding cassette transporter (Stein et al., 2006) act in the same pathway and independently of *PEN1*. It was suggested that *PEN2* and *PEN3* are involved in the cytoplasmic synthesis and transport of antimicrobial metabolites across the plasma membrane to the site of fungal penetration (Lipka et al., 2005; Stein et al., 2006). Recently, it was shown that *PEN2* is involved in the accumulation of

indole-glucosinolates that contribute to antifungal defence (Bednarek et al., 2009). So far, glucosinolates have mainly been described in defence responses to insects (Halkier and Gershenzon, 2006). The work of Bednarek et al. (2009) provides evidence of an independent glucosinolate metabolism that mediates antifungal defence.

When pathogens overcome the cell wall and are exposed to the plant cell plasma membrane (PM), a striking principle of immunity shared between animals and plants is brought to bear: the recognition of “self” and “non-self”. Animals as well as plants possess PM-resident pattern recognition receptors (PRRs) that allow them to recognize pathogen-associated molecular patterns (PAMPs; hereafter referred to as MAMPs (Microbe-Associated Molecular Patterns)) resulting in the induction of an immune response, MAMP-triggered immunity (MTI). MAMPs are highly conserved molecules that are not produced by the host and are indispensable to the microbe for fitness and/or viability (Nürnberg et al., 2004). The currently best understood MAMP recognition system is of the N-terminal 22 amino acid epitope from bacterial flagellin (flg22) by the *Arabidopsis* FLAGELLIN SENSING 2 (FLS2) receptor-like kinase (RLK) (Felix et al., 1999; Gomez-Gomez and Boller 2000). FLS2 consists of an extracellular leucine-rich repeat (LRR) domain and an intracellular serine/threonine kinase domain that are both required for the perception of flg22 and for subsequent downstream signalling (Gomez-Gomez et al., 2001). Early responses after flg22 perception comprise the induction of an early oxidative burst, nitric oxide (NO) and ethylene production, callose deposition and production of antimicrobial compounds (Felix et al., 1999; Zipfel and Felix, 2005). Furthermore, flg22 activates a MAP kinase cascade that consists of MEKK1, MKK4/5 and MPK3/6 and induces transcriptional reprogramming mediated by WRKY transcription factors (Asai et al., 2002; Tao et al., 2003; Navarro et al., 2004).

For a long time it was not clear whether MAMP perception contributes to plant disease resistance since most experiments were performed with purified MAMPs under artificial conditions. However, infection studies of *fls2* mutants revealed that plants lacking this MAMP receptor are more susceptible to the disease-causing virulent *Pseudomonas syringae* pv. *tomato* strain DC3000 (*Pst* DC3000) when applied to the leaf surface (Zipfel et al., 2004).

More recently, a number of other MAMP/PRR pairs have been identified in *Arabidopsis* and other plant species such as the bacterial elongation factor Tu (EF-Tu)

that is recognized by the EF-Tu receptor (EFR) in *Arabidopsis* (Kunze et al., 2004), fungal chitin recognized by the chitin oligosaccharide elicitor-binding protein (CEBiP) in rice (Kaku et al., 2006), or a heptaglucoside of oomycetes recognized by the β -glucan-binding protein in soybean (Fliegmann et al., 2004).

1.1.2. Pathogen effectors and effector-triggered immunity (ETI)

In order to gain access to plant nutrients, some pathogens are able to overcome MTI by expressing and delivering effectors into the plant host cell (Chisholm et al., 2006; Jones and Dangl, 2006). Effectors that successfully suppress host defences are termed virulence factors (*Vir*) and the interaction between a virulent pathogen and its susceptible host is defined as a compatible interaction (Abramovitch and Martin, 2004). The best characterized examples come from gram-negative bacteria that utilize a Type III Secretion System (TTSS) to inject between 20 and 100 effectors into the host cell that then interfere with components of PTI (Casper-Lindley et al., 2002; Alfano and Collmer 2004; Cunnac et al., 2004; Lindeberg et al., 2006). The TTSS effector AvrPtoB has recently been shown to target FLS2 for proteasomal degradation and to be required for full virulence of the *Pst* DC3000 strain (Göhre et al., 2008). AvrPto, another TTSS effector protein, was shown to suppress callose deposition at the cell wall when expressed under an inducible promoter in plants (Hauck et al., 2003). Fungi and oomycetes are also capable of delivering effectors into plant host cells. In contrast to bacteria, fungal and oomycete pathogens do not possess of a TTSS but form a specialized infection structure, the haustorium, which also delivers effectors (Chisholm et al., 2006; Whisson et al., 2007).

Pathogenic colonisation of host tissue facilitated by the suppression of PRR-mediated immune responses through effector proteins is not absolute. Host plants exert a further layer of defence that restricts pathogen growth in compatible interactions. This can be defined as post-invasive basal resistance (Glazebrook et al., 1997). The impact of basal resistance on plant immunity is illustrated by the identification of numerous mutants of *Arabidopsis* that exhibit enhanced virulent pathogen growth and hypersusceptibility compared to genetically-susceptible wild type (wt) plants (Cao et al., 1994; Glazebrook et al., 1996; Parker et al., 1996). A key regulator of basal resistance is *ENHANCED DISEASE SUSCEPTIBILITY 1 (EDS1)*. The loss of which results in abrogated post-invasive basal defence (see below) (Parker et al., 1996; Wiermer et al., 2005).

In response to pathogenic effectors *RESISTANCE* (*R*) genes evolved in plants that encode Resistance (*R*) proteins recognizing specific effector proteins and inducing the effector-triggered immunity (ETI) (Jones and Dangl, 2006). The recognition event confers a strong resistance; the pathogen is defined as avirulent and the interaction is called incompatible. Recognition of an effector gene product by the corresponding *R* gene product is defined as “gene-for-gene” or “race-specific” resistance and the recognized effector as an avirulence (*Avr*) factor (Flor, 1971). There are five structural classes of *R* proteins of which the predominant class is characterized by a central nucleotide binding site (NBS) and a carboxy-terminal leucine-rich repeat domain (LRR). NBS-LRR proteins are structurally related to mammalian Nod immune receptors (Dangl and Jones, 2001; Belkhadir et al., 2004; Ting and Williams, 2005). This class that can be further subdivided into two subclasses, one carrying an amino-terminal coiled-coil (CC) domain and a second possessing an amino-terminal domain related to the intracellular TIR signalling domains of the *Drosophila* Toll and mammalian interleukin (IL)-1 receptor (TIR). In the fully sequenced *Arabidopsis* accession Col-0 there are ~125 NBS-LRR *R*-genes of which ~60% belong to the TIR-NBS-LRR class and ~40% to the CC-NBS-LRR class (Dangl and Jones, 2001; Jones and Dangl 2006).

A possible mode of interaction between *R* and *Avr* gene product is a direct one where the *R* protein interacts physically with the pathogenic effector resulting in a defence response. So far, there are only a few examples of a direct recognition (Jia et al., 2000; Deslandes et al., 2003; Dodds et al., 2006). In consideration of the small number of *R* genes compared to the extensive arsenal of bacterial, fungal and viral effectors, it was postulated that *R*-proteins likely monitor common host targets attacked by effectors. Therefore it was proposed that many *R* proteins indirectly detect effector proteins rather than directly interact with them leading to the “guard hypothesis” (Van der Biezen and Jones, 1998; Dangl and Jones, 2001). Several interactions confirm to the guard model (Shao et al., 2003; Axtell and Staskawicz, 2003; Mackey et al., 2002, 2003) of which the best characterized example describes the monitoring of *Arabidopsis* RIN4 (RPM1 INTERACTING PROTEIN). RIN4, a plasma-membrane associated protein that is presumably involved in PTI (Kim et al., 2005; Jones and Dangl, 2006), is hyperphosphorylated by the two *Pseudomonas syringae* effector proteins AvrRpm1 and AvrB when delivered into the plant cell. The *R* protein RPM1 physically interacts with RIN4 and is activated, probably by the

changed phosphorylation status of RIN4, thereby triggering an immune response (Mackey et al., 2002). In addition, RIN4 is targeted by the *P. syringae* effector AvrRpt2 that proteolytically cleaves RIN4 (Axtell and Staskawicz, 2003; Mackey et al., 2003; Coaker et al., 2005). RPM1 is not able to detect the AvrRpt2-mediated cleavage of RIN4 and also does not detect AvrRpm1 and AvrB efficiently when AvrRpt2 is present (Ritter and Dangl, 1996). However, the CC-NBS-LRR protein RPS2 is able to sense AvrRpt2 activity and to trigger the defence response (Axtell and Staskawicz, 2003; Mackey et al., 2003).

It remains unclear how different R proteins trigger downstream responses. A study of barley *Mildew A 10* (*MLA10*) revealed interaction of *MLA10* with two repressors of basal defence, WRKY1 and WRKY2, in the nucleus after recognition of the *Blumeria graminis* f. sp. *hordei* effector protein AVR_{A10} resulting in the activation of an immune response (Shen et al., 2007). Hence, this study suggests one mechanism by which signals from distinct defence pathways might be integrated. Together with other studies, this work points to a requirement for a nuclear pool of NBS-LRR proteins to activate defences (Deslandes et al., 2003; Burch-Smith et al., 2007; Wirthmüller et al., 2007).

Downstream signalling after recognition of Avr proteins tends to require either *EDS1* in the case of TIR-NBS-LRR triggered responses or *NON RACE SPECIFIC DISEASE RESISTANCE 1* (*NDRI*) after CC-NBS-LRR defence activation (Aarts et al., 1998). Several studies showing contradictory cases as well as cases where *R* genes do not genetically require *EDS1* or *NDRI* (McDowell et al., 2000; Bittner-Eddy and Beynon, 2001; Xiao et al., 2001). Induced downstream responses comprise early changes in calcium fluxes, a localized burst of reactive oxygen species (ROS), activation of protein kinases and production of NO. In addition, incompatible plant-pathogen interactions often induce a hypersensitive reaction (HR) that is normally accompanied by programmed cell death (PCD) (Dangl and Jones, 2001; Nimchuk et al., 2003).

It is significant that ETI and basal resistance lead to a transcriptional reprogramming of a largely overlapping set of genes that mainly differs in the kinetics and quantity of gene expression (Tao et al., 2003; Bartsch et al., 2006).

1.2. Reactive oxygen species – a complex network of production, scavenging and signalling

Reactive oxygen species (ROS) are continuously generated in plants as byproducts of various metabolic pathways in different cellular compartments (Foyer and Harbinson, 1994). Abiotic and biotic stresses often lead to an enhanced production and a concomitant rapid increase of the cellular ROS concentration which is called oxidative burst (Apel and Hirt, 2004). ROS are characterized by their generation from molecular oxygen (O_2), either by energy transfer or electron transfer reactions (Klotz, 2002), and their high reactivity with other cellular components such as proteins or lipids thereby potentially causing irreversible damage (Pitzschke et al., 2006). Energy transfer reactions lead to the formation of singlet oxygen (1O_2) whereas electron transfer from various donors to O_2 results in superoxide ($O_2^{\cdot-}$) that is rapidly dismutated into hydrogen peroxide (H_2O_2). In the presence of transition metal ions (e.g. Fe^{II+} , Fe^{III+} , Cu^{II+}) H_2O_2 can be further reduced to the highly reactive hydroxyl radical (HO^{\cdot}) (Klotz, 2002; Apel and Hirt, 2004). Considering the potential cytotoxicity of ROS, plants evolved elaborated ROS scavenging systems consisting of non-enzymatic antioxidants and enzymatic scavengers that maintain an equilibrium between ROS production and scavenging under physiological conditions (Alscher et al., 1997; Noctor and Foyer, 2005). Research over the past years revealed that modulation of this equilibrium constitutes a complex signalling network that includes the interplay of different ROS, spatial fine-regulation of ROS scavengers and retrograde plastid-nucleus signalling (Noctor and Foyer, 2005; Fernandez and Strand, 2008; Miller et al., 2008).

1.2.1. Generation of ROS

Under physiological and abiotic stress conditions ROS are produced predominantly in the chloroplasts, peroxisomes and mitochondria (Apel and Hirt, 2004). The contribution of mitochondrial respiration to ROS generation is low compared to chloroplastic photosynthesis and photorespiration (in C3 plants) leading to ROS production in the peroxisomes (Purvis, 1997).

During photosynthesis, photosystem I (PS II) constantly produces 1O_2 which drastically increases during high light stress (Hideg et al., 2002). After light

absorption and excitation of the light harvesting complex II (LHC II) the energy is transferred to chlorophyll P680 in the reaction centre of PS II resulting in an electron transfer chain with subsequent sequential reduction of pheophytin, the quinones Q_A and Q_B and the plastoquinone (PQ) pool (Barber, 1998). Once Q_A , Q_B and the PQ pool are fully reduced, electron transfer is blocked leading to an uncompleted charge separation of the oxidized chlorophyll P680 and the reduced pheophytin thereby generating a triplet formation of P680 chlorophyll (Van Mieghem et al., 1989; Barber, 1998; Krieger-Liszkay, 2005). The excitation energy of chlorophyll P680 is then dissipated onto O_2 leading to the formation of 1O_2 (Durrant et al., 1990). Quenching of 1O_2 has been associated with the rapid turnover of the D1 protein, a central element of the PS II reaction centre (Aro et al., 1993; Hideg et al., 1994). When 1O_2 production exceeds D1 turnover, e.g. under high light stress or CO_2 deprivation, block of the electron chain and photoinhibition are the consequences (Hideg et al., 1998). Thus, plants have evolved protection mechanisms to prevent photoinhibition either by thermal dissipation of excess excitation energy (EEE) in the antennae of PS II (non-photochemical quenching) or transfer of excess electrons to additional electron sinks (photochemical quenching) (Ort and Baker, 2002). One of these additional electron sinks is O_2 that is utilized by photosystem I (PS I) and by the ribulose-1,5-bisphosphat-carboxylase/-oxygenase (RuBisCO) (Wingler et al., 2000; Ort and Baker, 2002). Under various stress conditions and restricted CO_2 availability O_2 is reduced to $O_2^{\bullet-}$ by the ferredoxin of the PS I and subsequently converted to H_2O_2 by Cu/Zn superoxide dismutase (Mehler reaction) (Mehler, 1951; Asada, 2000). In addition, in the presence of transition metals $O_2^{\bullet-}$ and H_2O_2 are able to form HO^{\bullet} , for which no physiological scavengers are yet known (Asada, 1999). HO^{\bullet} has a very short half-life (1 – 0,01 μ sec) and diffusion distance from its generation site (0,5 μ m) making it highly reactive. Therefore, it is important for the cell to scavenge $O_2^{\bullet-}$ and H_2O_2 rapidly (Asada, 1999; Pitzschke et al., 2006). Furthermore, in leaves of C3 plants O_2 is used as an electron sink by RuBisCO that provides the major route for H_2O_2 production during photosynthesis through photorespiration when CO_2 availability is scarce or temperature is increased. Under these conditions, RuBisCO catalyses a competitive reaction in which O_2 is favoured over CO_2 as a substrate. RuBisCO-catalyzed oxygenation produces phosphoglycolate that is converted into glycolate and translocated from the chloroplast to the peroxisomes where it is oxidized to H_2O_2 and glyoxylate (Ort and Baker, 2002).

In response to biotic stress, plants produce ROS as a line of defence to utilize the cytotoxicity of ROS against the pathogen, to strengthen the cell walls and to mediate downstream signalling for defence gene activation (Bradley et al., 1992; Levine et al., 1994; Lamb and Dixon, 1997). Upon pathogen attack, ROS are rapidly generated in the apoplast and comprise primarily $O_2^{\cdot-}$ and H_2O_2 (Doke, 1985; Apostol et al., 1989). During incompatible plant-pathogen interactions, the elicited oxidative burst occurs in a biphasic manner constituting an initial transient phase with low amplitude and a second prolonged phase of massive ROS accumulations. The latter has been correlated with disease resistance since compatible interactions induce only a transient oxidative burst (Lamb and Dixon, 1997). For a long time, the source of ROS production was unclear and several enzymes have been implicated in its production upon pathogen recognition. Mammalian phagocytes possess a NADPH-oxidase complex, the phagocyte oxidase (PHOX), that is activated upon pathogen recognition and catalyzes the production of $O_2^{\cdot-}$ using NADPH as donor molecule and O_2 as acceptor (Babior, 1999). Recent studies identified homologues of the plasma-membrane localized, O_2 -reducing catalytic subunit gp91^{PHOX} in several plant species such as *Oryza sativa*, *Nicotiana benthamiana* and *Arabidopsis* (Groom et al., 1996; Torres et al., 1998; Yoshioka et al., 2003). In *Arabidopsis*, there are ten such *respiratory burst oxidase homologue (AtRboh)* genes which have been implicated in apoplastic ROS production upon different environmental and developmental triggers (Torres and Dangl, 2005). With regard to plant defence, *AtRbohD* appears to provide the major source of ROS accumulation after infection with an avirulent pathogen and *AtRbohF* is involved in the regulation of the HR (Torres et al., 2002). Cell-wall bound peroxidases (POD) have been proposed as an additional source of ROS (Wojtaszek, 1997; Bolwell et al., 1998). In the presence of NADH, NADPH or related reductants, PODs are able to generate H_2O_2 in response to pathogen attack (Vera-Estrella et al., 1992). Finally, it was shown that the horse radish peroxidase can reduce H_2O_2 to HO^{\cdot} *in vitro* (Chen and Schopfer, 1999), and it was recently suggested that PODs generate HO^{\cdot} in the apoplast using H_2O_2 as a substrate (Kukavica et al., 2009).

1.2.2. ROS scavenging

Plants use non-enzymatic and enzymatic strategies to scavenge ROS. Non-enzymatic antioxidants comprise glutathione (GSH), ascorbate (Asc), tocopherol, flavonoids, alkaloids and carotenoids (Apel and Hirt, 2004; Mittler et al., 2004). Among these

scavenging molecules GSH and Asc are the major cellular redox buffers. Both molecules are oxidized by ROS forming either oxidized glutathione (GSSG) or monodehydroascorbate (MDA) and dehydroascorbate (DHA), respectively.

Enzymatic scavenging incorporates removal of ROS as well as recovery of oxidized antioxidants such as GSSG, MDA and DHA. Superoxide dismutase (SOD), dismutating $O_2^{\cdot-}$ to H_2O_2 , catalase, converting H_2O_2 into H_2O and $\frac{1}{2} O_2$, and alternative oxidases (AOX), minimizing $O_2^{\cdot-}$ production, act only as scavengers and are not involved in antioxidant recovery. By contrast, ascorbate peroxidase (APX), monodehydroascorbate reductase (MDAR), dehydroascorbate reductase (DHAR) and glutathione reductase (GR) form an ascorbate-glutathione cycle to detoxify H_2O_2 . This cycle includes consumption and recovery of Asc and GSH thereby using NAD(P)H as reducing equivalent. In addition, in the glutathione-peroxidase cycle the glutathione peroxidase (GPX) scavenges H_2O_2 by using GSH that is then recovered by GR and NAD(P)H (Apel and Hirt, 2004; Mittler et al., 2004).

There are multiple isoforms of APX and SOD in plants that exert their function in different subcellular compartments. While AOXs are associated with the thylakoid and mitochondrial inner membrane, CAT localizes only to peroxisomes and GPX is exclusively cytosolic (Mittler et al., 2004). In this context also ferritins should be mentioned that do not scavenge ROS but remove transition metals and therefore help to prevent the formation of HO^{\cdot} (Ravet et al., 2009).

1.2.3. ROS signalling

In recent years it became evident that ROS form a complex signalling network regulated by the active modulation of ROS production and scavenging that is mediated by at least 152 genes, the so-called ROS gene network (Mittler et al., 2004). Thus, signalling results from changes of the cellular as well as of the compartmental redox homeostasis and could be achieved in different ways: (i) by activation/repression of redox sensitive transcription factors, (ii) by antioxidant-mediated sensing of an altered cellular redox homeostasis and (iii) by activation of ROS sensors and subsequent signal transduction (Apel and Hirt, 2004; Noctor and Foyer, 2005; Mittler et al., 2004; Miller et al., 2008). Elucidation of the precise signalling activity of each ROS faces the problem that different ROS are produced simultaneously (Fryer et al., 2002). H_2O_2 has been postulated as major ROS signal since it is stable and less reactive compared to other ROS and, importantly, can cross

plant membranes. Several genetic approaches have assessed the impact of different ROS on nuclear gene expression by compiling gene expression profiles of mutants lacking or over expressing specific ROS scavengers, respectively, and after engineered induction of specific ROS (Op den Camp et al., 2003; Gadjev et al., 2006; Laloi et al., 2006, 2007). Among a large set of genes induced by $^1\text{O}_2$, $\text{O}_2^{\cdot-}$ and H_2O_2 a number of genes could be identified that were differentially expressed in response to specific ROS pointing to defined signalling roles for each ROS. Intriguingly, antagonistic crosstalk between $^1\text{O}_2$ and H_2O_2 signalling has also been proposed (Laloi et al., 2007). It is noteworthy that in these approaches ROS production originating in chloroplasts resulted in rapid nuclear gene expression changes suggesting operation of retrograde plastid-nucleus signalling. Furthermore, the source of ROS production seems to be crucial, since a certain ROS can cause different effects depending on the compartment it was derived from (Miller et al., 2007).

A paradigm for ROS signalling beyond ROS cytotoxicity comes from studies investigating the conditional *flu* (*fluorescent*) mutant in *Arabidopsis* (Meskauskiene et al., 2001; Op den Camp et al., 2003; Wagner et al., 2004; Danon et al., 2005; Lee et al., 2007). *Flu* mutants generate $^1\text{O}_2$ in the chloroplasts in response to a dark/light shift. In *flu* mutant seedlings the induction of $^1\text{O}_2$ results in rapid bleaching and mortality (Meskauskiene et al., 2001) while mature plants exhibit a strong growth reduction and necrotic lesions (Op den Camp et al., 2003). A genetic screen for suppressors of the *flu* mutant identified the *EXECUTER 1* (*EX 1*) and *EXECUTER 2* (*EX 2*) genes. While the precise functions of EX1 and EX2 are unknown, they are associated with the thylakoid membranes of chloroplasts (Wagner et al., 2004; Lee et al., 2007). The *ex1/flu* mutant over accumulates $^1\text{O}_2$ but fully abrogates the *flu* phenotype and partially suppresses $^1\text{O}_2$ -mediated nuclear gene expression. The *ex1/ex2/flu* mutant fully suppressed $^1\text{O}_2$ -induced nuclear gene expression but still maintains elevated $^1\text{O}_2$ levels (Lee et al., 2007). These studies demonstrated that the phenotypes exhibited by the *flu* mutant are not the result of $^1\text{O}_2$ cytotoxic effects but require chloroplast-nucleus signalling leading to transcriptional output.

1.2.4. ROS and cell death

Besides $^1\text{O}_2$ other ROS have been implicated in the initiation of cell death (Vranova et al., 2002; Dat et al., 2003) as part of plant growth and development programmes and in response to environmental triggers such as pathogen attack (Van Breusegem and

Dat, 2006). After successful pathogen recognition, plants exhibit an HR that presumably requires an orchestrated accumulation of different ROS to induce cell death whereas a key signalling role has been assigned to apoplast-generated H₂O₂ (Dangl and Jones, 2001; Torres et al., 2002; Overmyer et al., 2003). A recent study has shown that *Arabidopsis* RBOH-generated ROS contribute to HR cell death since *rboh* mutants display reduced ROS generation and PCD after infection with avirulent bacteria (Torres et al., 2002). Strikingly, elicitation of the HR also requires light pointing to an involvement of chloroplastically produced ROS (Goodman and Novacky, 1994).

Studies on the *lesion simulating disease resistance 1 (lsd1)* mutant revealed important insights into cell death regulation. *Lsd1* mutants are unable to restrict cell death beyond the site of HR (Dietrich et al., 1997) and exogenous generation of O₂^{•-} is sufficient to induce so-called run-away cell death (RCD) in *lsd1* (Jabs et al., 1996). In addition, high light and low CO₂ promote lesion formation in *lsd1* that can be blocked by photosynthetic electron transport inhibitors (Mateo et al., 2004). Surprisingly, ROS produced by *AtRbohD* and *AtRbohF* negatively regulate RCD in *lsd1* while SA promotes it (see below) (Aviv et al., 2002; Torres et al., 2005). It was suggested that LSD1 negatively regulates cell death by interacting with the basic leucine zipper (bZIP) transcription factor AtbZIP10 and retaining it from the nucleus (Kaminaka et al., 2006). After perception of an appropriate ROS-derived signal, LSD1 releases AtbZIP10 to the nucleus where it activates transcription of HR related genes. Furthermore, LSD1 interacts with the LOL1 (LSD-one-like 1) protein that positively regulates cell death in an unknown manner (Epple et al., 2003). Therefore, LSD1 seems to act as a molecular hub mediating oxidative stress responses.

Besides chloroplasts, mitochondria have also been implicated in ROS production resulting in PCD (Maxwell et al., 2002; Tiwari et al., 2002; Yu et al., 2002; Yao et al., 2004, 2006). Studies on the *accelerated cell death 2 (acd2)* provided evidence for the involvement of a mitochondrial oxidative burst in the HR and suggested the requirement of crosstalk between chloroplasts and mitochondria to mediate PCD (Yao et al., 2004, 2006).

Cell death induction not only requires production of ROS, but also coordinated suppression of ROS scavenging (Mittler et al., 1999; Delledonne et al., 2001) and the interaction with other signalling molecules such as nitric oxide (NO) and the plant hormones SA, ethylene and jasmonic acid (JA) (see below) (Delledonne et al., 2001;

de Jong et al., 2002; Overmyer et al., 2005; Mur et al., 2006). For example, NO and $O_2^{\cdot-}$ can react to produce peroxynitrite ($ONOO^-$) that is able to cause cell death in animals (Bonfoco et al., 1995). By contrast, $ONOO^-$ seems not to be crucial for cell death induction in plants. In fact, formation of $ONOO^-$ was suggested to prevent an imbalance of NO and H_2O_2 that otherwise synergistically trigger PCD (Delledonne et al., 2001; Zago et al., 2006).

1.3. EDS1 – a regulatory node for immune and oxidative stress responses

EDS1 was originally identified in a screen for *Arabidopsis* mutants that are defective in *R* gene-mediated resistance to isolates of the obligate biotroph oomycete *Hyaloperonospora parasitica* (Parker et al., 1996). Subsequent analysis revealed that *EDS1* constitutes a central regulatory node in the plant innate immune system and plays an important role in oxidative stress signalling (Wiermer et al., 2005).

1.3.1. EDS1 and plant innate immunity

EDS1 is a mediator of basal resistance, defence responses triggered by TIR-NBS-LRR immune receptors and is required for early signalling events resulting in the induction of an oxidative burst and expression of the HR (Feys et al., 2001; Rusterucci et al., 2001). Most *EDS1*-activated responses require *PAD4* (PHYTOALEXIN DEFICIENT 4), an interaction partner of *EDS1* (Feys et al., 2001). *EDS1/PAD4* triggered defence leads to the accumulation of SA and amplification of the defence response around the infection site, including promotion of their own expression (Feys et al., 2001). While *eds1* mutants show a complete loss of TIR-NBS-LRR mediated resistance upon infection with avirulent isolates of *H. parasitica*, *pad4* mutants still retain a delayed HR but fail to restrict pathogen growth (Feys et al., 2001). Further studies showed that functional redundancy between *PAD4* and *SAG101* (*SENESCENCE ASSOCIATED GENE 101*), a second interactor of *EDS1*, accounts for the partially compromised resistance phenotype of *pad4* (Feys et al., 2005). However, *EDS1* and *PAD4* are equally required for basal resistance in response to virulent pathogens (Aarts et al., 1998; Feys et al., 2001). After infection with virulent *H. parasitica* or *Pst*, *eds1* and *pad4* mutant plants exhibited similarly enhanced levels of

pathogen growth compared to the susceptible wt (Feys et al., 2001) indicative of a loss of post-invasive basal resistance.

How *EDS1* and its interacting partners exert their function is still unclear. Localization and molecular interaction experiments revealed that *EDS1* forms homodimers in the cytosol while *EDS1-PAD4* heteromers localize to the cytosol and the nucleus and the *EDS1-SAG101* complex is exclusively localized to the nucleus (Feys et al., 2005). The three proteins share a lipase-like domain but so far no lipolytic activity could be shown and mutations of conserved amino-acid residues in the lipase domain of *EDS1* or *PAD4* do not interfere with their role in disease resistance (S. Rietz and J. Parker, unpublished data).

1.3.2. *EDS1* and ROS signalling

Although *EDS1* and *PAD4* are not required for defence responses triggered by the CC-NBS-LRR immune receptor *RPM1* both are needed for the generation of a ROS/SA-dependent defence signal amplification loop (Rusterucci et al., 2001). *RPM1*-triggered defence induces RCD in the *lsd1* mutant that requires *EDS1* and *PAD4* for propagation. This activity is genetically separable from the *EDS1/PAD4* roles in *R* gene mediated HR and disease resistance (Rusterucci et al., 2001). In addition, *eds1* and *pad4* abrogate RCD in *lsd1* caused by photo-oxidative stress due to high light conditions that promote EEE (Mateo et al., 2004). The failure of *lsd1* to acclimate to EEE is associated with reduced catalase activity, stomatal conductance and thus sequential decreased CO₂ availability, resulting in ROS overload that are all dependent on *EDS1* and *PAD4*. Subsequent studies suggested that an over-reduction of the PQ pool generates signals that require *EDS1*-, and partially *PAD4*-, dependent transduction leading to ROS and ethylene accumulation and resulting in RCD in the *lsd1* mutant (Mühlenbock et al., 2008).

Notably, *EDS1* is also required for signalling events in the conditional *flu* mutant (Ochsenbein et al., 2006). However, the *eds1* mutation does not abolish *flu* initiation of cell death but *eds1/flu* mutant plants recover faster from ¹O₂-mediated growth inhibition and suppress the spread of necrotic lesions. In addition, elevated levels of SA and expression of *PR1* and *PR5* genes in *flu* also depend on *EDS1*.

Together, these data suggest that *EDS1* has distinct key regulatory functions in mediating disease resistance and oxidative stress responses.

1.4. Salicylic Acid

The phytohormone SA is a phenolic beta-hydroxy benzoic acid that plays an important role in response to biotic and abiotic stresses in plants. In particular, SA is required to mount an adequate defence response after infection with various pathogens and it has also been implicated in the elicitation of the HR in certain resistance responses. In addition, SA-conjugates as well as the crosstalk with other plant hormone signalling pathways such ethylene- and JA-signalling seem to play a crucial role in plant defence.

1.4.1. SA synthesis and its role in plant disease resistance

SA can be synthesised via two different pathways that both utilize chorismate as initial substrate. One pathway uses chorismate-derived phenylalanine that is converted via different intermediates into SA (Wildermuth, 2006). A second pathway synthesises SA in the chloroplasts in a two step reaction mediated by ISOCHORISMATE SYNTHASE 1 (ICS1) converting chorismate into isochorismate and ISOCHORISMATE PYRUVATE LYSASE (IPL) that catalyzes the conversion into SA (Wildermuth et al., 2001; Wildermuth, 2006; Strawn et al., 2007). It was shown that this pathway provides the major route for pathogen induced SA accumulation in *Arabidopsis*. Knockouts of the *SID2* (*SALICYLIC ACID INDUCTION DEFICIENT 2*) gene encoding ICS1 fail to accumulate SA in response to pathogens and exhibit enhanced susceptibility (Nawrath and Metraux, 1999; Wildermuth et al., 2001). The importance of SA accumulation upon pathogen infection was reinforced by studies with plants expressing the bacterial *NahG* gene whose gene product, a bacterial salicylate hydrolase, hydrolyzes SA to catechol thereby fully depleting the SA pool. These plants failed to express *PR* genes and exhibited hypersusceptibility towards virulent and avirulent pathogens (Gaffney et al., 1993; Delaney et al., 1994; Kachroo et al., 2000). However, negative effects of catechol on plant disease resistance have to be taken into account when interpreting these results (van Wees and Glazebrook, 2003). Nevertheless, external application of SA or synthetic SA analogues such as dichloro-isonicotinic acid (INA) or benzo(1,2,3)thiadiazole-7-carbothioic acid S-methyl ester (BTH) restored resistance

and *PR* gene expression in *sid2* mutants and *NahG*-expressing plants (Nawrath and Metraux, 1999).

SA accumulation upon pathogen challenge can be regulated by *EDS1/PAD4* or *NDR1* (Feys et al., 2001; Shapiro and Zhang, 2001) depending on the *R gene* trigger. In *eds1* and *pad4* mutants, SA application induces defence gene expression and is therefore positioned downstream of EDS1 and PAD4 (Feys et al., 2001). SA contributes to a positive feedback loop in which it stimulates *EDS1/PAD4* expression thereby potentiating signalling.

SA-dependent signalling in *Arabidopsis* is mediated by the redox sensitive *NONEXPRESSOR OF PR GENES (NPR1)* (Cao et al., 1994; Delaney et al., 1995). Under conditions of redox equilibrium NPR1 appears to be present as an oligomer in the cytosol that is formed through intramolecular disulfide bonds. SA-induced changes of cellular redox homeostasis lead to a reduction of the disulfide bonds thereby releasing NPR1 monomers to the nucleus and activating the transcription of defence genes (Mou et al., 2003; Tada et al., 2008). In addition, NPR1 interacts in the nucleus with the TGA1 (TGACG-sequence-specific binding-protein 1) transcription factor in a redox-sensitive manner thereby increasing the DNA binding capacity of TGA1 (Despres et al., 2003).

1.4.2. SA, ROS and cell death

Alterations of SA levels can have direct effects on the efficiency of photosynthesis and acclimation to EEE thereby also regulating the production of H₂O₂ (Mateo et al., 2004, 2006). It was suggested that SA promotes H₂O₂ accumulation by inhibiting ROS scavengers thus forming an amplification loop in which H₂O₂ promotes SA accumulation (Chen et al., 1993; Leon et al., 1995; Klessig et al., 2000). Initially, this amplification loop was proposed to drive the HR and establish resistance (Draper, 1997). Recent studies, however, showed that SA is not necessarily required for HR elicitation since *NahG* plants and *sid2* mutants are able to trigger HR (Feys et al., 2001; Overmyer et al., 2003). Reports about SA-dependent cell death induction are contradictory. In several mutants a spontaneous cell death phenotype is correlated with enhanced SA accumulation. Cell death in these mutants was abrogated by SA depletion and re-initiated by exogenous application of SA or BTH (Lorrain et al., 2003). By contrast, it has been shown that SA also negatively regulates cell death and that elevated SA levels do not result in a spontaneous cell death phenotype,

respectively (Rate et al., 1999; Clough et al., 2000; Rate and Greenberg, 2001; Devadas and Raina, 2002). ROS and SA can also have antagonistic effects on cell death regulation as shown in the *lsd1* mutant (Torres et al., 2005): SA and BTH application results in the spread of necrotic lesions in *lsd1* that is negatively regulated by *AtrbohD* and *AtrbohF*.

SA-dependent resistance and cell death induction also depend on the crosstalk of SA with ethylene and JA. While SA and ethylene can interact synergistically or antagonistically, SA-JA crosstalk is mainly antagonistic (Robert-Seilaniantz et al., 2007). A recent study showed that *EDS1* and *PAD4* induce ethylene production that is required for cell death induction in *lsd1* suggesting an interplay of SA and ethylene (Mühlenbock et al., 2008). Furthermore microarray analysis revealed that SA and ethylene might function together to induce the same set of defence genes (Schenk et al., 2000) while ethylene potentiates SA-dependent *PR1* expression (Lawton et al., 1994).

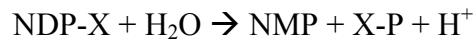
There is large body of evidence for negative crosstalk between SA and JA (Kunkel and Brooks, 2000). A good example comes from several *Pst* strains that produce the phytotoxin coronatine, a mimic of methyljasmonate which activates defence against necrotrophs. By promoting JA-dependent signalling via coronatine delivery, *Pst* utilize an endogenous negative regulation system of SA dependent defence and this may tip the balance towards disease. This was reinforced by the *Arabidopsis coi1* (*coronatine insensitive 1*) mutant that is more resistant to *Pst* and this is associated with more rapid SA-dependent expression of *PR1* (Kloek et al., 2001; Zhao et al., 2003).

1.5. The nudix hydrolase NUDT7 – a negative regulator of EDS1

NUDT7 has been shown independently in several gene expression microarray experiments to be upregulated after infection with avirulent pathogens (Bartsch et al., 2006; Ge et al., 2007; Adams-Phillips et al., 2008). *Nudt7* mutant plants resemble constitutive defence mutants and recent studies suggested a role for *NUDT7* as a negative regulator of *EDS1*-mediated defence signalling and oxidative stress responses (Bartsch et al., 2006; Ge et al., 2007).

1.5.1. Nudix hydrolases

The nudix hydrolase NUDT7 is one of 32 nudix hydrolases present in *Arabidopsis* (McLennan, 2006). Nudix hydrolases are a superfamily of Mg²⁺-requiring enzymes that are widespread among eukaryotes, bacteria, archaea and viruses (Bessman et al., 1996; McLennan, 2006). This class of enzymes mainly consists of pyrophosphohydrolases that catalyze the hydrolysis of **nucleoside diphosphates** linked to other moieties **X** (NDP-X) to yield nucleoside monophosphate (NMP) plus X-P:



The NUDT enzyme substrate range includes intact and oxidatively damaged nucleoside triphosphates, dinucleoside polyphosphates, nucleoside-sugars, capped RNA and dinucleotide coenzymes (Bessman et al., 1996; Mildvan et al., 2005). These substrates are either toxic or have a signalling activity and nudix hydrolases play protective, regulatory and signalling roles in metabolism by removing such molecules (Mildvan et al., 2005). The centre of catalysis is the so-called Nudix box, a highly conserved 23-residue sequence motif, GX₅EX₇REX₃EEXGU (where U is Ile, Leu or Val) that is found in all members of the superfamily (McLennan, 2006).

NUDT7 has *in vitro* hydrolase activity on ADP-ribose and NADH (Ogawa et al., 2005; Olejnik et al., 2005; Jambunathan and Mahalingam, 2006) but this could not be confirmed *in vivo* (Ge et al., 2007). The subcellular localization of NUDT7 is predicted as cytosolic by software predictions but has not been shown *in vivo* (Ogawa et al., 2005). Crosslinking experiments with glutaraldehyde revealed the ability of NUDT7 to form homodimers (Olejnik et al., 2005).

1.5.2. NUDT7 in plant defence and oxidative stress signalling

Arabidopsis plants lacking *NUDT7* are reduced severely in growth, exhibit spontaneous leaf cell death that is restricted to single cells, and accumulate elevated SA levels (Bartsch et al., 2006). In addition, *nudt7* mutants show constitutive expression of defence markers such as *PRI*, *PR2* and *AIG1* (Jambunathan and Mahalingam, 2006; Ge et al., 2007) and are hyper resistant towards a virulent isolate of *H. parasitica* (Bartsch et al., 2006). Other studies suggested a hyper resistance phenotype of *nudt7* towards virulent and avirulent strains of *Pst* (Jambunathan and Mahalingam, 2006; Ge et al., 2007). *NUDT7* was shown to be upregulated in an *EDSI*-dependent manner in a gene expression microarray experiment aimed at the

identification of novel components of *EDSI*-mediated defence signalling (Bartsch et al., 2006). Further, genetic analysis revealed that the *nudt7* phenotype depends on *EDSI*. Therefore, it was proposed that *NUDT7* acts as a negative regulator of *EDSI*-triggered defence signalling (Bartsch et al., 2006). Surprisingly, the cell death phenotype of *nudt7* plants does not depend on SA as was shown for other cell death mutants (Brodersen et al., 2005; Torres et al., 2005). By contrast, SA depletion in *nudt7/sid2* mutants exacerbates spontaneous leaf cell death drastically pointing to an SA-independent defence branch triggered by *EDSI* (Bartsch et al., 2006).

Reports on the redox homeostasis of *nudt7* mutant plants are contradictory demonstrating either enhanced ROS accumulation (Jambunathan and Mahalingam, 2006) or no ROS accumulation (Ge et al., 2007). However, pharmacological induction of oxidative stress results in a strong growth retardation of *nudt7* plants suggesting a role for *NUDT7* in maintaining the cellular redox balance (Ge et al., 2007).

1.6. Aims of the thesis

The importance of *EDSI*-dependent signalling in plant innate immunity is evident from several studies (Parker et al., 1996; Aarts et al., 1998; Feys et al., 2001). Recent data also reveal a key regulatory function for *EDSI* in mediating oxidative stress signalling (Rusterucci et al., 2001; Mateo et al., 2004; Ochsenbein et al., 2006; Mühlenbock et al., 2008). However, little is known about how the *EDSI* pathway works and is controlled. Expression of the nudix hydrolase *NUDT7* is tightly *EDSI*-dependent and *NUDT7* is positioned genetically as a negative regulator of *EDSI* resistance signalling (Bartsch et al., 2006). I aimed to characterize *NUDT7* activity and the relationship of *NUDT7* to *EDSI* in order to define more closely key processes governing plant innate immunity and programmed cell death.

EDSI-dependent *nudt7-1* growth retardation, spontaneous leaf cell death and elevated salicylic acid levels suggested that *NUDT7* regulation is part of intrinsic *EDSI* stress pathway. I tested this hypothesis by co-expression studies of *EDSI* and *NUDT7* and analysed *NUDT7* transcript and protein levels upon activation of *EDSI*-dependent and *EDSI*-independent defence responses. *EDSI* and *NUDT7* transcripts are responsive to MAMP treatment (Zipfel et al., 2004; Phillips-Adams et al., 2008). Thus, hyper-responsiveness of *nudt7-1* to MAMPs leading to increased MAMP-triggered immunity (MTI) by microbes was postulated to induce the *nudt7-1* phenotype. I

investigated a potential role for *EDSI* and *NUDT7* in MTI by multiple assays. *EDSI*-mediated ROS signalling causes cell death and growth retardation (Rusterucci et al., 2001; Mateo et al., 2004; Mühlenbock et al., 2008) and *nudt7* mutants are hypersusceptible to oxidative stress (Ge et al., 2007). In addition, SA is involved in redox regulation (Mateo et al., 2006) and *EDSI*-dependent programmed cell death (PCD) in *nudt7* is exacerbated by SA depletion (Bartsch et al., 2006). Therefore, I used the *nudt7* mutant as a genetic tool to gain deeper insight to i) mechanisms of *EDSI*-mediated oxidative stress signalling ii) the impact of SA on the regulation of PCD in *EDSI*-triggered oxidative stress signalling and iii) the position of *NUDT7* in this signalling pathway.

2. Materials and Methods

2.1. Materials

2.1.1. Plant materials

Arabidopsis wild-type and mutant lines use in this study are listed in Table 2.1 and 2.2, respectively.

Table 2.1 Wild-type *Arabidopsis* accessions used in this study

Accession	Abbreviation	Original source
Columbia-0	Col-0	J. Dangl ^a
Landsberg- <i>erecta</i> -0	Ler-0	Nottingham <i>Arabidopsis</i> Stock Center

^a University of North Carolina, Chapel Hill, NC, USA

^b Nottingham, UK

Table 2.1 Mutant and transgenic *Arabidopsis* lines used in this study

Mutant allele	Accession	Mutagen	Reference/Source
	Col-0		
<i>eds1-2</i>	/(Ler-0) ^a	FN	Bartsch et al., 2006
<i>fls2</i>	Col-0	T-DNA	
<i>fmo1-1</i>	Col-0	T-DNA	Bartsch et al., 2006
<i>nud7-1/eds1-2</i>	Col-0	T-DNA/FN	Bartsch et al., 2006
<i>nudt7-1</i>	Col-0	T-DNA	Bartsch et al., 2006
<i>nudt7-1/eds1-2/sid2-1</i>	Col-0	T-DNA/FN/EMS	this study
<i>nudt7-1/fmo1-1</i>	Col-0	T-DNA	this study
<i>nudt7-1/pad4-1</i>	Col-0	T-DNA/EMS	this study
<i>nudt7-1/rbohD</i>	Col-0	T-DNA/ <i>dSpm</i>	this study
<i>nudt7-1/sid2-1</i>	Col-0	T-DNA/EMS	Bartsch et al., 2006
<i>pad4-1</i>	Col-0	EMS	Glazebrook et al., 1997
<i>rbohD</i>	Col-0	<i>dSpm</i>	Torres et al., 2002
<i>sid2-1</i>	Col-0	EMS	Wildermuth et al., 2001
<i>CaMV35S::cNUDT7-strepII</i>	Col-0	Floral dipping of <i>nudt7-1</i>	M. Bartsch ^b , unpublished

^a *Ler eds1-2* allele introgressed into Col-0 genetic background, 8th backcrossed generation

^b Centro Nacional de Biotecnología, Dep. of Plant Molecular Genetics, C/ Darwin 3, 28049 Madrid

EMS: ethylmethane sulfonate; FN: fast neutron; *dSpm*: defectice *Suppressor-mutator*;

T-DNA: transfer-DNA

2.1.2. Pathogens

2.1.2.1. *Hyaloperonospora parasitica*

Hyaloperonospora parasitica isolate NOCO2 was used for infection studies in this work. *H. parasitica* NOCO2 was derived from isolated conidia from single seedlings (Holub et al., 1994).

Table 2.2 *H. parasitica* isolate NOCO2 and its interaction with *Arabidopsis* ecotypes

<i>Arabidopsis</i> ecotype	<i>H. parasitica</i> NOCO2
Col-0	compatible
Ler-0	incompatible (RPP5)

2.1.2.2. *Pseudomonas syringae* pv. *tomato*

Pseudomonas syringae pv. *tomato* strain DC3000 expressing the avirulence determinants *avrRps4* (Hinsch and Staskawicz, 1996) or *avrRpm1* (Grant et al., 1995) from the broad host range plasmid pVSP61 (Innes et al., 1993) or DC3000 containing empty pVSP61 were used in this study. The *P. syringae* pv. *tomato* isolates were originally obtained from R. Innes (Indiana University, Bloomington Indiana, USA). In addition, *P. syringae* pv. *tomato* lacking the effector genes *AvrPto/AvrPtoB* (*Pst* DC3000 Δ *AvrPto/AvrPtoB*) was used (Xiao et al., 2007).

2.1.3. Oligonucleotides

Primers used in this study are listed in Table 2.4. Oligonucleotides were purchased from Sigma-Aldrich (Deisenhofen, Germany), Operon (Cologne, Germany) or Metabion (Martinsried, Germany). Lyophilised primers were resuspended in nuclease-free water to a final concentration of 100 pmol/ μ l (= 100 μ M), working stocks were diluted to 10pmol/ μ l (=10 μ M).

Table 2.3 List of primers used in this study

Primer	Sequence (5' \rightarrow 3')	Purpose
ActF	TGCGACAATGGAAGCTGGAATG	Actin2 RT-PCR
ActR	CTGTCTCGAGTTCCTGCTCG	Actin2 RT-PCR
105/E2	ACACAAGGGTGATGCGAGACA	<i>eds1-2</i> mutant detection
EDS4	GGCTTGTATTCATCTTCTATCC	<i>eds1-2</i> mutant detection
EDS6	GTGGAAACCAAATTTGACTTAG	<i>eds1-2</i> mutant detection

MB58	TCAATGGATGGATTGTTCCCC	<i>fmo1-1</i> genotyping For
MB59	GGCAACAATTAACAGTTACTCGCA	<i>fmo1-1</i> genotyping Rev
MB111	CCAATAAACAAAGGGCACGGA	<i>nudt7-1</i> genotyping For
MB112	CCACTCCTCTCCTGGACAACG	<i>nudt7-1</i> genotyping Rev
pad4-1 for	GCGATGCATCAGAAGAG	<i>pad4-1</i> genotyping For
pad4-1 rev	TTAGCCCAAAGCAAGTATC	<i>pad4-1</i> genotyping Rev
MS7	GGATACTGATCATAGGCGTGGCTCCA	<i>rbohD</i> genotyping For
MS12	GTCGCCAAAGGAGGCGCCGA	<i>rbohD</i> genotyping Rev
MS10	CTTATTTTCAGTAAGAGTGTGGGGTTTTGG	<i>dSpm</i> detecion
MS4	GCAGTCCGAAAGACGACCTCGAG	<i>sid2-1</i> mutant detection For
MS5	CTATCGAATGATTCTAGAAGAAGC	<i>sid2-1</i> mutant detection Rev
LBa1	TGGTTCACGTAGTGGGCCATCG	LB primer for SALK
EG46	CGAAGACACAGGGCCGTA	qRT PCR <i>EDS1</i> For
EG48	AAGCATGATCCGCACTCG	qRT PCR <i>EDS1</i> Rev
MS35	GCTTCTCTTTCGCATTGGAG	qRT PCR <i>NUDT7</i> For
MS36	GCAGCCTCCACAAGATTAGC	qRT PCR <i>NUDT7</i> Rev
EG68	AGATCCAGGACAAGGAGGTATTC	qRT PCR Ubiquitin For
EG69	CGCAGGACCAAGTGAAGAGTAG	qRT PCR Ubiquitin Rev
MS29	CTGCGACTCAGGGAATCTTCTAA	qRT PCR UBC21 For
MS30	TTGTGCCATTGAATTGAACCC	qRT PCR UBC21 Rev

For = forward; Rev = reverse

2.1.4. Enzymes

2.1.4.1. Restriction endonucleases

Restriction enzymes were purchased from New England Biolabs (Frankfurt, Germany) unless otherwise stated. Enzymes were supplied with 10x reaction buffer.

MS (Murashige and Skoog) liquid medium

MS powder including vitamins and MES buffer	4,8g/l
Sucrose	10g/l

For MAMP assays flg22 peptide was added at the indicated concentrations from a 10mM stock. Plant agar and MS powder including vitamins and MES buffer was purchased from Duchefa (Haarlem, The Netherlands). Flg22 was provided by S. Robatzek^a.

^a Max-Planck-Institute for Plant Breeding Research, Carl-von-Linné-Weg 10, 50829 Cologne, Germany

Escherichia coli media**LB (Luria-Bertani) broth**

Tryptone 10,0g/l

Yeast extract 5,0g/l

NaCl 5.0 g/l

pH 7.0

For LB agar plates 1.5% (w/v) agar was added to the above broth.

Pseudomonas syringae media**NYG broth**

Peptone 5g/l

Yeast extract 3g/l

Glycerol 20ml/l

pH 7.0

For NYG agar plates 1,5% (w/v) agar was added to the above broth.

2.1.8. Antibodies

Listed below are primary and secondary antibodies used for immunoblot detection

Table 2.4 Primary antibodies

Antibody	Source	Dilution	Reference
α -EDS1	rabbit polyclonal	1:500 TBS-T + 2% milk	S. Rietz ^a
α -NUDT7	rabbit polyclonal	1:500 TBS-T + 5% milk	this study
α -GFP	mouse monoclonal	1:2000 TBS-T + 2% milk	Roche (Mannheim, Germany)
α -Histone H3	rabbit polyclonal	1:5000 TBS-T	Abcam (Cambridge, UK)
α -Hsc70	mouse polyclonal	1:5000 TBS-T + 1% BSA	Stressgen (Victoria, Canada)

^a Max-Planck-Institute for Plant Breeding Research, Carl-von-Linné-Weg 10, 50829 Cologne, Germany

Table 2.5 Secondary antibodies

Antibody	Feature	Dilution	Reference
goat anti-rabbit IgG-HRP	HRP	1:5000 TBS-T + 5% milk	Santa Cruz (Santa Cruz, USA)
goat anti-mouse IgG-HRP	HRP	1:5000 TBS-T + 1% BSA	Santa Cruz (Santa Cruz, USA)

HRP = horse radish peroxidase

2.1.9. Buffers and solutions

General buffers and solutions are displayed in the following listing. All buffers and solutions were prepared with Milli-Q® water. Buffers and solutions for molecular biological experiments were autoclaved and sterilised using filter sterilisation units. Buffers and solutions not displayed in this listing are denoted with the corresponding methods.

DNA extraction buffer (Quick prep)

Tris 200 mM
NaCl 250 mM
EDTA 25 mM
SDS 0.5%
pH 7,5 (HCl)

DNA gel loading dye (6x)

Sucrose 4g
EDTA (0,5 M) 2ml
Bromphenol blue 25mg
H₂O to 10ml

DAB solution	25mg 3,3'-Diaminobenzidine (Sigma) 25ml H ₂ O 25μl 1N HCl Place the solution in a water-bath at 42 ⁰ C for 6-8 hours
Ethidium bromide stock solution	Ethidium bromide 10 mg/ml H ₂ O Dilute 1:40000 in agarose solution
Honda buffer	Ficoll 400 5g Dextran T40 10g Sucrose 27,38g Tris 0,606g MgCl ₂ 0,407g H ₂ O to 200 ml pH 7,4 Before use add 10mM β Mercaptoethanol and protease inhibitor cocktail for plant cell and tissue extracts (Sigma).
Lactophenol trypan blue	Lactic acid 10ml Glycerol 10ml H ₂ O 10ml Phenol 10g Trypan blue 10mg Before use dilute 1:1 in ethanol.
PCR reaction buffer (10x)	Tris 100mM KCl 500mM MgCl ₂ 15mM Triton X-100 1 % pH 9,0 Stock solution was sterilised by autoclaving and used for homemade Taq DNA polymerase.
Ponceau S	Ponceau S working solution was Prepared by dilution of ATX Ponceau S concentrate (Fluka) 1:5 in H ₂ O.
SDS-PAGE:	
Resolving gel buffer (4x)	Tris 1,5M pH 8,8 (HCl)
Running buffer (10x)	Tris 30,28g Glycine 144,13g SDS 10g H ₂ O to 1000ml Do not adjust pH.

Sample buffer (2x)	Tris 0,125M SDS 4% Glycerol 20% (v/v) Bromphenol blue 0,02% Dithiothreitol (DTT) 0,2M pH 6,8
Stacking gel buffer (4x)	Tris 0,5M pH 6,8 (HCl)
TAE buffer (50x)	Tris 242g EDTA 18,6g Glacial acetic acid 57,1ml H ₂ O to 1000ml pH 8,5
TBS buffer	Tris 10mM NaCl 150mM pH 7.5 (HCl)
TBST buffer	Tris 10mM NaCl 150mM Tween20 0,05% pH 7.5 (HCl)
TE buffer	Tris 10mM EDTA 1mM pH 8.0 (HCl)
Western blotting: Transfer buffer (10x)	Tris 58,2g Glycine 29,3g SDS (10%) 12,5ml H ₂ O to 1000ml pH 9,2 Before use dilute 80ml 10x buffer with 720ml H ₂ O and add 200ml methanol.

2.2. Methods

2.2.1. Maintenance and cultivation of *Arabidopsis* plant material

Arabidopsis seeds were germinated by sowing directly onto moist compost (Stender AG, Schermbeck, Germany) containing insecticide (10mg/l Confidor WG70 (Bayer, Germany)) or jiffy-9 pots (Jiffy International AS, Ryomgaard, Denmark) supplemented with Wuxal fertilizer (Nitzsch; Kreuztal, Germany). Seeds were cold treated by placing sawn pots on a tray with a lid and incubating them in the dark at

4°C for three days. Pots were subsequently transferred to a controlled environment growth chamber, covered with a propagator lid and maintained under short day conditions (10 hour photoperiod, light intensity of approximately 200 μ Einsteins/m/sec, 23°C day, 22°C night, and 65% humidity). Propagator lids were removed when seeds had germinated. If required for setting seed, plants were transferred to long day conditions (16 hour photoperiod) to allow early bolting and setting of seed. To collect seed, aerial tissue was enveloped with a paper bag and sealed with tape at its base until siliques shattered.

2.2.2. Generation of *Arabidopsis* F₁ and F₂ progeny

Fine tweezers and a magnifying-glass were used to emasculate an individual flower. To prevent self-pollination, only flowers that had a well-developed stigma but immature stamen were used for crossing purpose. Fresh pollen from three to four independent donor stamens was dabbed onto each single stigma. Mature siliques containing F₁ seed were harvested and allowed to dry. Approximately five F₁ seeds per cross were grown as described above and allowed to self pollinate. Produced F₂ seeds were collected and stored for subsequent genotyping.

2.2.3. *Arabidopsis* seed sterilization

For in vitro growth of *Arabidopsis*, seed had to be sterilised. Approximately 50 – 100 *Arabidopsis* seeds were put into a mini column in a 2ml closable microcentrifuge tube. 500 μ l 70% EtOH and 0,1% Tween20 were added and shaken for 2min. Tubes were centrifuged for 10sec and liquid was removed. 500 μ l 100% EtOH were added to the seeds and incubated for 1min. Samples were centrifuged again for 10sec and EtOH was removed. Seeds were dried under sterile hoods for approximately 1 hour before sowing.

2.2.4. Inoculation and maintenance of *Hyaloperonospora parasitica*

H. parasitica isolates were maintained as mass conidiosporangia cultures on leaves of their genetically susceptible *Arabidopsis* ecotypes over a 7 day cycle (see 2.1.2.1). Leaf tissue from infected seedlings was harvested into a 50ml Falcon tube 7 days after inoculation. Conidiospores were collected by vigorously vortexing harvested leaf material in sterile dH₂O for 15sec and after the leaf material was removed by filtering through miracloth (Calbiochem) the spore suspension was adjusted to a concentration

of 4×10^4 spores/ml dH₂O using a Neubauer counting cell chamber. Plants to be inoculated had been grown under short day conditions as described (section 2.2.1). *H. parasitica* conidiospores were applied onto 2-week-old seedlings by spraying until imminent run-off using an aerosol-spray-gun. Inoculated seedlings were kept under a propagator lid to create a high humidity atmosphere and incubated in a growth chamber at 18°C and a 10 hours light period. For long-term storage *H. parasitica* isolate stocks were kept as mass conidiosporangia cultures on plant leaves at -80°C.

2.2.5. Quantification of *H. parasitica* sporulation

To determine sporulation levels, seedlings were harvested 5 - 6 days after inoculation in a 50ml Falcon tube and vortexed vigorously in 5 - 10ml water for 15sec. Whilst the conidiospores were still in suspension 12µl were removed twice and spores were counted under a light microscope using a Neubauer counting cell chamber. For each tested Arabidopsis genotype, three jiffy pots containing approximately 30 seedlings were infected per experiment and harvested spores from all seedlings of each pot were counted twice with sporulation levels expressed as the number of conidiospores per gram fresh weight.

2.2.6. DAB staining

To determine H₂O₂ accumulations in foliar tissue, leaves were excised and placed in 15ml Sarstedt tube (Nümbrecht, Germany) and immersed in DAB solution. The opened tube was placed in a plastic desiccator and vacuum was applied. After 2min, vacuum was released and DAB-infiltrated leaves were placed in a plastic box and kept at high humidity in the dark. After 10-12 hours, leaves were transferred into a fixation solution (3:1:1 ethanol: lactic acid: glycerol) and incubated for 8 hours. Fixation solution was exchanged for chloral hydrate solution (2,5 g/ml H₂O) for over night incubation. The next day, chloral hydrate solution was removed and leaves were stored in 70% glycerol. Samples were mounted onto glass microscope slides in 70% glycerol and examined using a light microscope (Axiovert 135 TV, Zeiss, Germany) connected to a Nikon DXM1200 Digital Camera.

2.2.7. Lactophenol trypan blue staining

Lactophenol trypan blue staining was used to visualise necrotic plant tissue and *P. parasitica* mycelium (Koch and Slusarenko, 1990a). Leaf material was placed in a 15ml Sarstedt tube (Nümbrecht, Germany) and immersed in lactophenol trypan blue. The tube was placed into a boiling water bath for 2min followed by destaining in 5ml chloral hydrate solution (2,5 g/ml H₂O) for 2 hours and a second time overnight on an orbital shaker. After leaf material was left for several hours in 70% glycerol, samples were mounted onto glass microscope slides in 70% glycerol and examined using a light microscope (Axiovert 135 TV, Zeiss, Germany) connected to a Nikon DXM1200 Digital Camera.

2.2.8. Quantification of cell death

Untreated and paraquat treated leaves from similar developmental stages were stained with lactophenol trypan blue as described under 2.2.7. All samples have been blinded to guarantee unbiased analysis. Leaves were examined for dead cells using a light microscope (Axiovert 135 TV, Zeiss, Germany) and representative leaf areas were marked with square of 1mm² using Diskus 4.2 Software (Hilgers, Königswinter, Germany). Dead cells were counted within this square. In each experiment, 5 leaves per genotype and treatment were used for cell death quantification.

2.2.9. Maintenance of *P. syringae* pv. *tomato* cultures

Pseudomonas syringae pv. *tomato* strains described in 2.1.2.2 were streaked onto selective NYG agar plates containing rifampicin (100µg/ml) and kanamycin (50µg/ml) from -80° C DMSO stocks. Streaked plates were incubated at 28°C for 48 hours before storing at 4°C and refreshed weekly.

2.2.10. *P. syringae* pv. *tomato* inoculations for time course experiments and growth assays

P. syringae cultures of the denoted strains were started from bacteria grown on NYG agar plates. One day prior to inoculation, fresh cultures were generated on NYG agar plates with Rifampicin (100µg/ml) and Kanamycin (50µg/ml). Freshly grown bacteria were resuspended in 10mM MgCl₂ and OD600 was determined. For vacuum-infiltration the concentration of bacteria was adjusted to 1 x 10⁷cfu/ml (OD600 =

0,02) in 600ml of 10mM MgCl₂ containing 0,002% Silwet L-77 (Lehle seeds, USA). Jiffy pots with 3 plants, grown under short day conditions for five weeks, were routinely used for time course experiments. The evening before vacuum-infiltration, plants were watered and kept under a dH₂O-humidified lid. Vacuum infiltration of the plants was accomplished by inverting the jiffy pots and carefully submerging all leaf material in 600ml of diluted bacterial suspension in a plastic desiccator. Vacuum was applied and maintained within the desiccator for 2min before being gradually released. Plants were removed from the desiccator and remaining non-infiltrated leaves were removed. The excess of bacterial solution was washed off by inverting the pots and gently agitating them in water.

For spray-inoculation the concentration of bacteria was adjusted to 1×10^8 cfu/ml (OD₆₀₀ = 0,2) in 100ml of 10mM MgCl₂ containing 0,02% Silwet L-77. Single pots with 5 plants, grown under short day conditions for five weeks, were routinely used for bacterial growth assays. The evening before spray-inoculation, plants were watered and kept under a dH₂O-humidified lid. Bacteria were applied on leaves by spraying until imminent run-off using an aerosol-spray-gun. Day zero samples were taken three hour after infiltration by using a cork borer (\varnothing 0.4cm) to excise and transfer 3 leaf discs from 3 independent plants to a 2ml centrifuge tube. This was repeated with two more batches of 3 leaf discs from 3 independent plants. The discs were then incubated in 300 μ l of sterile 10mM MgCl₂ containing 0,02% Silwet at 28°C. Subsequently, 100 μ l of each sample were plated onto NYG agar (Rifampicin 100 μ g/ml; Kanamycin 50 μ g/ml). Day three samples were taken in an identical manner to that of d0. For each sample a dilution series ranging between 10^1 and 10^{-5} was made and 25 μ l aliquots from each dilution were spotted sequentially onto a single NYG agar plate (Rifampicin 100 μ g/ml, Kanamycin 50 μ g/ml). All bacteria plates were incubated at 28°C for 48 hours before colony numbers were determined.

2.2.11. Fresh weight analysis of soil-grown plants

Plants were grown for 4 weeks under conditions described in section 2.2.1. After 4 weeks, 3 samples of 3 plants each were weighed and the weight of a single plant was estimated. Fresh weight analysis after paraquat treatment was performed 37 days after germination the same way.

2.2.12. Sterile growth

Magenta boxes (Sigma-Aldrich Deisenhofen, Germany), were autoclaved. Under laminar flow hood 50ml of autoclaved MS solid medium was poured in all Magentas and the medium was let to solidify. Upon solidification, sterilized *Arabidopsis* seeds were sown on the medium surface and the Magentas were sealed. For stratification the Magentas were kept for two days at 4°C in the dark and then transferred in a short day (8 hours light/day) growth chamber. After four weeks Magentas were open and samples taken for fresh weight analysis.

2.2.13. Flg22 growth assay

Seeds were sterilized as described above and sown on MS plates without antibiotics. For stratification plates were incubated for two days at 4°C in the dark. Afterwards they were transferred in a growth chamber with standard growth condition (12 h/day light). After 7 days, seedlings were transferred in 24 well microtiter plates (Nunc, Denmark) containing in each well 500µl of autoclaved MS liquid medium without or with flg22 (10nM, 100nM or 1µM). Plates were closed and their lids sealed with hypoallergenic non-woven tape (Leukopor, Germany). Plates were then placed on shakers in growth chamber with standard growth conditions (12 hours/day light). After 7 days, 24 samples of 2 plants each were weighed and the weight of a single plant was estimated.

2.2.14. Oxidative stress analysis

Methyl viologen (paraquat) (Sigma) was applied as previously described by Get et. al. (2007). Plants were grown for three weeks on jiffy-9 pots as described above. After 3 weeks, paraquat was applied in a concentration of 5µM in dH₂O containing 0,02% Silwet L-77 onto leaves using a hand spray bottle. Application was performed three times in an interval of 4 days. 4 days after the last paraquat application, plant tissue was harvested and prepared for particular analysis.

2.2.15. Biochemical methods

2.2.15.1. *Arabidopsis* total protein extraction for immunoblot analysis

Total protein extracts were prepared from 3- to 5-week-old plant materials. Liquid nitrogen frozen samples were homogenized 2 x 15sec to a fine powder using a Mini-

Bead-Beater-8™ (Biospec Products) and 1,2mm stainless steel beads (Roth) in 2ml centrifuge tubes. After the first 15sec of homogenisation samples were transferred back to liquid nitrogen and the procedure was repeated. 150µl of 2x SDS-PAGE sample buffer was added to 50mg sample on ice. Subsequently, samples were boiled for 7 min while shaking at 700rpm in an appropriate heating block. Samples were stored at -20°C if not directly loaded onto SDS-PAGE gels.

2.2.15.2. Protein purification using StrepII affinity purification

StrepII affinity protein purification was performed according to the protocol described by Witte et al., with modifications described below (Witte et al., 2004). For one purification, 2 g of Arabidopsis leaf material was ground in liquid nitrogen and thawed in 1ml StrepII extraction buffer listed below. The slurry (about 1,5ml) was placed in 2x 2ml micro centrifuge tube and then centrifuged for 10min at 4°C (14000rpm). The supernatant was ultra centrifuged for 15min at 4°C (100000rpm). After centrifugation, supernatants of one sample were combined and transferred to a new micro centrifuge tube, sampled, and 300µl slurry of StrepTactin Sepharose (IBA GmbH, Göttingen, Germany) was added. The Sepharose matrix is based on Sepharose 4FF with a bead size of 45–165µm. All samples taken for electrophoresis analysis were mixed with a 2 x SDS-loading buffer and heated for 5 min to 90°C prior to loading. Binding was performed by incubation in an end-over-end rotation wheel for 60min at 4°C. The slurry was transferred into a micro spin column (BioRad 732-6204, Hercules, CA) and the flow-through collected and sampled (Flow through). The resin was washed twice with 1ml and four times with 0,5ml StrepII washing buffer. For elution, 80µl of Elution buffer representing the void volume of the system were carefully applied to the resin but not recovered. Four times 100µl Elution buffer were passed through and collected in two pools of 200µl. From each pool, 20µl were sampled for SDS-PAGE analysis. The rest of eluates were pooled and concentrated using Vivaspin500 (VIVASCIENCE, Hannover, Germany) up to 20µl. The concentrated eluates were mixed with a 2 x SDS-loading buffer and heated for 5 min to 90°C prior to SDS-PAGE and immunoblot analysis.

Table 2.7: StrepII purification buffers

StrepII extraction buffer		StrepII washing buffer		StrepII elution buffer	
Tris-HCl ^a	100mM	Tris-HCl	50mM	Tris-HCl	10mM
EDTA	5mM	EDTA	0,5mM	NaCl	150mM
NaCl	100mM	NaCl	100mM	DTT	2mM
DTT	10mM	DTT	2mM	Triton	0,05%
ABESF ^b	0,5mM			Desthiobiotine	10mM
Aprotinin	5µg/ml				
Leupeptin	5µg/ml				
AVIDINE	100µg/ml				
Pi ^c	1 : 100				
Triton X-100	0,50%				

a Tris-HCl: pH8

b AEBSF: 4-(2-aminoethyl)benzenesulfonyl fluoride hydrochloride

c Proteinase Inhibitor cocktail (Sigma p9599)

2.2.15.3. Nuclear fractionation for immunoblot analysis

Nuclear fractionations were performed according to the protocol described by Kinkema *et al.* (2000), which is based on that described by Xia *et al.* (1997), with minor modifications: 1,5g fresh weight of unchallenged leaf tissues grown under short day conditions (as described in 2.2.1) were homogenised in 3ml Honda buffer using a pre-cooled mortar and pestle and then filtered through a 62µm (pore size) nylon mesh. Triton X-100 (10% working solution) was added to a final concentration of 0,5% and the solution was slowly mixed by swirling. The mixture was incubated on ice for 15min. The extract was then centrifuged at 1500 g for 5min. An aliquot of the nuclei-depleted fraction was saved and the pellet washed by gentle resuspension in 2.5ml Honda buffer containing 0.1% Triton X-100. The sample was centrifuged again at 1500 g for 5min. The pellet was resuspended in 2.5ml Honda buffer and 620µl ml aliquots were transferred to 1.5 ml microcentrifuge tubes. The preparations were centrifuged at 100 g for 5 min to pellet starch and cell debris. The supernatants were transferred to new microcentrifuge tubes and centrifuged at 2000 g for 5 min to pellet the nuclei. Nuclear pellets were resuspended in 200µl 2 x SDS-PAGE sample buffer, boiled for 10min, and pooled. The nuclear and nuclei-depleted fractions were run on 10% and 15% SDS-PAGE gels. α -HSC70 and α - histone H3 antibodies were used as cytosolic and nuclear markers, respectively.

2.2.15.4. Isolation of microsomal membranes

To isolate microsomal membranes 0,5g of 4-week-old leaves grown in short day conditions (see 2.2.1) were homogenised in liquid nitrogen. The ground tissue was thawed under further homogenisation in 1 ml extraction buffer (100mM Tris-HCl pH 7,5, 12% sucrose, 1 mM EDTA, 5 mM DTT and 1x protease inhibitor cocktail for plant cell and tissue extracts (Sigma)). The homogenate was passes through two layers of Miracloth (Calbiochem). The filtrate was transferred to a microcentrifuge tube and centrifuged at 2000 *g* and 4°C for 15min in a bench top centrifuge to remove cell debris and nuclei. 100µl of the supernatant were kept as a crude extract fraction whilst 600µl of the supernatant were transferred to an ultracentrifugation tube (Beckmann) and centrifuged for 1 hour at 100.000 *g* and 4°C (Optima™ MAX-E ultracentrifuge, Beckmann Coulter, USA). 600µl supernatant were kept as a soluble fraction and the pellet was washed with extraction buffer. After washing, the pellet was resuspended in 600µl of extraction buffer containing 1% (v/v) Triton X-100 using an ultrasonic bath. One volume of 2x SDS-PAGE sample buffer was added to the all fractions and samples were boiled for 5min to denature proteins. Samples were stored at -20° C.

2.2.15.5. Denaturing SDS-polyacrylamide gel electrophoresis (SDS-PAGE)

Denaturing SDS-polyacrylamide gel electrophoresis (SDS-PAGE) was carried out using the Mini-PROEAN® 3 system (BioRad) and discontinuous polyacrylamide (PAA) gels. Gels were made fresh on the day of use according to the manufacturer instructions. Resolving gels were poured between to glass plates and overlaid with 500µl isopropanol. After gels were polymerised for 30 – 45min the alcohol overlay was removed and the gel surface was rinsed with dH₂O. Excess water was removed with filter paper. A stacking gel was poured onto the top of the resolving gel, a comb was inserted and the gel was allowed to polymerise for 30 - 45min. In this study, 10% and 15% resolving gels were used, overlaid by 4 % stacking gels. Gels were 0,75 mm in thickness.

If protein samples were not directly extracted in 2x SDS-PAGE sample buffer proteins were denatured by adding 1 volume of 2x SDS-PAGE sample buffer to the protein sample followed by boiling for 5min.

After removing the combs under running water, each PAA gel was placed into the electrophoresis tank and submerged in 1x running buffer. A pre-stained molecular weight marker (Precision plus protein standard dual colour, BioRad) and denatured

protein samples were loaded onto the gel and run at 80 - 100V (stacking gel) and 100 – 150V (resolving gel) until the marker line suggested the samples had resolved sufficiently.

2.2.15.6. Immunoblot analysis

Proteins that had been resolved on acrylamide gels were transferred to Hybond™-ECL™ nitrocellulose membrane (Amersham Biosciences) after gels were released from the glass plates and stacking gels were removed with a scalpel. PAA gels and membranes were

pre-equilibrated in 1x transfer buffers for 10min on a rotary shaker and the blotting apparatus (Mini Trans-Blot® Cell, BioRad) was assembled according to the manufacturer instructions. Transfer was carried out at 100V for 90-120min. The transfer cassette was dismantled and membranes were checked for equal loading by staining with Ponceau S for 5min before rinsing in copious volumes of deionised water. Ponceau S stained membranes were scanned and thereafter washed for 5min in TBS-T before membranes were blocked for 1 hour at room temperature in TBS-T containing 5% blotting grade milk powder (Roth). The blocking solution was removed and membranes were washed briefly with TBS-T. Incubation with primary antibodies was carried out overnight by slowly shaking on a rotary shaker at 4°C in the conditions shown in Table 2.5. Next morning the primary antibody solution was removed and membranes were washed 3 x 15min with TBS-T at room temperature on a rotary shaker. Primary antibody-antigen conjugates were detected using a horseradish peroxidase (HRP)-conjugated goat anti-rabbit secondary antibody. Membranes were incubated in the secondary antibody solution for 1 hour at room temperature by slowly rotating. The antibody solution was removed and membranes were washed as described above. After being washed as described above, detection immediately followed. Detection was performed by chemiluminescence using the SuperSignal® West Pico Chemiluminescent kit or a 3:1 mixture of the SuperSignal® West Pico Chemiluminescent- and SuperSignal® West Femto Maximum Sensitivity-kits (Pierce) according to the manufacturer instructions. Luminescence was detected by exposing the membrane to photographic film (BioMax light film, Kodak).

2.2.15.7. In-gel MAP kinase assay

Seeds were sterilized as described above and sown on MS plates without antibiotics. For stratification plates were incubated for two days at 4°C in the dark. Afterwards they were transferred in a growth chamber with standard growth condition (12 hours/day light). After 7 days, seedlings were transferred in 24 well microtiter plates (Nunc, Denmark) containing in each well 500µl of autoclaved MS liquid medium and grown for 10 more days. After 10 days, MS liquid medium was filled up to 500µl again and after 2 hours flg22 was added to a final concentration of 100nM. After 0, 5, 10 and 30minutes aerial tissue was transferred to 2ml eppendorf microcentrifuge tubes and immediately frozen in liquid nitrogen. Liquid nitrogen frozen samples were homogenized 2 x 15sec to a fine powder using a Mini-Bead-Beater-8TM (Biospec Products) and 1,2mm stainless steel beads (Roth). 100µl protein extraction buffer (Buffer E) (buffers listed below) was added per 50mg fresh weight. Samples were centrifuged at 14000rpm for 20min at 4°C. Supernatant was transferred to new eppi. 20% of sample was mixed with an equal volume of 2x SDS-PAGE sample buffer and boiled for 8min. Sample was then separated on an SDS-PAGE gel containing myelin basic protein (5mg ml⁻¹). SDS-page gels were then washed with several buffers to renature the separated proteins:

Buffer F 3x30min at room temperature

Buffer G 2x30min at 4°C , then over night at 4°C

Buffer H 1x30min at RT

After renaturation, gels were incubated with Buffer H containing 2µM ATP and 5µCi radioactive γ -³²P-ATP for 90min. Gels were washed 6x30min with 1% phosphoric acid and rinsed with dH₂O. Kinase activity was visualized by Typhoon phosphor imager.

Table 2.6 In-gel MAP Kinase Buffers

Buffer contents	Buffer E	Buffer F	Buffer G	Buffer H
1M Tris-HCl ph 7,5	750µl	7,5ml	7,5ml	2,5ml
0,5M EGTA	150µl	/	/	20µl
0,5M EDTA	150µl	/	/	/
1M DTT	30µl	150µl	300µl	100µl
Protease inhibitor ^a	4µl/sample	/	/	/
1M NaF ^a	150µl	1,5ml	1,5ml	
1M Na ₃ VO ₄ ^a	75µl	30µl	30µl	10µl
1M β-glycerophosphate ^a	750µl	/	/	/
BSA	/	150g	/	/
TritonX	/	300µl	/	/
3M MgCl ₂	/	/	/	400µl
Water	12855µl	fill up to 300ml	fill up to 300ml	fill up to 100ml

^a chemicals derived from Sigma

2.2.15.8. Ethylene Measurements

Plants were grown 4 weeks as described above. After 4 weeks, samples were taken using a cork borer (ø 0,6cm) to excise 24 leaf discs from at least 12 independent plants. Leaf discs were floated over night on dH₂O before transferring 3x8 leaf discs per genotype and treatment into hermetic vials containing either 1ml dH₂O or 1ml dH₂O with 100nM flg22. Vials were sealed with rubber septa and incubated on a shaker for 4 hours at room temperature. After 4 hours ethylene production was measured by gas chromatography (GC). The analysis was performed on an Agilent 6890 GC connected to an Agilent 5975N mass selective detector (MSD, Agilent, Santa Clara, USA) operating in split mode with a ratio of 10 to 1. 100µl of the gas phase were taken from the hermetically closed vial with a gas-tight syringe and injected in the GC. Ethylene was separated on an Agilent GS-GasPro column (60m, ø 0,32mm) at 90°C and 1.4ml/min. The MSD was run in the "selected ion monitoring" (SIM) mode, measuring Ethylene fragment ions of 24,1; 25,1; 26,1 and 27,1 amu. Additionally to the fragment masses, the identification of the ethylene peak was based on the retention time of an ethylene standard (Fluka, Deisenhofen, Germany) run under same conditions and the ratio of ion abundances. To relatively quantify ethylene the area sum of all four ion counts was integrated using Chemstation software (Agilent). For more precise analysis, integrals of the void volume and the ethylene peaks were calculated and their ratio to each other was determined. For each genotype

and treatment, average was calculated from three replicates. The obtained value was then used to express relative ethylene quantities in the different samples.

2.2.16. Antibody production and purification

2.2.16.1. Protein expression in *E. coli*

The pGEX-2TM-GST::cNUDT7::his plasmid (M. Bartsch and J. Parker, unpublished) was expressed in *Escherichia coli* strain BL21 (DE3) (pLysS). The *E. coli* clones were cultured in 5ml LB medium overnight at 37°C. 500ml of new LB medium containing appropriate antibiotics were re-inoculated with 2ml of those cultures and incubated at 37°C until the bacterial growth reached an OD600 0.9. By adding 0,5mM IPTG protein expression was induced. Cultures were grown for 3 more hours at 37°C. Bacterial cells were pelleted by centrifugation at 4000rpm at 4°C for 20min. The pellets were washed 3 times with 30ml H₂O. After freezing pellet at -20°C overnight, total protein was extracted by incubation with native lysis buffer (50mM NaH₂PO₄, 300mM NaCl, 10mM Imidazol, 10% glycerol, 1mg/ml lysozyme, 10µg/ml DNase I) and subsequent sonication. Pellet was spun down at 14000rpm for 15min at 4°C and supernatant was removed. The pellet was then dissolved and incubated over night in denaturing lysis buffer (50mM Tris pH8, 8M Urea, 250mM NaCl, 10mM Imidazole, 10µM β-mercaptoethanol). Pellet was spun down again and supernatant was processed with Nickel-NTA affinity resin (Quiagen, Hilden, Germany) according to the manufactures instruction to purify NUDT7 protein. Immunization of rabbits was performed at BioGenes (Berlin) following their standard methods.

2.2.16.2. Antibody purification

Purified NUDT7 protein was fractionated on SDS-PAGE and transferred onto a PVDF membrane. The blotted proteins were visualized by Ponceau S. A membrane region containing a band corresponding to the size of GST::cNUDT7::his was cut, sliced into small pieces and collected in 2ml eppendorf tube. After rinsing membrane pieces with TBS buffer, membranes were incubated with TBS containing 1% BSA and 0.05% Tween20 for 2.5 hours at 4°C. After removing all buffers from the tube, 400µl of antiserum with 1600µl of TBS were added into the tube, incubated at 4°C for 4 hours. The membrane pieces were washed 4 times with 2ml of TBS for 5 min at 4°C. The bound antibodies were then eluted with 450µl of 0,1M Glycine, 0,5M NaCl, 0,05% Tween20, pH2,6 (with HCl) for 1,5 min at 4°C. The elution buffer was

collected in a new tube containing 50µl of 1M Tris-HCl pH8,0. Elution was repeated and 2 x 500µl of purified antibody were pooled.

2.2.17. Molecular biological methods

2.2.17.1. Isolation of genomic DNA from *Arabidopsis* (Quick prep for PCR)

One leaf of a plant was put into a 1,5 ml microcentrifuge tube was closed and 400 µl of DNA extraction buffer were added. A micropestle was used to grind the tissue in the tube until the tissue was well mashed. The solution was centrifuged at maximum speed for 5min in a bench top microcentrifuge and 300µl supernatant were transferred to a fresh tube. One volume of isopropanol was added to precipitate DNA and centrifuged at maximum speed for 5 minutes in a bench top microcentrifuge. The supernatant was discarded carefully. The pellet was washed with 70% ethanol and dried. Finally the pellet was dissolved in 100µl 10mM Tris-HCl pH 8,0 and 1µl of the DNA solution was used for a 20µl PCR reaction mixture. The aliquots were stored at -20°C.

2.2.17.2. Isolation of total RNA from *Arabidopsis*

Total RNA was prepared from 3- to 6-week-old plant materials. Liquid nitrogen frozen samples (approximately 100mg) were homogenized 2 x 15sec to a fine powder using a Mini-Bead-Beater-8™ (Biospec Products) and 1.2mm stainless steel beads (Roth) in 2ml centrifuge tubes. After the first 15sec of homogenisation samples were transferred back to liquid nitrogen and the procedure was repeated. 1ml of TRI® Reagent (Sigma) was added and samples were homogenised by vortexing for 1min. Samples were centrifuged for 10min. at 4° C at 12000 g and supernatants incubated for 5min at room temperature to dissociate nucleoprotein complexes. 0,2ml of chloroform was added and samples were shaken vigorously for 15sec. After incubation for 3min at room temperature samples were centrifuged for 15min at 12000 g and 4°C. 0,5ml of the upper aqueous, RNA containing phase were transferred to a new microcentrifuge tube and RNA was precipitated by adding 0,5 volumes of isopropanol and incubation for 10min at room temperature. Subsequently, samples were centrifuged for 10min at 12000 g and 4°C. The supernatant was removed and the pellet was washed by vortexing in 1ml of 70% ethanol. Samples were again centrifuged for 10min at 12000 g and 4°C, pellets were air dried for 10min and

dissolved in 20 μ l H₂O. Samples were incubated for 5min at 55°C and then immediately stored at -80°C.

2.2.17.3. Reverse transcription-polymerase chain reaction (RT-PCR)

RT-PCR was carried out in two steps. SuperScript™ II RNase H⁻ Reverse Transcriptase (Invitrogen) was used for first strand cDNA synthesis by combining 1 - 1.5 μ g template total RNA, 1 μ l oligo dT₁₈ V (0.5 μ g/ μ l, V standing for an variable nucleotide), 5 μ l dNTP mix (each dNTP 2.5mM) in a volume of 13,5 μ l (deficit made up with H₂O). The sample was incubated at 65°C for 10min to destroy secondary structures before cooling on ice for one minute. Subsequently the reaction was filled up to a total volume of 20 μ l by adding 4 μ l of 5x reaction buffer (supplied with the enzyme), 2 μ l of 0.1M DTT and 0.5 μ l reverse transcriptase. The reaction was incubated at 42°C for 60min before the enzyme was heat inactivated at 70°C for 10min. For subsequent normal PCR, 1 μ l of the above RT-reaction was used as cDNA template.

2.2.17.4. Polymerase chain reaction (PCR)

Standard PCR reactions were performed using home made *Taq* DNA polymerase. All PCRs were carried out using a PTC-225 Peltier thermal cycler (MJ Research). A typical PCR reaction mix and thermal profile is shown below.

Table 2.7 PCR reaction mix (20 μ l total volume)

Component	Volume
Template DNA	0,1 - 20ng
10x PCR reaction buffer	2 μ l
dNTP mix (2,5 mM each: dATP, dCTP, dGTP, dTTP)	2 μ l
Forward primer (10 μ M)	1 μ l
Reverse primer (10 μ M)	1 μ l
<i>Taq</i> DNA polymerase (4U/ μ l)	0,5 μ l
Nuclease free water	to 20 μ l total volume

Table 2.8 Thermal profile

Stage	Temperature (°C)	Time period	No. of cycle
Initial denaturation	95	3min	1x
Denaturation	95	30sec	
Annealing	50-60	30sec	30-40x
Extension	72	1min per kb	
Final extension	72	3min	1x

2.2.17.5. Quantitative real time (qRT) PCR

qRT PCR reactions were performed using iQTM SYBR® Green Supermix containing 100mM KCL, 6mM MgCl₂, 40mM Tris-HCl pH 8,4, 0,4mM of each dNTP, SYBR Green I and iTaq DNA polymerase (50 U/ml) (BioRad, Hercules, USA). All qRT PCRs were carried out using iQTM5 multicolor real-time PCR detection system (BioRad, Hercules, USA). Data were analysed with iQTM5 Optical System Software by the comparative $\Delta\Delta C_T$ method. A typical qRT PCR reaction mix and thermal profile is shown below.

Table 2.9 qRT PCR reaction mix

Component	Volume
Template cDNA	0,1 - 20ng
Forward primer (10 μ M)	1 μ l
Reverse primer (10 μ M)	1 μ l
iQ TM SYBR® Green Supermix	12,5 μ l
Nuclease free water	to 25 μ l total volume

Table 2.10 Thermal profile

Stage	Temperature (°C)	Time period	No. of cycle
Initial denaturation	95	3min	1x
Denaturation	95	30sec	
Annealing	60	30sec	40x
Extension	72	30sec	

2.2.17.6. Agarose gel electrophoresis of DNA

DNA fragments were separated by agarose gel electrophoresis in gels consisting of 1–3% (w/v) SeaKem® LE agarose (Cambrex, USA) in TAE buffer. Agarose was dissolved in TAE buffer by heating in a microwave. Molten agarose was cooled to 50°C before 2,5 μ l of ethidium bromide solution (10 mg/ml) was added. The agarose was pored and allowed to solidify before being placed in TAE in an electrophoresis tank. DNA samples were loaded onto an agarose gel after addition of 2 μ l 6x DNA loading buffer to 10 μ l PCR-reaction. Separated DNA fragments were visualised by placing the gel on a 312nm UV transilluminator and photographed.

2.2.18. Microarray analysis

2.2.18.1. Sample preparation

Plants of the Col-0, *nudt7-1*, *nudt7-1/sid2-1*, *nudt7-1/eds1* and *nudt7-1/sid2-1/eds1-2* genotypes were grown on soil for 4 weeks as described under 2.2.1.. Leaf material

was harvested exactly after 28 days of growth. This was performed 3 times to obtain 3 independent replicates for microarray analysis. To reduce transcriptional variations due to intrinsic circadian programs in *Arabidopsis*, leaf material of all three independent replicates was harvested 6 hours after illumination of the growth chambers. For each replicate, leaf material from the same developmental stage of different plants per genotype was pooled and RNA was extracted according to the protocol described under 2.2.16.2. RNA quality and concentration was measured in a spectrophotometer according to the manufacturer's instructions (BioPhotometer, Eppendorf AG, Hamburg, Germany). The absorption ratio 260/280 of all 15 samples was between 1,7 – 1,8 indicating that good quality RNA was isolated (low protein contamination). Complementary RNA labelling, hybridisation and data collection from the hybridised GeneChip were performed by the Integrated Functional Genomic service unit of the Interdisciplinary Center for Clinical Research (IZKF) in Münster (Germany), according to the standard manufacturer's protocol (Affymetrix GeneChip technical analysis manual). In brief, total RNA was reverse transcribed using SuperScript™ II RNase H⁻ Reverse Transcriptase (Invitrogen™) and T7(dT)₂₄ primer. The first strand cDNA was used for double-strand cDNA synthesis. Purified double-strand cDNA was used to generate biotin-labelled cRNA by in vitro transcription reactions. cRNA was fragmented and used for hybridisation to GeneChip Arabidopsis ATH1 Genome Array (Affymetrix, Santa Clara, USA). After the washing and staining procedure the arrays were scanned in an Agilent GeneArray Scanner (Agilent, Santa Clara, USA).

2.2.18.2. Data analysis

GeneSpring GX software version 10.0 (Agilent, Santa Clara, USA) was used for analysis of the raw data. Raw data of all chips were processed from CEL-files and summarized using GCRMA algorithm. This procedure included background correction and normalization of raw data of each chip to the median of all samples. Normalization per gene was also performed to median of all samples. Replicate structure of the experiment was then defined by grouping the three independent samples per each genotype. Normalized signal intensity values of each gene were averaged across the three replicates per genotype. Before filtering data and applying statistical analysis, quality of all chips was assessed by quality control measures. Efficiency of the labelling reaction and hybridization was controlled by comparing

normalized signal intensity values and 3'/5' hybridization ratios of two housekeeping genes (GAPDH and UBQ11) and prokaryotic control samples (BIOB, BIOC, CREX and BIODN). Raw signal intensity values of all entities were then filtered to remove low and saturated signal values, respectively. Percentile cut-offs were set at 20 and 100. All entities were retained in which at least 1 out of 15 samples had values within this range.

Statistical analysis was performed by using ANOVA test. P-value computation was done asymptotically and Benjamini Hochberg FDR was chosen as correction method for multiple testing correction. Only genes were considered that were differentially expressed in all samples compared to each other with a significance of $p < 0,05$. This test listed all genes that were significantly differentially expressed in any of the comparisons. Applying a post-hoc Tuckey test evaluated whether differences between any two pairs of means are significant. This test revealed that e.g. Gene *A* is significantly different expressed in the comparison Col-0 vs. *nudt7-1* but not in a comparison *nudt7-1* vs. *nudt7-1/sid2-1*. Lists were generated containing the significantly differentially expressed genes for each possible comparison. These lists were then subjected to fold change analysis. All genes were considered whose expression changed at least two fold. Further analysis was performed as described in results section (3.4).

3. Results

3.1. Generation of NUDT7 antibody and transgenic lines over expressing NUDT7

3.1.1. Generation of antisera recognizing NUDT7 protein

In order to perform molecular analyses of NUDT7 protein, antisera against recombinant NUDT7 protein were generated and α -NUDT7 antibody was purified and characterized. The pGEX-2TM-GW *Escherichia coli* expression vector was used to express recombinant NUDT7 protein fused to N-terminal GST and C-terminal histidine affinity purification tags (M. Bartsch and J. Parker, unpublished data). Purified recombinant GST-NUDT7-his protein was used by the company BioGenes (Berlin) to boost two rabbits (rabbit 8556 and rabbit 8557) four times. The resulting antiserum from rabbit 8556 was cleaned using recombinant GST-NUDT7-his protein immobilized onto a PDVF membrane and specific antibody against GST-NUDT7-his was purified. The obtained α -NUDT7 antibody specifically detected NUDT7 protein in total protein extracts from *Arabidopsis* leaves (Figure 3.1A). NUDT7 protein was detected at the predicted size of 32 KDa (Kilo Dalton) in total protein extracts from wildtype (WT) plants (accession Columbia-0, hereafter Col-0) but not in the *nudt7-1* mutant. NUDT7 antibody purified from rabbit 8556 antiserum was used throughout this work.

3.1.2. Complementation analysis of epitope-tagged NUDT7 over expresser lines

In order to characterize further the NUDT7 protein and its potential *in vivo* function, NUDT7 over expresser (OE) lines were generated (Bartsch and Parker, unpublished). *Arabidopsis nudt7-1* null mutant plants (accession Col-0) were transformed with constructs for constitutive expression of an AtNUDT7 StrepII affinity tag fusion protein under the *CaMV 35S* promoter (p35S::NUDT7-StrepII). Three independent, homozygous transgenic single insertion lines were selected and were characterized for complementation of the *nudt7-1* phenotype. The NUDT7 OE lines 4 and 7 complemented *nudt7-1* growth to WT levels while NUDT7 OE line 10 exhibited intermediate growth between WT and *nudt7-1* (Figure 3.2A and 3.2C).

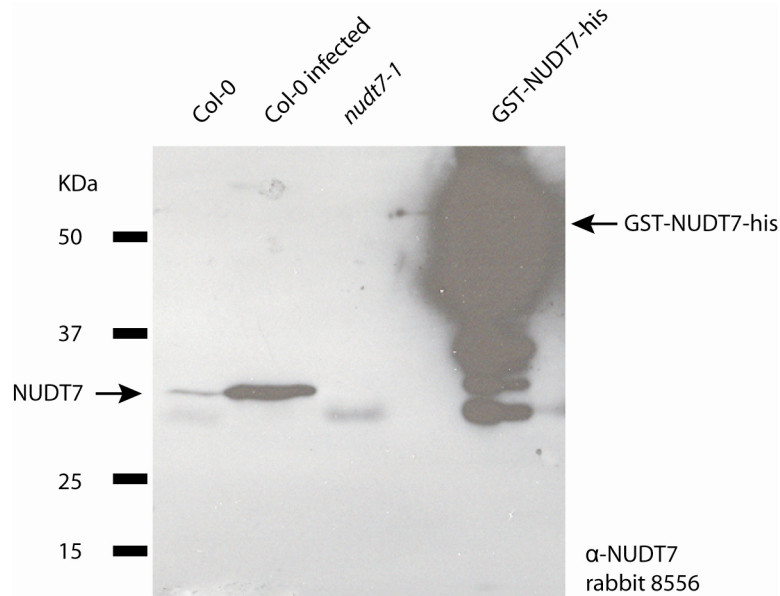


Figure 3.1: Specificity of α -NUDT7 antibody.

α -NUDT7 antibody specifically recognizes NUDT7 protein. NUDT7 antibody was purified from antiserum of immunised rabbit 8556. The antiserum was incubated with recombinant GST-NUDT7-his bound to a PVDF-western blotting membrane. Antibody that bound to epitopes of GST-NUDT7-his was then eluted and tested against total protein extracts from leaf material in a 1:500 dilution in TBS-T buffer containing 5% milk. Col-0 infected = Col-0 leaf tissue 24hpi *Pst avrRPM1*; NUDT7-GST = NUDT7 protein affinity tagged with GST and expressed *in vitro* in *E. coli*

Western blot analysis revealed that all OE lines expressed NUDT7 protein to much higher levels than WT (Figure 3.2C).

Of the three OE lines, OE4 expressed NUDT7 at the highest level whereas OE line 7 and OE line 10 had similar levels of NUDT7 protein. To investigate the basal resistance of the NUDT7 OE lines, I inoculated plants with virulent *H. parasitica* isolate NOCO2 that is recognized by *RPP5* in the Landsberg (Ler-0) background but not in Col-0 (Parker et al., 1996). The enhanced basal resistance phenotype of *nudt7-1* plants towards *H. parasitica* NOCO2 was reverted to WT levels of basal resistance in OE4 (Figure 3.2D). NUDT7 OE line 7 and OE10 failed to complement fully since both lines exhibited similar levels of enhanced basal resistance as *nudt7-1*. Based on the high protein levels and the failure to fully complement the basal resistance phenotype of *nudt7-1* plants, I concluded that over expressed NUDT7-StrepII protein is only partially functional.

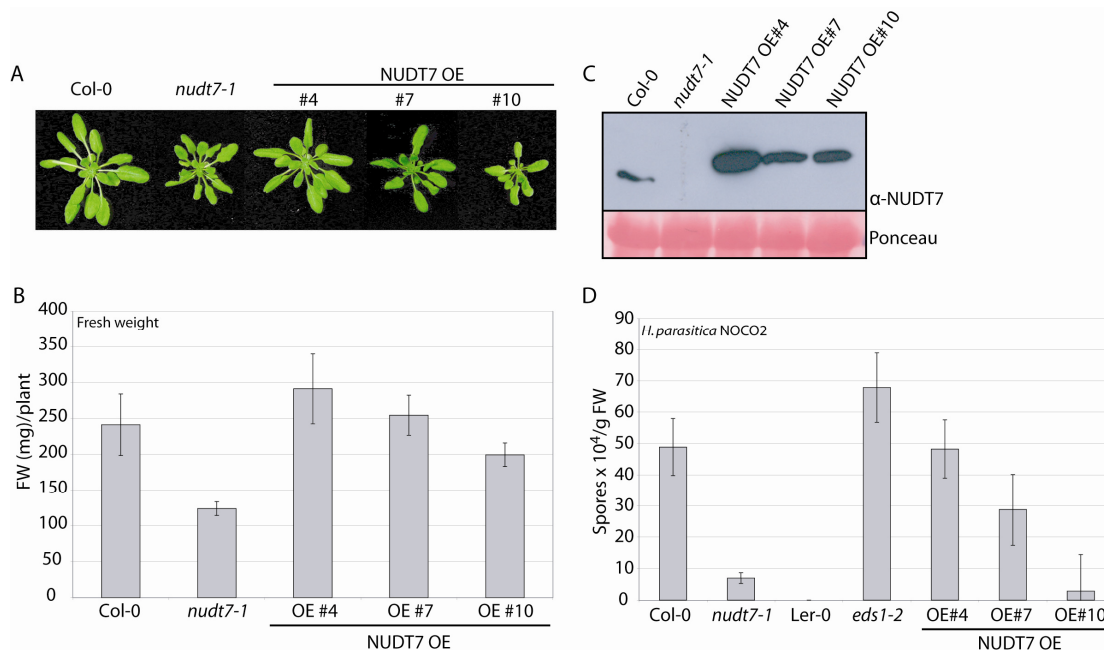


Figure 3.2: Complementation studies of NUDT7 over expresser lines.

(A) NUDT7 OE lines vary in complementing *nudt7-1* growth phenotype. Pictures are representative for 4-week-old soil-grown plants.

(B) Fresh weight analysis of 4-week-old soil-grown plants. Fresh weight of 12 plants per genotype was measured and average was calculated. Error bars represent standard deviation (SD). Experiment was repeated at least three times with similar results.

(C) NUDT7 OE accumulate more NUDT7 protein compared to wt. Total protein was extracted from leaves of 4-week-old plants and analysed with α -NUDT7 antibody. Ponceau staining served as loading control.

(D) NUDT7 OE lines exhibit different degrees of basal resistance. 3-week old soil-grown plants were inoculated with *H. parasitica* NOCO2 with 4×10^4 spores/ml. Sporulation was analysed 6 days post inoculation with a Neubauer counting chamber. Experiment was repeated at least three times with similar results.

This is further supported by the fact that NUDT7 OE10 also fails to complement the *nudt7-1* growth phenotype. It is likely that the strepII affinity tag interfered with NUDT7 protein function. Although the strepII tag is small in size (8 amino acids) (Witte et al., 2004), it might affect the folding of NUDT7 and therefore also affect protein function. However, there were no untagged NUDT7 OE lines generated making it difficult to prove this conclusion. During the progress of this work, the scientific focus changed wherefore no further NUDT7 fusion proteins were generated and analyzed.

3.2. Analysis of *NUDT7* transcript and protein expression

3.2.1. Co-regulation of *EDSI* and *NUDT7* in response to stress

Previous work showed that the phenotype exhibited by the *nudt7-1* mutant is fully *EDSI*-dependent and that *NUDT7* negatively regulates *EDSI*-dependent signalling (Bartsch et al., 2006). Both genes are constitutively expressed in all tissues in *Arabidopsis* (Wiermer, 2005; Jambunathan and Mahalingam, 2006) and required to mediate abiotic and biotic stress responses (Wiermer et al., 2005; Jambunathan and Mahalingam, 2006; Ge et al., 2007; Adams-Philipp et al., 2008; Mühlenbock et al., 2008).

These data prompted me to investigate whether there is a co-regulation of *EDSI* and *NUDT7* during plant development and in response to stress. Analysis of the expression profile of *EDSI* and *NUDT7* using the ATTED-II co-expression database (Obayashi et al., 2008) revealed a high co-expression of both genes after induction of several stresses (abiotic, biotic and chemotoxic) whereas the co-expression profile at different developmental stages was not tightly linked (Figure 3.3A). Calculating the Pearson's correlation coefficient resulted in a correlation coefficient of 0,66 for the co-expression of *EDSI* and *NUDT7*. This result points to a tight linkage of the expression of *EDSI* and *NUDT7* in response to stress. I concluded that *EDSI* and *NUDT7* are both required for various stress responses indicated by their co-expression profile.

These data and work from Bartsch et al. (2006) suggested a close relationship of *NUDT7* and *EDSI* in response to stress. However, both studies could not provide evidence whether *NUDT7* has a direct or indirect negative regulatory effect on *EDSI* and whether this occurs at the transcriptional or post-translational level.

In order to investigate if the regulatory effect of *NUDT7* on *EDSI* is of direct or indirect nature, I determined transcript and protein levels of *EDSI* in the *nudt7-1* mutant and *vice versa* in healthy, four-week-old soil-grown plants. The *eds1-2* mutation was generated by fast neutron mutagenesis of Landsberg-0 (Ler-0) seedlings (Aarts et al., 1998) and introgressed in the Col-0 background (Bartsch et al., 2006). In Col-0 *nudt7-1* plants, the *NUDT7* gene was disrupted by T-DNA (Transfer-DNA) insertion (Bartsch et al., 2006). Both mutants are null mRNA mutants (Aarts et al., 1998; Bartsch et al., 2006).

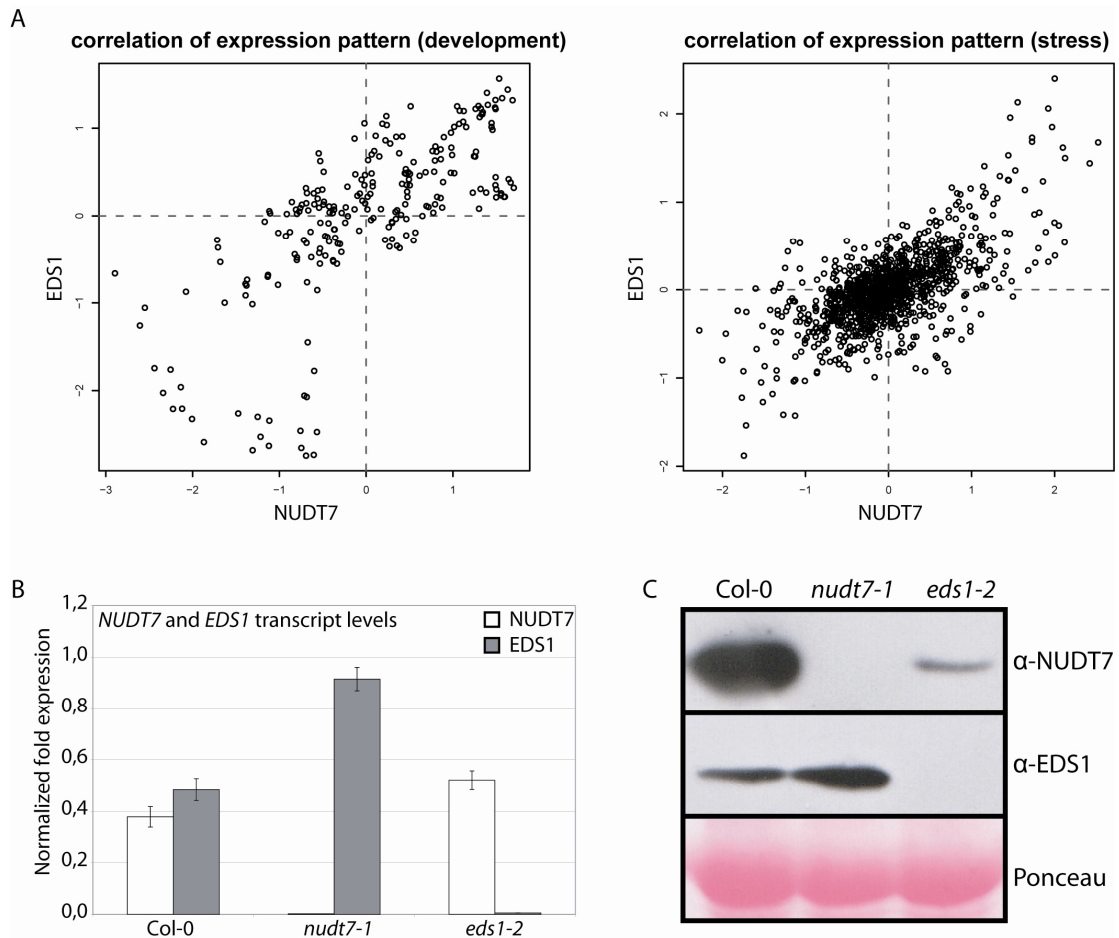


Figure 3.3: Scatter plot graphs displaying the co-expression of *EDS1* and *NUDT7* and determination of *EDS1* and *NUDT7* transcript and protein levels.

(A) Co-expression study of *EDS1* and *NUDT7* using the Co-expression Viewer tool from the ATTED-II database (<http://atted.jp/>). Left panel shows the co-expression of both genes at different developmental stages. Right panel displays the expression of *EDS1* and *NUDT7* after induction of various stresses (abiotic, biotic and chemotoxic stress).

(B) Quantitative real-time PCR to determine transcript levels of *NUDT7* and *EDS1* in Col-0 wt, *nudt7-1* and *eds1-2*. Total RNA was extracted from 4-week-old soil-grown plants and ubiquitin was used for normalization. Error bars represent standard error ($n = 3$). Experiment was repeated at least three times with similar results.

(C) Total protein extracts of indicated genotypes of 4-week-old soil-grown plants. Samples were probed with *NUDT7* and *EDS1* antibodies to determine protein levels. Note that *NUDT7* Western blot is overexposed for Col-0 sample to be able to detect signal in *eds1-2* sample. Similar results were observed in at least three independent experiments.

NUDT7 and *EDS1* transcripts were expressed at a similar level in WT (Figure 3.3B). In the *nudt7-1* mutant, *EDS1* transcripts were upregulated. By contrast, *NUDT7* transcript levels were only slightly elevated in *eds1-2* compared to Col-0. Elevated *EDS1* transcript levels in *nudt7-1* were reflected by a moderate increase in EDS1 protein accumulation (Figure 3.3C). *NUDT7* showed strongly depleted protein levels in the *eds1-2* mutant background. This result clearly shows that *NUDT7* has a negative impact on the expression of *EDS1*. *EDS1* seems to be required for post-translational accumulation of *NUDT7* protein rather than acting on *NUDT7* gene expression.

To assess the possibility of a direct interaction of EDS1 and *NUDT7*, I performed immunoprecipitations (IP) using the *NUDT7* OE line 4 (see section 3.1.2). Although I concluded that over expressed *NUDT7*-strepII fusion protein was only partially functional, this line was considered to express sufficient amounts of functional transgenic *NUDT7* for co-IP studies since OE line 4 complemented the *nudt7-1* phenotype to WT levels (Figure 3.2).

The strepII affinity purification is a rapid one step purification (Witte et al., 2004). Using this fast purification procedure would increase the likelihood of co-purifying transiently bound interactors. Furthermore, this method has been successfully established for analysis of proteins derived from leaf tissue (Witte et al., 2004).

For StrepII affinity purification, I used unchallenged leaf tissue from *NUDT7* OE line 4. In parallel, I processed tissue from Col-0 WT and *nudt7-1* plants that served as negative controls. The collected fractions were separated by SDS-PAGE and analyzed by immunoblotting. Ponceau staining of the western blot membrane revealed a single band in the concentrated eluate and the boil-off (BO) from the StrepTactin sepharose that corresponds with the predicted size of *NUDT7*-strepII (Figure 3.4A). This result indicated that *NUDT7*-strepII was successfully purified. A potential interaction of *NUDT7* and EDS1 was analyzed by probing the different fractions with α -*NUDT7* and α -EDS1 antibody. *NUDT7* protein was detected in the input fractions of WT and *NUDT7* OE line 4 and in the eluate fractions of *NUDT7* OE line 4 (Figure 3.4B). By contrast, EDS1 was only detectable in the input and in the flow through fractions of *NUDT7* OE line 4. Therefore, this result suggests that *NUDT7* and EDS1 do not directly interact with each other.

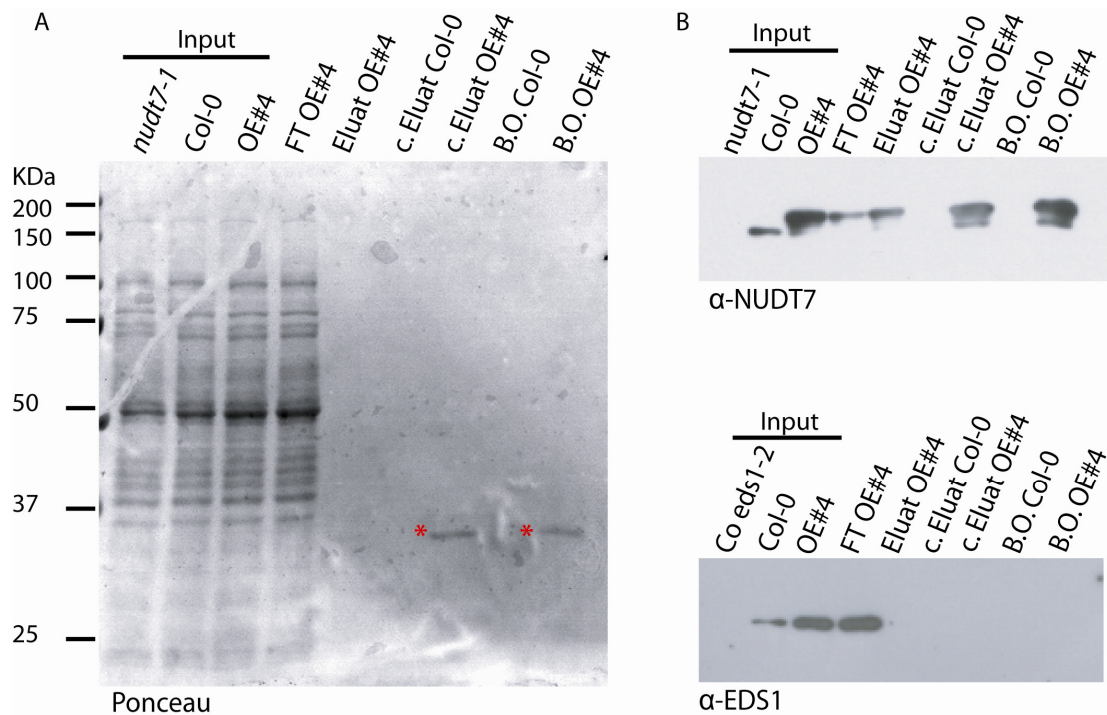


Figure 3.4: StrepII affinity purification from NUDT7 OE line 4 to detect potential interaction between NUDT7 and EDS1

(A) Analysis of StrepII purification by Ponceau staining. The different fractions collected during the purification procedure were separated by SDS-PAGE and analyzed by Ponceau staining and on an immunoblot using α -NUDT7 and α -EDS1 antibodies. Soluble extracts were prepared using StrepII extraction buffer from unchallenged leaf tissue of 4-week-old Col-0, *nudt7-1* and NUDT7 OE line 4 plants (Input). Extracts were incubated with StrepTactin sepharose and unbound fractions were collected (flow through (FT)). After washing steps, bound protein was eluted four times with 100 μ l elution buffer. 40 μ l of the eluate was mixed with 2x SDS-loading buffer (Eluate) and 360 μ l were concentrated using Vivaspin500 (c. Eluate). After elution, SDS-loading buffer was added to StrepTactin sepharose and boiled for 5min at 96°C (B.O.). NUDT7-strepII is indicated by red asterisks. **(B)** Immunoblot analysis of StrepII purification. All fractions were analyzed using α -NUDT7 (upper Western blot) and α -EDS1 (lower Western blot) antibodies. Western blot analysed with α -NUDT7 corresponds to Ponceau staining shown in (A). Experiment was repeated two times with similar results.

Final confirmation can be obtained by IPs using α -NUDT7 and α -EDS1 to purify the respective protein in WT plants and testing for co-purification of EDS1 and NUDT7, respectively.

Together, these analyses point to an indirect regulation of *EDS1* and *NUDT7* by which *EDS1* is promoting either the synthesis or the stabilization of a negative regulator of the EDS1 pathway in healthy leaf tissues.

3.2.2. *NUDT7* transcript and protein are upregulated in response to avirulent bacteria

NUDT7 was identified in a gene expression micro array experiment as being upregulated after *Pst AvrRPS4* inoculation in an *EDSI*-dependent manner (Bartsch et al., 2006). The same experiment revealed a strong upregulation of *NUDT7* after inoculation with *Pst AvrRPM1* that was largely independent of *EDSI*. *AvrRPS4* is recognized by *RPS4* in an *EDSI*-dependent TIR-NBS-LRR *Avr* protein interaction (Wirthmüller et al., 2007). *AvrRPM1* that is detected by the CC-NBS-LRR protein *RPM1* (Mackey et al., 2002) induces resistance independent of *EDSI* (Aarts et al., 1998). In order to gain more information on the *NUDT7* response to pathogen infection, I performed time course experiments. Col-0 WT plants were infected either with *Pst AvrRPS4* or *Pst AvrRPM1* and samples were taken at 0, 3, 6, 12 and 24 hour (h) time points after infection. Controls were infiltrated with 10mM $MgCl_2$ and samples were taken at the indicated time points.

After infection with *Pst AvrRPS4*, *NUDT7* transcripts were strongly upregulated 9 h post inoculation (hpi) (Figure 3.5A). Transcript levels declined again and reached similar levels after 24 hpi as at 0 hpi. In consistency with transcript upregulation, *NUDT7* protein accumulation peaked at 9 hpi and correlated with reduction of transcripts at 12 and 24 hpi (Figure 3.5B). $MgCl_2$ infiltration did not cause significant increases in *NUDT7* transcript or protein levels (Supplemental Figure 1A and 1B). In response to *Pst AvrRPM1* inoculation, *NUDT7* transcripts were strongly induced 3 hpi and 6 hpi (Figure 3.5A). At later time points, transcript levels decreased to 0 hpi levels. Although *NUDT7* protein was also upregulated 3 hpi, *NUDT7* protein accumulation was not consistent with *NUDT7* transcript reduction (Figure 3.5B). I found similar levels of *NUDT7* protein at 6, 9 and 12 hpi that were reduced at 24 hpi. Control samples infiltrated with 10mM $MgCl_2$ showed no induction of *NUDT7* transcript and protein (Supplemental Figure 1A and 1B).

I also explored whether *NUDT7* upregulation coincides with pathogen-induced cell death. Coincidence of *NUDT7* upregulation and induction of cell death would support the suggested role for *NUDT7* in cell death regulation.

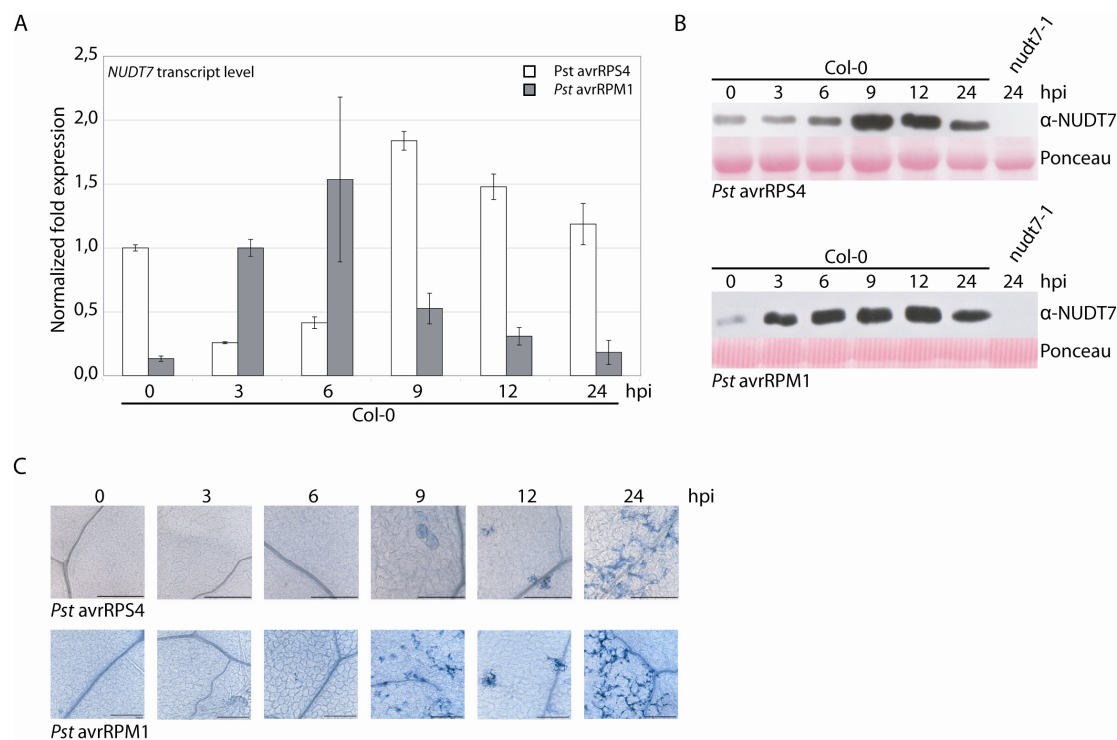


Figure 3.5: Regulation of *NUDT7* transcript and protein levels and appearance of cell death in response to avirulent *P. syringae* infection.

(A) *NUDT7* mRNA is upregulated after infection with both, *Pst avrRPS4* or *Pst avrRPM1*. 4-week-old plants were vacuum-infiltrated with 5×10^7 colony forming units (cfu) of the respective *Pst* strain. Leaf material was collected at the indicated time points and total RNA was extracted. Transcript levels were determined by quantitative real-time PCR using *UBC21* (*Ubiquitin Conjugating Enzyme 21*) as reference gene. Error bars represent standard deviation (SD). Infection experiments were repeated three times with similar results. The results of one experiment after infection with the respective pathogen are shown.

(B) *NUDT7* protein follows upregulation of mRNA after infection with *Pst* strains. Leaf material was harvested after indicated time points and total protein was extracted. *NUDT7* protein was analysed on a Western blot with α -*NUDT7* antibody. Ponceau staining served as loading control.

(C) Appearance of cell death coincides with *NUDT7* mRNA upregulation. 3-5 leaves were taken at indicated time points after inoculation and stained with trypan blue to detect plant cell death. Bars = 200 μ m.

Plant cell death monitored by trypan blue staining appeared 9 hpi with *Pst avrRPS4* and therefore coincided with *NUDT7* upregulation (Figure 3.5C). Initial cell death in response to *Pst avrRPM1* inoculation was detected 6 hpi which was 3 hours later than *NUDT7* transcript and protein induction. Induction of plant cell death was not detected upon $MgCl_2$ infiltration (Supplemental Figure 1C).

These data show that *NUDT7* expression responds to both, TIR-NBS-LRR and CC-NBS-LRR triggered plant defence. Furthermore, the results obtained after infection

with *Pst AvrRPM1* support the data shown in Figure 3.3A and 3.3B suggesting a post-transcriptional regulation of NUDT7 protein. It will require further analysis whether the difference in NUDT7 protein accumulation and cell death induction in response to *Pst AvrRPS4* and *Pst AvrRPM1* can be correlated to the distinct functions of *EDS1* upon AvrRPS4 and AvrRPM1 triggers.

3.2.3. NUDT7 localization is not altered upon pathogen challenge

The *in vivo* function of NUDT7 is unknown. Also, the localization of NUDT7 is predicted as being cytosolic (Ogawa et al., 2005) but has not been shown *in vivo*. I investigated where NUDT7 protein is localized *in vivo* and whether its localization changes after pathogen infection since the subcellular localization of NUDT7 could allow conclusion about its activity. I performed nuclear and microsomal fractionations with healthy and *Pst avrRPM1* challenged plant material. NUDT7 was present in the nuclear-depleted but not in the nuclear fraction independent of pathogen challenge (Figure 3.6A). Moreover, NUDT7 protein fractionated in the soluble pool in both, healthy and pathogen-infected plants (Figure 3.6B). There was no NUDT7 protein detectable in the microsomal fractions. I concluded that NUDT7 is soluble and localizes exclusively to the cytosol.

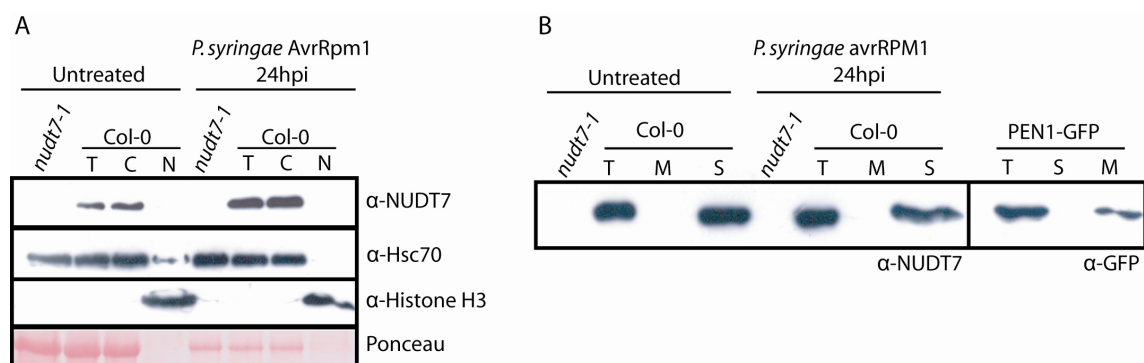


Figure 3.6: Localization studies of NUDT7 protein in healthy and pathogen-infected leaf tissue.

(A) NUDT7 protein localizes to the cytosol. Healthy and pathogen-infected plant tissue was separated into nuclei and nuclei-depleted fractions. Infections with *Pst avrRPM1* were performed as described under (2A). T = Total fraction; C = Cytosolic fraction; N = Nuclear fraction. Fractions were probed with indicated antibodies. Hsc70 served as cytosolic control and HistoneH3 as nuclear control. Experiment was repeated at least three times with the same result.

(B) NUDT7 protein is exclusively soluble. Separation of healthy and pathogen-infected leaf tissue of indicated genotypes into soluble and microsomal fractions by ultracentrifugation. PEN1-GFP was co-purified in the same experiment and served as a microsomal marker. T = Total fraction; M = Microsomal fraction; S = Soluble fraction. Fractions were analysed by immunoblotting with α -NUDT7 and α -GFP antibody. Experiment was repeated three times with the same result.

3.3. Impact of defence-related mutants on the *nudt7-1* phenotype

3.3.1. EDS1 triggers an SA-antagonized defence pathway

Arabidopsis nudt7-1 mutant plants exhibit an exacerbated growth retardation and cell death phenotype when depleted of salicylic acid (SA) in the *nudt7-1/sid2-1* mutant (Figure 3.7) (Bartsch et al., 2006). It was unknown whether this SA-antagonized phenotype requires *EDS1*. I tested this hypothesis by crossing the *eds1-2* mutation into the *nudt7-1/sid2-1* mutant background. The enhanced growth retardation caused by SA depletion (Figure 3.7A and 3.7B) and exacerbated cell death (Figure 3.7C) of *nudt7-1/sid2-1* were suppressed in *nudt7-1/sid2-1/eds1-2* and restored to Col-0 WT levels. Enhanced susceptibility towards virulent *H. parasitica* NOCO2 was not altered in *nudt7-1/sid2-1/eds1-2* plants compared to *nudt7-1/sid2-1* (Figure 3.7D).

Thus, *EDS1* mediates two distinct signalling events that are both negatively regulated by *NUDT7*. *EDS1* induces the accumulation of SA and induces a positive feedback-loop through which it promotes its own expression leading to further activation of defence responses (Feys et al., 2001). In addition, *EDS1* triggers a pathway that is negatively regulated by SA leading to the initiation of cell death and suppression of growth. The results shown in Figure 3.7D provide further evidence for the requirement of SA in basal resistance and positioning of SA accumulation downstream of *EDS1*.

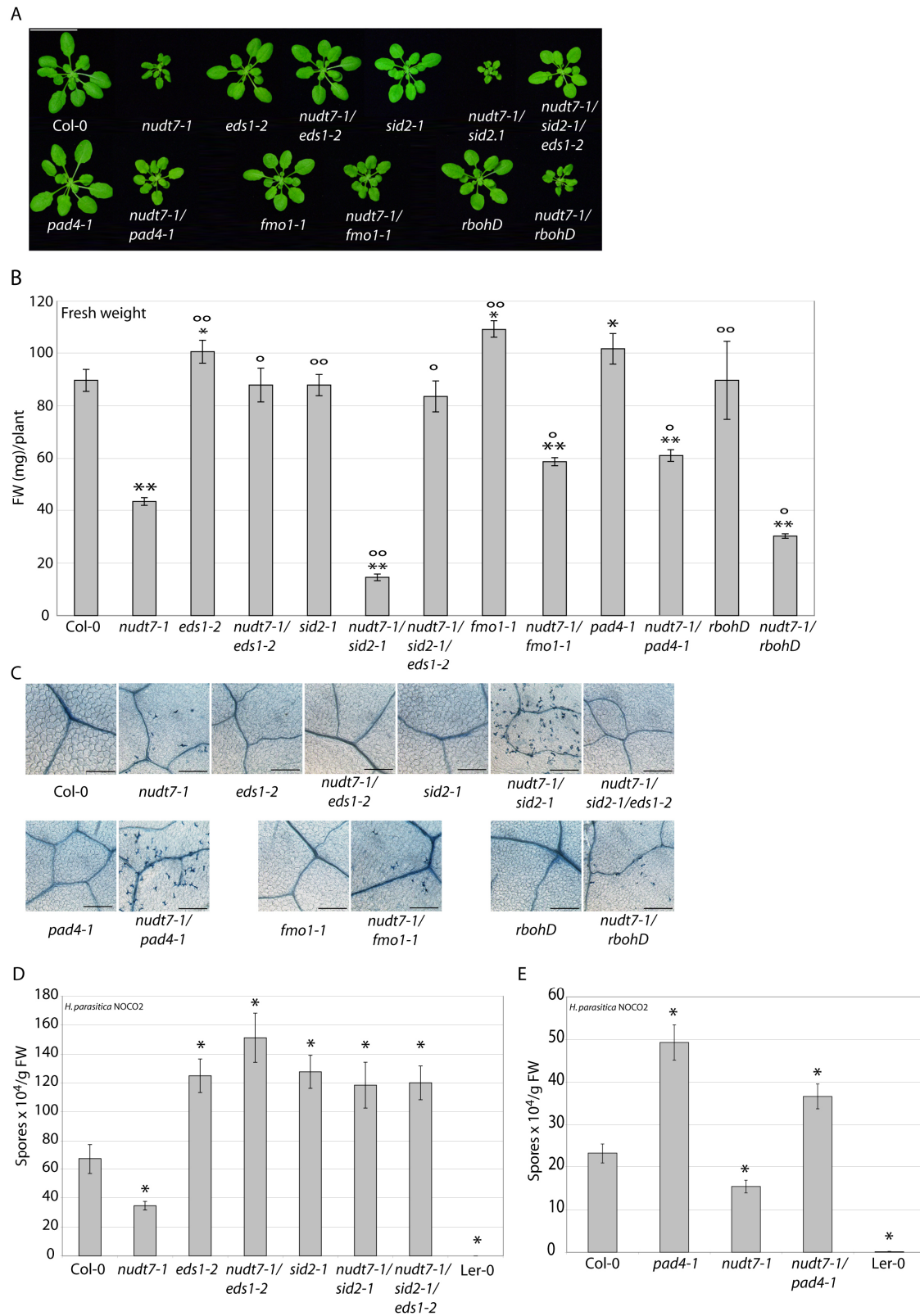


Figure 3.7: Analysis of the impact of defence mutants on the *nudt7-1* phenotype

(A) The *eds1-2* mutation abolishes growth retardation of *nudt7-1*. Pictures are representative of mutant phenotypes of 4-week-old soil-grown plants. Bar = 3cm.

(B) Fresh weight (FW) analysis of 4-week-old-soil-grown plants. Error bars represent standard error (SE) (n=9). * $p < 0,05$, ** $p < 0,001$ (student's t-test for pairwise comparison of wt and different mutants); ° $p < 0,01$, °° $p < 0,0001$ (student's t-test for pairwise comparison of *nudt7-1* and different mutants). Experiment was repeated at least three times with similar results.

(C) Spontaneous leaf cell death in the *nudt7-1* mutant background depends only on *EDS1*. Leaves of 4-week-old plants were stained with trypan blue to detect cell death. Three leaves per genotype were stained and the experiment was repeated at least three times with the same results.

(D) Enhanced basal resistance in *nudt7-1* depends on SA and *EDS1*. 2-week old plants were inoculated with *H. parasitica* NOCO2 with 4×10^4 spores/ml. Sporulation on plants was analysed five days post inoculation with a Neubauer counting chamber. Error bars represent SE (n=3). * $p < 0,055$ (student's t-test for pairwise comparison of wt and mutants). Experiment was repeated at least three times with similar results.

(E) *pad4-1* compromises enhanced basal resistance of *nudt7-1*. Inoculation was performed as described under (D). Error bars represent SE (n=3). * $p < 0,05$ (student's t-test for pairwise comparison of wt and mutants). Experiment was repeated at least three times with similar result.

3.3.2. The *nudt7-1* phenotype is influenced by other defence mutations

PAD4 is an interaction partner of EDS1 and required to mount an adequate defence response to virulent pathogens (Zhou et al., 1998; Feys et al., 2001). Genetic epistasis analysis revealed that *PAD4* and *EDS1* are required for SA-dependent defence signalling (Brodersen et al., 2002). This is reinforced by the fact that *pad4* mutants fail to accumulate SA after infection with virulent and avirulent *Pst* that trigger EDS1-dependent resistance (Feys et al., 2001). The close relationship between *EDS1* and *PAD4* prompted me to investigate whether the *pad4* mutation abrogates the *nudt7-1* phenotype as the *eds1* mutation does. For this reason I crossed *nudt7-1* with *pad4-1* to generate the *nudt7-1/pad4-1* double mutant. Growth analysis revealed that *nudt7-1/pad4-1* plants exhibit intermediate growth between *nudt7-1* and WT (Figure 3.7A and 3.7B). Enhanced basal resistance of the *nudt7-1* mutant was abrogated by the *pad4-1* mutation (Figure 3.7E). *Nudt7-1/pad4-1* plants were more susceptible than WT but less susceptible compared to *pad4-1*. These results suggest that *PAD4* affects different signalling events leading to the *nudt7-1* phenotype. Whether the intermediate phenotype of *nudt7-1/pad4-1* mutant is the direct result of the *pad4-1* mutation or an indirect consequence of a possible disturbed interaction between *EDS1* and *PAD4* is not clear. Significantly, *nudt7-1/pad4-1* plants showed an exacerbated cell death phenotype similar to *nudt7-1/sid2-1* mutants (Figure 3.7C). Also, SA levels were depleted in the *nudt7-1/pad4-1* mutant (M. Bartsch and J. Parker, unpublished data).

Thus, reduced SA levels in the *nudt7-1/pad4-1* mutant likely account for the enhanced cell death phenotype.

FMO1 (*Flavin-Dependent Mono-oxygenase*) was identified in the same gene expression microarray experiment as *NUDT7* and was shown to be upregulated in an *EDS1*-dependent manner after inoculation with *Pst avrRPS4* and *Pst avrRPM1* (Bartsch et al., 2006). Defects in *FMO1* compromise basal resistance, TIR-NBS-LRR triggered resistance and systemic acquired resistance (SAR) (Bartsch et al., 2006; Koch et al., 2006; Mishina and Zeier, 2006). Further analysis suggested a role for *FMO1* in an *EDS1*-regulated but SA-independent pathway that mediates resistance and promotes cell death at pathogen infection sites (Bartsch et al. 2006; Mishina and Zeier, 2006). By contrast, systemic induction of *FMO1* requires SA and is impaired in SAR-deficient SA pathway mutants (Mishina and Zeier, 2006).

I assessed whether the *fmo1* mutation alters *EDS1*-dependent growth, cell death and basal resistance phenotype of the *nudt7-1* mutant. The *nudt7-1/fmo1-1* mutant exhibited intermediate growth between *nudt7-1* and wt (Figure 3.7A and 3.7B). By contrast, the *fmo1-1* mutation did not alter *nudt7-1* cell death (Figure 3.7C) or basal resistance phenotypes (data not shown). I concluded from this that the positive regulatory role of *FMO1* on *EDS1*-mediated resistance has only a minor effect on signalling events causing the *nudt7-1* phenotype.

The NADPH oxidase *AtRbohD* was shown to negatively regulate SA-induced cell death in the *lsd1* mutant (Torres et al., 2005). Cell death in the *nudt7-1* mutants seems not to be caused but rather negatively regulated by SA. Therefore I tested whether *AtRbohD* affects SA-independent cell death in *nudt7-1*. I found that the *rbohD* mutation exacerbated *nudt7-1* growth retardation (Figure 3.7A and 3.7B) but had no effect on the spontaneous leaf cell death phenotype (Figure 3.7C). Thus, *AtrbohD* is not involved in signalling events leading to cell death in the *nudt7-1* mutant.

3.4. The roles of *EDS1* and *NUDT7* in basal resistance and oxidative stress responses

3.4.1. *Nudt7-1* growth retardation is abolished under sterile conditions

The study from Bartsch et al. (2006) and results presented in here led to the conclusion that deregulated *EDS1*-signalling likely causes the *nudt7-1* phenotype. In *nudt7-1* plants, the *EDS1* pathway could then either be constitutively active or require an external trigger leading to deregulated defence signalling. I tested whether constitutive *EDS1*-signalling results in *nudt7-1* growth retardation by growing plants under sterile conditions. Growth of 4-week-old sterile grown *nudt7-1* plants was not different compared to WT plants (Figure 3.8).

I concluded that *EDS1*-dependent growth retardation of *nudt7-1* plants required an external trigger. This is supported by a recent study showing that under certain growth conditions *nudt7* plants also exhibit a WT-like growth on soil (Ge et al., 2007).

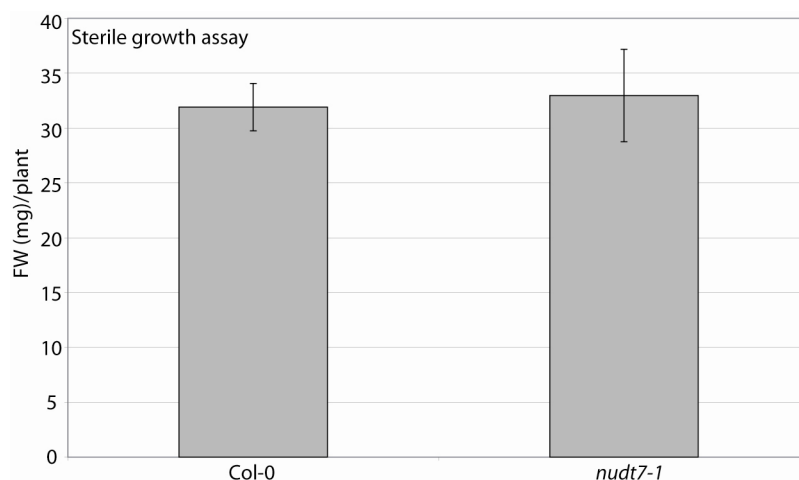


Figure 3.8: Col-0 and *nudt7-1* plant growth under sterile conditions

Growth retardation observed for soil-grown *nudt7-1* plants is abrogated under sterile conditions. Plants were grown for four weeks under sterile conditions on MS-medium. Fresh weight of nine plants per genotype was measured and experiment was repeated at least three times with similar results. Error bars represent SE (n=9).

3.4.2. *Nudt7-1* mutant plants are not hyper-responsive to the MAMP flg22

Perception of highly-conserved microbial molecules like bacterial flagellin or elongation factor Tu (EF-Tu) by pattern recognition receptors leads to the activation of a pre-invasive defence mechanism called PAMP (pathogen-associated molecular

patterns)-triggered immunity (PTI) (hereafter referred to as MAMP (microbe-associated molecular pattern)-triggered immunity (MTI)) (Jones and Dangl, 2006). Recently, it was reported that *NUDT7* transcripts are up-regulated in response to flagellin and that mRNA levels of the pathogen inducible genes *PRI* (*PATHOGENESIS-RELATED 1*) and *AIG1* (*AVRRPT2-INDUCED GENE 1*) increased in the *nudt7* mutant after treatment with several MAMPs (Ge et al., 2007; Adams-Phillips et al., 2008).

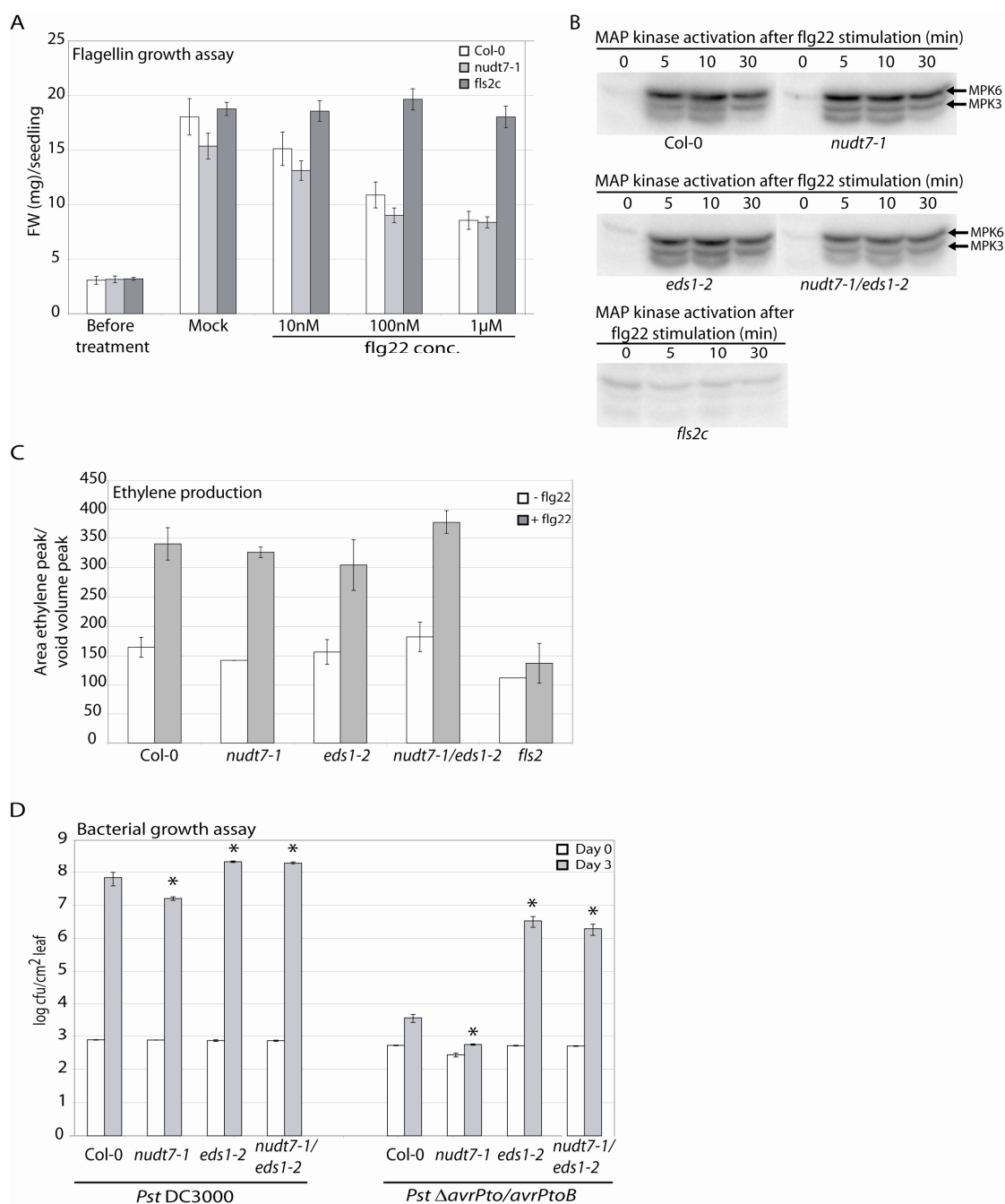


Figure 3.9: Response of *nudt7-1* mutants after induction of MAMP-triggered immunity.

(A) *nudt7-1* mutant plants are not hyper-responsive to flg22. To determine growth inhibition after flg22 stimulation, seedlings were grown for seven days on MS-plates before transferring into liquid MS medium with different concentrations of flg22 or only MS-medium (Mock). After seven days of treatment, the fresh weight of the seedlings was measured. Error bars represent SE (n=24). Experiment was repeated at least 3 times with similar results.

(B) In-gel MAP kinase assay to investigate the activation of MPK6 (upper band) and MPK3 (middle band) in response to flg22 stimulation. Sterile grown seedlings have been stimulated with 1 μ M flg22 and total protein was subsequently extracted after indicated time points. Samples were separated on a SDS-PAGE gel containing myelin basic protein as MAPK substrate. After renaturation, an in-gel MAP kinase assay was performed and kinase activity was visualized by autoradiography. Experiment was repeated twice with similar results.

(C) Ethylene production in response to flg22 stimulation. Leaf discs of 4-week-old soil-grown plants were incubated either with or without 1 μ M flg22 in hermetic vials for 4 hours. Ethylene production was measured subsequently by gas chromatography and displayed by the ratio of the ethylene peak area to void volume peak area. Similar results were obtained in three independent experiments.

(D) *EDS1* triggers enhanced basal resistance in *nudt7-1* mutant plants. *Pst* DC3000 or the weakly virulent *Pst* Δ Pto/PtoB was sprayed onto leaves of 4-week-old plants of the indicated genotypes at 1×10^8 cfu/ml. Bacterial growth (cfu/cm²) was determined 3h (white bars) and 3 days (grey bars) after infection. Error bars represent SE (n=3). *p < 0,05 (Student's t-test for pairwise comparison of wildtype and mutant). Similar result was observed in at least three independent experiments.

This suggests an involvement of *NUDT7* in MAMP-triggered pre-invasive resistance. However, *nudt7* plants exhibit an increased basal resistance that occurs at a post-invasive level after infection with a virulent isolate of the oomycete *H. parasitica* that will have largely suppressed MTI (Bartsch et al., 2006; Ge et al., 2008; Jambunathan and Mahalingam, 2006). While *EDS1* is a key regulator of post-invasive defence responses (Aarts et al., 1998; Feys et al., 2001) no substantial *EDS1* contribution has been found in pre-invasive resistance, although it is transcriptionally upregulated after flagellin treatment (Zipfel et al., 2004).

In order to assess whether the enhanced basal resistance of *nudt7-1* plants occurs at a pre-invasive or a post-invasive level and whether this depends on *EDS1*, I treated plants with flagellin to test for enhanced MTI in *nudt7-1*. I first investigated whether the reduction of growth in *nudt7-1* plants is caused by a hyper-responsiveness to pathogens or MAMPs to which the plants are exposed when grown on soil.

Perception of the 22-amino acid peptide flg22 derived from the bacterial elicitor flagellin leads to a significant growth retardation of Col-0 plants (Gomez-Gomez et al., 1999). To investigate if *nudt7-1* plants exhibit an increased growth retardation to

flg22 treatment I incubated sterile grown Col-0, *nudt7-1* and *fls2* (flagellin receptor mutant used as negative control) plants with different concentrations of flg22 and analyzed their fresh weight. While a clear dose-responsiveness was observed, none of the applied flg22 concentrations led to a higher growth retardation of *nudt7-1* mutant plants compared to Col-0 WT plants (Figure 3.9A). Therefore I concluded that the decreased growth of *nudt7-1* plants is unlikely to be caused by a hyper-responsiveness to MAMPs.

Although flg22 treatment did not lead to increased growth retardation of *nudt7-1* compared to WT, differences between Col-0 and *nudt7-1* in MAMP-triggered signalling could be more subtle. Therefore I investigated early events induced by flg22 perception. To see if potential changes in the signalling cascade after flg22 perception also involve *EDS1* I included the *eds1-2* and *nudt7-1/eds1-2* mutant plants in these experiments.

An early event in MAMP signalling after flg22 perception is the rapid activation of a MAP kinase cascade including MPK3 and MPK6 (Nühse et al., 2000; Asai et al., 2002). I tested whether activation of MPK3 and MPK6 was altered in sterile grown *nudt7-1* and *eds1-2* mutant plants after flg22 stimulation. In all genotypes tested, except for *fls2* that served as negative control, I found similar activation of the MAP kinases 3 and 6. Thus, no differences were observed in the activation pattern of Col-0, *eds1-2* and *nudt7-1* mutants, respectively (Figure 3.9B).

The production of ethylene and the induction of an oxidative burst are two other early down-stream responses after flagellin perception (Bauer et al., 2001; Felix et al., 1999; Gomez-Gomez et al., 1999). I measured the production of ethylene in response to flg22 in leaves of 4-week-old soil-grown plants (Figure 3.9C) and the induction of an oxidative burst after stimulation of sterile grown seedlings with flg22 (data not shown). In all of these assays the *nudt7-1* and the *eds1-2* mutants responded in the same way as Col-0 WT. I concluded that neither *EDS1* nor *NUDT7* are involved in MAMP-triggered signalling after the perception of flg22.

Although flg22 treatment did not result in altered responses in *nudt7-1* plants compared to WT, there is still the possibility of primed MTI in *nudt7-1* that confers enhanced resistance. I tested this hypothesis by two different experiments. First, I infected plants with a fully virulent *Pst* strain to investigate whether *nudt7-1* plants are more resistant compared to wt. In a second experiment, plants were inoculated with a virulent *Pst* strain that lacks the effectors *avrPto* and *avrPtoB* and that suppresses the

MTI response less than *Pst* DC3000 (Lin et al., 2005). If *nudt7-1* plants exhibit primed MTI, bacterial growth of a less virulent *Pst* strain in wt and *nudt7-1* plants should be more similar due to the strongly impaired suppression of MTI. In both experiments, bacteria were applied to the leaf surface since studies on the *fls2* mutant revealed that direct infiltration into intercellular space presumably by-passes initial steps of bacterial infection that are required to induce MTI (Zipfel et al., 2004).

I infected 4-week-old soil-grown *nudt7-1* and *eds1-2* mutant plants by spraying virulent *P. syringae* DC3000 onto the leaves. Bacterial growth was determined after 0 and 3 days (Figure 3.9D, left panel). *Nudt7-1* mutant plants showed significantly less bacterial growth compared to Col-0 WT whereas mutant plants in the *eds1-2* background were hyper susceptible. Infection with *Pst* Δ *avrPto/avrPtoB* was performed as with *Pst* DC3000 and resulted in reduced bacterial growth in all genotypes compared to *Pst* DC3000 infection (Figure 3.9D, right panel). Growth of both strains was approximately one log less in *nudt7-1* compared to WT (Figure 3.9D). Also, growth of *Pst* Δ *avrPto/avrPtoB* in the *eds1-2* mutants was still higher than in Col-0 WT but less than compared to *eds1-2* mutant plants infected with *Pst* DC3000.

I concluded that less efficient suppression of MTI by the *Pst* Δ *avrPto/avrPtoB* strain accounts for the reduced growth in all tested genotypes. Similar differences of bacterial growth between WT and *nudt7-1* after inoculation with both strains suggest that enhanced resistance in *nudt7-1* plants does not rely on primed MTI but on enhanced post-invasive basal resistance that is *EDSI*-dependent.

3.4.3. *Nudt7-1* plants are rendered hyper susceptible towards oxidative stress by *EDSI*-mediated signals

Previous reports implicate *EDSI* in oxidative stress signalling, most clearly after induction of photo-oxidative stress. For example, *EDSI* is required to trigger runaway cell death and stomatal conductance in *lsd1* mutants that fail to acclimate to EEE and experience chloroplastic ROS overload (Rusterucci et al., 2001; Mateo et al., 2004). Further analysis revealed that *EDSI* acts upstream of ROS (H₂O₂) accumulation and regulates signalling events leading to programmed cell death and light acclimation (Mühlenbock et al., 2008). Also, it has been shown that *EDSI* is upregulated after release of singlet oxygen in chloroplasts of the *flu* mutant in an SA-independent

manner (Ochsenbein et al., 2006). *EDSI* promotes the spread of necrotic lesions and prevents the recovery of *flu* mutants from singlet oxygen stress.

It was reported recently by others that *nudt7* plants have normal growth but become stunted after induction of oxidative stress by paraquat (Ge et al., 2007). Paraquat inhibits ferredoxin reduction in PS I and, by subsequent auto-oxidation into a radical, leads to the production of superoxide and H_2O_2 (Babbs et al., 1989). By contrast, I found that soil-grown *nudt7-1* plants under normal conditions exhibited stunting compared to WT and accumulated high levels of H_2O_2 without external induction of oxidative stress (Figure 3.10). I reasoned that the soil induces oxidative stress causing the growth retardation of *nudt7-1* mutant plants. Therefore, I grew plants on commercial medium (jiffy-7 soil pellets; Jiffy International AS, Denmark). Growing *nudt7-1* plants on jiffy soil pellets reduced the extent of leaf curling and growth stunting (Figure 3.10). In addition, spontaneous leaf cell death was strongly reduced and H_2O_2 accumulation was abrogated.

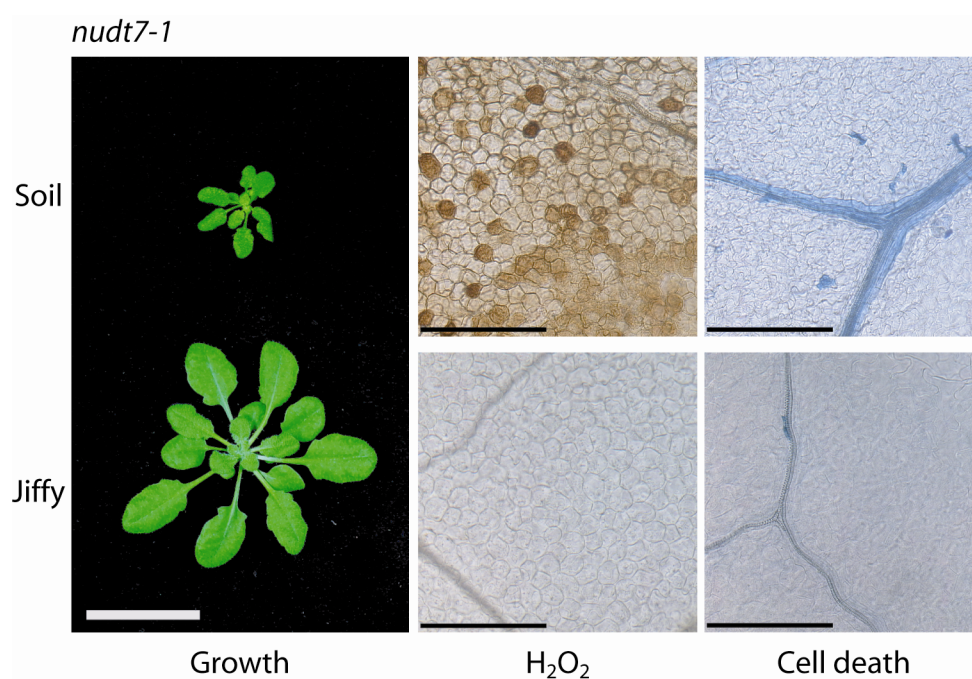


Figure 3.10: Phenotypes exhibited by *nudt7-1* on different soils

Nudt7-1 plants were grown on soil and commercial jiffy soil for four and five weeks, respectively. Leaves were stained with 3,3-Diaminobenzidine to detect H_2O_2 accumulations (middle panel) and with trypan blue to detect cell death (right panel). White bar (left panel) = 3cm; Black bar (middle and right panel) = 200 μ m. Pictures are representative for observed differences of *nudt7-1* plants grown on the respective soils.

In order to test whether the phenotype observed on soil-grown *nudt7-1* plants could be induced and whether this requires *EDS1*-mediated oxidative stress signalling, I applied paraquat at a mild dosage of 5 μ M multiple times over a period of 12 days. Application of paraquat led to a severe growth retardation of *nudt7-1* plants compared to Col-0 WT plants; the observed developmental phenotype was similar to the one displayed by soil-grown plants (Figure 3.11A and 3.11B).

By contrast, *eds1-2* and *nudt7-1/eds1-2* mutants plants did not show significant growth retardation after paraquat treatment (Figure 3.11A and 3.11B). When the induction of cell death after paraquat treatment was determined, there was a strong induction in the *nudt7-1* mutant compared to Col-0 WT that was suppressed in the *nudt7-1/eds1-2* double mutant (Figure 3.11C). Cell death was quantified by trypan blue staining to detect plant cell death in leaves and subsequent counting of dead cells per mm² in representative leaf areas. Detection of H₂O₂ by DAB (3,3 Diaminobenzidine) stainings revealed high accumulation of H₂O₂ in *nudt7-1* that were abolished in the *nudt7-1/eds1-2* double mutant (Figure 3.11D). H₂O₂ accumulation in paraquat-treated *nudt7-1* plants are also comparable to the levels exhibited by soil-grown *nudt7-1* plants (Figure 3.10, Figure 3.11D).

I concluded from these data that the *nudt7-1* phenotype observed on soil-grown plants seems to be caused by oxidative stress that is induced by de-regulated *EDS1*-dependent defence signalling. Moreover, these findings support a role of *EDS1* in oxidative stress signalling leading to the accumulation of ROS and the induction of cell death.

I tested whether the oxidative stress response is correlated with protein levels of *EDS1* and *NUDT7*. Steady state levels of *EDS1* protein after oxidative stress induction were higher in both WT and *nudt7-1* compared to steady state levels in untreated plants (Figure 3.12A). By contrast, *NUDT7* protein levels did not increase in response to oxidative stress in WT but in the *eds1-2* mutant.

Together, these data suggest that the *nudt7* mutant lowers the threshold for *EDS1*-dependent responses to oxidative stress and pathogens.

I also tested whether oxidative stress induction affects the subcellular localization of *NUDT7* or leads to changes in the nuclear pool of *EDS1* as pathogen infection does (A. Garcia and J. Parker, unpublished data). Paraquat application did not lead to an obvious change in subcellular localization of *NUDT7* and did not result in measurable

changes in the nuclear pool of EDS1 (Supplemental Figure 2; A. Garcia and J. Parker, unpublished data).

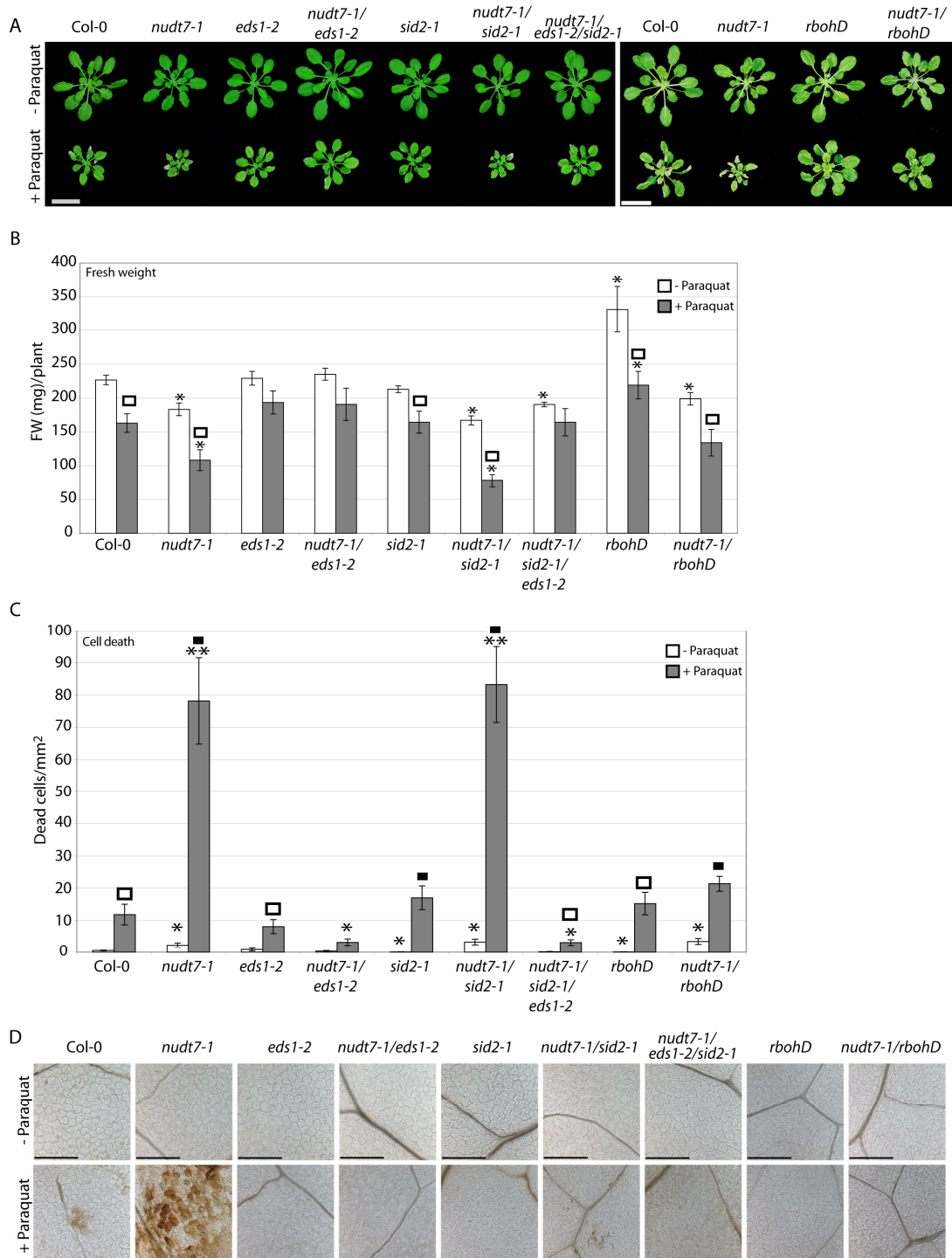


Figure 3.11: Oxidative stress responses of different *nudt7-1* mutants and their dependence on *EDS1* and SA.

(A) Application of paraquat leads to a growth retardation of Col-0 plants that is exacerbated in the *nudt7-1* mutant background. Plants were grown for three weeks on commercial medium (Jiffy[®]-soil) and then sprayed with 5 μ M paraquat three times at an interval of 4 days. Representative pictures were taken 4 days after the last paraquat application. The experiment was repeated independently at least three times with similar results. Bar = 3cm.

(B) Quantification of plant growth +/- paraquat. Mean FW and SE values (n=27) were calculated from the results of three independent experiments. \square p < 0,05 (student's t-test for pairwise comparison of nontreated and treated plants); *p < 0,05 (student's t-test for pairwise comparisons of respective WT and mutant).

(C) Exacerbated cell death in *nudt7-1* in response to paraquat requires *EDS1* and *AtRbohD* but not SA. Quantification of cell death +/- paraquat. Dead cells were counted on a representative area in five leaves/genotype. Observed cell death was single dead cells as shown in Figure 5C. Mean and SE values (n=15) were calculated from the results of three independent experiments. \square p < 0,005, \blacksquare p < 0,0001 (Student's t-test for pairwise comparison of nontreated and treated plants); *p < 0,02, **p < 0,001 (Student's t-test for pairwise comparisons of respective WT and mutant).

(D) H₂O₂ accumulation in *nudt7-1* after paraquat treatment depends on *EDS1*, SA and *AtRbohD*. After treatment as described under (A), 3-5 leaves per genotype were stained with 3,3-Diaminobenzidine (DAB) to detect H₂O₂. Bars = 200 μ m. Experiment was repeated multiple times with similar results.

3.4.4. SA promotes H₂O₂ accumulation but has no effect on the induction of cell death in response to paraquat application

Nudt7-1 plants possess high levels of SA (Bartsch et al., 2006) and SA has been shown to regulate H₂O₂ production in the chloroplast (Mateo et al., 2004, 2006). Moreover, SA depletion exacerbates *EDS1*-dependent initiation of cell death and growth retardation of *nudt7-1* plants, as shown in Figure 3.7. To investigate whether SA suppresses *EDS1*-dependent cell death by modulating chloroplastic ROS, I tested the response to external induction of oxidative stress of *nudt7-1/sid2-1* and *nudt7-1/sid2-1/eds1-2* mutants.

Paraquat treatment led to a similar growth reduction of *nudt7-1/sid2-1* and *nudt7-1* plants that was abolished in the *eds1-2* mutant background. By contrast, *sid2-1* mutant plants behaved like Col-0 WT (Figure 3.11A and 3.11B). Quantification of cell death revealed a similar number of dead cells in healthy *nudt7-1* and *nudt7-1/sid2-1* plants (Figure 3.11C). Paraquat application induced cell death in the *nudt7-1/sid2-1* mutant to the same extent as in *nudt7-1*. The number of dead cells in *sid2-1* was not significantly different compared to Col-0 WT in response to oxidative stress. By contrast, cell death was almost completely compromised in the *nudt7-1/sid2-1/eds1-2*

mutant in healthy and paraquat treated plants. Paraquat application did not result in H₂O₂ accumulation in *nudt7-1/sid2-1* and *nudt7-1/sid2-1/eds1-2* mutants (Figure 3.11D). Faint H₂O₂ staining reveal dead cells in *nudt7-1/sid2-1*.

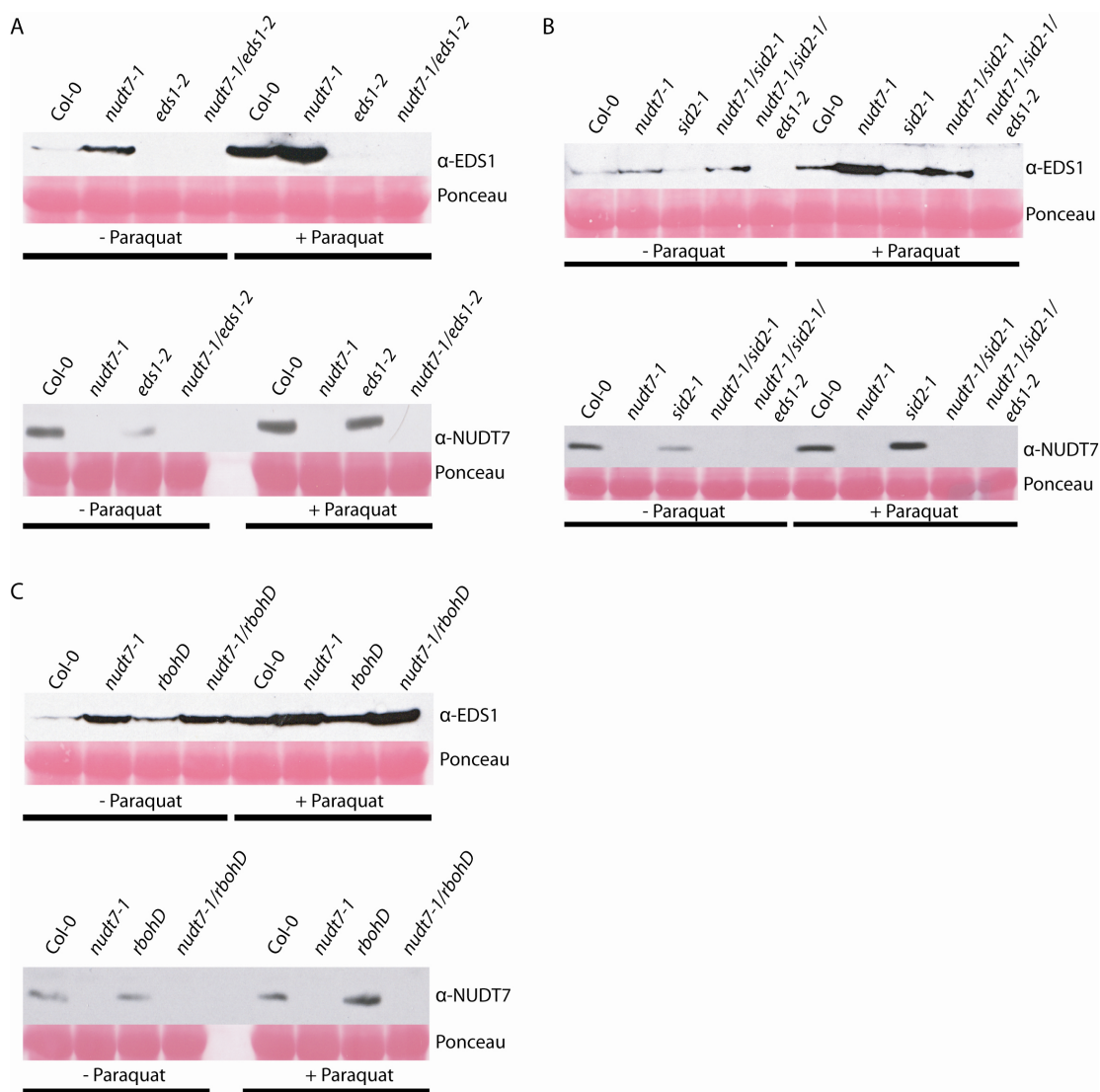


Figure 3.12: Western blot analysis of EDS1 and NUDT7 protein with and without paraquat treatment.

(A) EDS1 but not NUDT7 is strongly upregulated in Col-0 after oxidative stress induction. EDS1 and NUDT7 protein levels were analysed after treatment described under Figure 3.11A. Protein was extracted from aerial tissue of the indicated genotypes. Analysis was performed using anti-EDS1 and anti-NUDT7 antibody. Ponceau staining served as loading control. The result was repeated in at least three independent experiments.

(B) Depletion of SA reduces EDS1 and NUDT7 protein levels. Analysis performed as described in (A). The same expression pattern was observed in at least three independent experiments.

(C) The *rbohD* mutation does alter *EDS1* protein levels in *nudt7-1*. Western blot analysis was described in (A). Experiment was repeated at least three times with the same result.

Similar EDS1 protein levels were observed in healthy *nudt7-1* and *nudt7-1/sid2-1* plants and were strongly increased after paraquat application (Figure 3.12B). EDS1 protein was upregulated to a higher extent in *nudt7-1* compared to *nudt7-1/sid2-1* which is probably due to a missing SA-dependent positive feedback-loop in *nudt7-1/sid2-1* through which promotes *EDS1* expression (Feys et al., 2001). Notably, EDS1 protein was strongly depleted in healthy *sid2-1* mutant plants but increased to the level found in Col-0 WT after paraquat treatment. The same trend was observed for NUDT7 protein in paraquat treated *sid2-1* mutants.

These results show that SA tends to promote accumulation of H₂O₂. I concluded further that residual cell death and initiation of cell death in response to oxidative stress in *nudt7-1* and *nudt7-1/sid2-1* is SA-independent and requires functional *EDS1*.

3.4.5. *Nudt7-1/rbohD* displays an *eds1-2* like phenotype after paraquat treatment

Beside its role in cell death regulation, the NADPH oxidase *AtRbohD* plays a central role in the production of apoplastic ROS in response to avirulent pathogens (Torres et al., 2002, 2005). During the late response to light stress, steady-state transcript levels of the ROS scavengers *APX1* and *CAT1* declined in the *rbohD* mutant and the authors suggested that *AtRbohD* is required to maintain their expression by an amplification loop (Davletova et al., 2005). I was interested whether *AtRbohD* affects the H₂O₂ accumulation in the *nudt7-1* mutant. In addition, I wanted to investigate whether *AtRbohD* has a regulatory impact on chloroplast-derived oxidative stress signals that cause cell death.

Healthy *nudt7-1* and *nudt7-1/rbohD* plants are both reduced in size compared to Col-0 WT plants whereas increased growth retardation of *nudt7-1/rbohD* in response to paraquat was intermediate between Col-0 and *nudt7-1* (Figure 3.11A and 3.11B). Untreated *rbohD* mutants exhibited enhanced growth compared to WT while paraquat application led to a significant reduction of plant size. *Nudt7-1* and *nudt7-1/rbohD* mutants exhibited similar number of dead cells in healthy leaves. Induction of cell death in *nudt7-1/rbohD* did not exceed Col-0 WT levels after paraquat treatment (Figure 3.11C). H₂O₂ accumulation was not detectable in the *rbohD* or *nudt7/rbohD* mutants after application of paraquat indicating that H₂O₂ accumulation in response to paraquat is dependent on *AtRbohD* activity (Figure 3.11D).

EDS1 protein levels in untreated *rbohD* plants were elevated compared to Col-0 WT and the same levels of EDS1 protein were seen in *nudt7-1* and *nudt7-1/rbohD* (Figure 3.12C). After application of paraquat, EDS1 protein levels were increased in all samples. NUDT7 protein accumulated to similar levels in Col-0 and *rbohD* irrespective of paraquat treatment.

The strong increase of EDS1, absence of H₂O₂ accumulation, and failure to initiate exacerbated cell death in response to paraquat in *nudt7-1/rbohD* suggest that *RbohD* acts downstream of *EDS1*. However, *EDS1*-mediated growth retardation is only partially suppressed by the *rbohD* mutation indicating that *EDS1* signals via multiple different pathways.

Collectively, I concluded that there are different requirements for *EDS1*-dependent ROS signalling leading to initiation of cell death in *nudt7-1* and runaway cell death in *lsd1*, respectively. This is supported by the results showing that cell death initiation in *nudt7-1* upon oxidative stress trigger is independent of SA and promoted by AtRbohD generated ROS. *EDS1*-dependent runaway cell death in *lsd1* was shown to be induced by SA and negatively regulated by AtRbohD (Torres et al., 2005).

3.5. A gene expression microarray to identify genes in *nudt7-1* and *nudt7-1/sid2-1* that are regulated in an *EDS1*-dependent manner

Soil-grown *nudt7-1* mutants exhibit a phenotype that points to a deregulated defence pathway triggered by *EDS1* (Figure 5; Bartsch et al., 2006). Signalling events in this mutant presumably include rather late responses of *EDS1*-mediated immunity because the defence pathways are constitutively activated. Nonetheless, I considered *nudt7-1* as a good model system to identify further components of *EDS1*-triggered signalling by a gene expression microarray. The fact that SA depletion exacerbates the *nudt7-1* phenotype in an *EDS1*-dependent manner (Figure 3.7) suggests a novel negative regulatory role for SA in *EDS1*-signalling. For this reason, adding *nudt7-1/sid2-1* to this analysis allowed me to investigate the role of SA in *EDS1*-mediated signalling and to gain new insights in its role in modulating ROS signals. With regard to the results described above I was particularly interested in genes potentially involved in redox homeostasis and cell death.

Nudt7-1 and *nudt7-1/sid2-1* mutant plants that exhibited a developmental phenotype shown in Figure 3.7A were grown on soil. Col-0, *nudt7-1/eds1-2* and *nudt7-1/sid2-1/eds1-2* served as controls for this experiment.

Genotypes used for the microarray experiment

Col-0
nudt7-1
nudt7-1/sid2-1
nudt7-1/eds1-2
nudt7-1/sid2-1/eds1-2

Table 3.1: List of WT and mutant genotypes that were used for gene expression microarray analysis

Plants of these five genotypes were grown for four weeks in the same growth chamber. Leaf material from different plants of the same genotype was then harvested, pooled and RNA was extracted. This was repeated twice to obtain three independent biological replicates per genotype. After verification of the purity of total RNA, samples were sent to the IFG (Center for Integrated Functional Genomic) Münster for copy DNA (cDNA) synthesis and hybridization on Affymetrix ATH1 chips. The Genespring 10.0 software was used to analyze the datasets including normalization, quality control and filtering of all entities (see “Materials and Methods” section 2.2.18).

I extracted all genes whose expression changed significantly ($p < 0,05$) and at least two-fold in *nudt7-1* compared to Col-0 WT (Figure 3.13 (A)). *EDS1*-dependency was determined by comparing all genes differentially expressed in Col-0 vs. *nudt7-1* to genes differentially expressed in *nudt7-1* vs. *nudt7-1/eds1-2*. Overlapping genes were considered a being regulated in an *EDS1*-dependent manner in *nudt7-1*. The same analysis was performed for *nudt7-1/sid2-1* compared to the respective *eds1-2* mutant. The effect of SA on the expression of these genes was investigated by checking the list of defined *EDS1*-dependent genes in *nudt7-1* against the list of defined *EDS1*-dependent genes in *nudt7-1/sid2-1* (Figure 3.13 (B)). This comparison resulted in three different groups of genes (Supplemental Table 1):

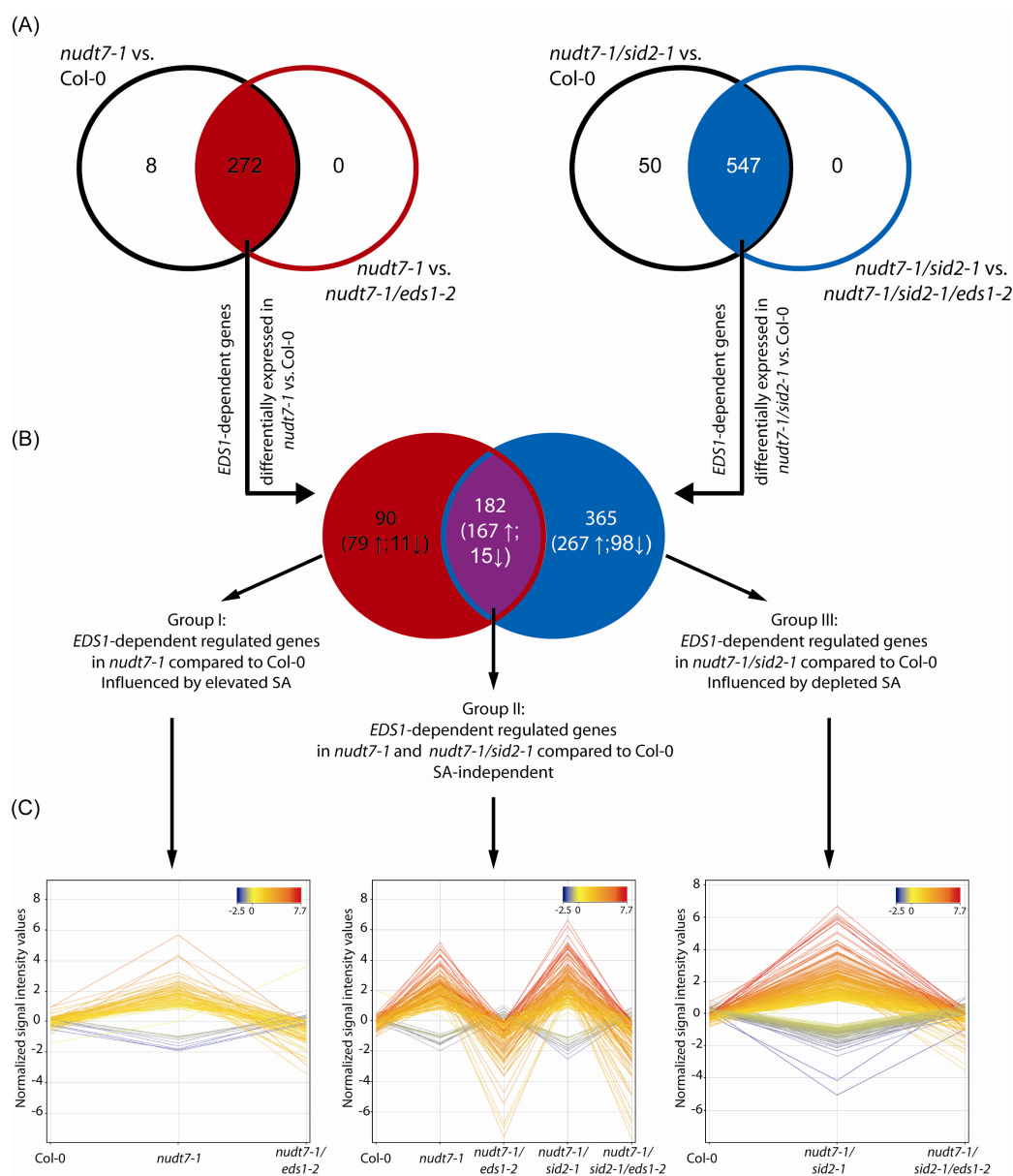


Figure 3.13: Identification of *EDS1*-dependent regulated genes in *nudt7-1* and *nudt7-1/sid2-1* and the influence of SA on their expression.

(A) Comparison of genes that are differentially expressed in *nudt7-1* compared to Col-0 and to *nudt7-1/eds1-2* (left Venn diagram). Right Venn diagram illustrates the comparison of *nudt7-1/sid2-1* to Col-0 and to *nudt7-1/sid2-1/eds1-2*, respectively. Intersections show the number of identified *EDS1*-dependent genes. Only genes that were significantly ($p < 0,05$) and at least two-fold differentially expressed in each comparison were considered. **(B)** Both intersections were compared with each other to investigate the influence of SA on the expression of the identified *EDS1*-dependent genes. Red section shows differentially expressed genes that are influenced by elevated SA levels (Group 1). Violet section shows the number of genes that are differently expressed in an SA-independent manner (Group 2). SA depletion affects the expression of genes in the blue section (Group 3). Numbers and arrows in brackets indicate the number of up- (↑) and downregulated (↓) genes, respectively. Up- and downregulated genes of all three groups were visualized in profile plot graphs **(C)**. Normalized signal intensity values for each gene in the respective genotype are displayed.

Group 1) genes that are expressed in an *EDSI*-dependent manner and that are induced/repressed by elevated SA levels (90 genes)

Group 2) genes that are expressed in an *EDSI*-dependent manner independent of SA (182 genes)

Group 3) genes that are expressed in an *EDSI*-dependent manner and that are induced/repressed by depleted SA levels (365 genes)

The three different groups were visualized in profile plot graphs showing the expression of each gene in the respective genotype (Figure 3.13 (C)).

In addition, Group 2 contained 23 genes that were significantly and at least two-fold differently expressed between *nudt7-1* and *nudt7-1/sid2-1* (Supplemental Table 2). Although, differential expression of these genes in both genotypes was *EDSI*-dependent, SA had an amplifying or suppressive effect on them.

All identified genes were then compared to genes annotated for the terms oxidative stress and cell death on TAIR (www.arbidopsis.org). Also, I performed a functional categorization using the MIPS functional catalogue database (<http://mips.gsf.de/projects/funcat>) and sought for genes that were categorized for terms either associated with redox stress or cell death. The identified genes are compiled in Table 3.2 and 3.3.

In Group 1, two members of the glutaredoxin family are highly upregulated suggesting enhanced $O_2^{\cdot-}$ production in *nudt7-1*. Glutaredoxins are involved in recovery of ascorbate that scavenges $O_2^{\cdot-}$ thereby producing H_2O_2 (Table 3.2). By contrast, one gene with similar function in ascorbate recovery, *DHAR1*, was down-regulated. Group 2 comprises mainly genes that are either ROS stress markers or that have elusive cellular functions. Strikingly, I did not find an upregulation of H_2O_2 scavengers in the *nudt7-1* mutant but only upregulated genes that are involved in production of H_2O_2 . By contrast, several genes recently described as ROS scavengers or participating in ROS scavenging were upregulated in Group 3. In particular, the peroxidase *PRXR5* was strongly upregulated in the SA-depleted *nudt7-1/sid2-1* mutant. The same holds true for two ferritins and the alternative oxidase *AOX 1D*. I concluded that elevated SA levels in *nudt7-1* suppress the scavenging of H_2O_2 whereas depletion of SA in *nudt7-1/sid2-1* results in H_2O_2 scavenging. This finding correlates with the results described above that show reduced H_2O_2 accumulation in *nudt7-1/sid2-1* compared to *nudt7-1* (Figure 3.11D).

The presence and expression of particular ROS scavengers in Group 1 and Group 3 and absence of ROS scavengers in Group 2 suggests that different ROS predominate in *nudt7-1* and *nudt7-1/sid2-1*. I addressed this hypothesis by comparing the gene lists with lists of marker genes specifically differentially regulated in response to $^1\text{O}_2$, $\text{O}_2^{\bullet-}$ or H_2O_2 (Gadjev et al., 2006) (Supplemental Table 3). Marker genes for $^1\text{O}_2$ and H_2O_2 were similarly present in Groups 1, 2 and 3 (Supplemental Table 3A and 3B). Strikingly, I found only two marker genes for $\text{O}_2^{\bullet-}$ in Group 1, none in Group 2 and 30 marker genes were expressed in Group 3 (Supplemental Table 3b). It is important to note that the two genes identified in Group 1 were down-regulated and therefore showed opposite expression than previously described (Gadjev et al., 2006). Although, H_2O_2 marker genes were not elevated in Group 1 as expected, my data reveal increased SA-dependent H_2O_2 accumulation in *nudt7-1*. Combining this result with the exclusive presence of $\text{O}_2^{\bullet-}$ marker genes in Group 3, I propose that SA not only promotes the accumulation of H_2O_2 but also antagonizes $\text{O}_2^{\bullet-}$ accumulation. It is not clear whether this is mediated by SA directly or indirectly.

Probe Set ID	AGI	Gene Title	Gene symbol	Description	Fold change <i>nudt7-1</i> vs <i>nudt7-1/eds1-2</i>	Fold change <i>nudt7-1/sid2-1</i> vs <i>nudt7-1/sid2-1/eds1-2</i>	Fold change <i>nudt7-1/sid2-1</i> vs <i>nudt7-1</i>
Group I genes - EDS1-dependent expressed genes, influenced by elevated SA							
262832_s_at	AT1G14870 /// AT1G14880	expressed protein		Responsive to oxidative stress (Luhua et al., 2008)	22,48		
265067_at	AT1G03850	glutaredoxin family protein		Recovery of ascorbate (Asc) from dehydroascorbate (DHA) (Mittler et al., 2004)	17,32		
261443_at	AT1G28480	glutaredoxin family protein	AtGRX480	SA-inducible transcription, <i>NPR1</i> -dependent (Ndamukong et al., 2007); recovery of Asc from DHA (Mittler et al., 2004)	12,91		
251840_at	AT3G54960	thioredoxin family protein	AtRDI1	Enzyme regulation by reducing disulfide bridges (Mittler et al., 2004)	4,15		
261149_s_at	AT1G19550 /// AT1G19570	putative dehydroascorbate reductase	AtDHAR1/ similar to AtDHAR1	Recovery of Asc from DHA (Mittler et al., 2004)	-2,57		
Group II genes - EDS1-dependent but SA-independent expressed genes							
254385_s_at	AT4G21830 /// AT4G21840	methionine sulfoxide reductase domain-containing protein / SelR domain-containing protein		Upregulated in response to singlet oxygen (AT4G21830) (Danon et al., 2006)	70,74	80,04	
259410_at	AT1G13340	expressed protein		Responsive to oxidative stress (Luhua et al., 2008)	15,50	22,82	
256337_at	AT1G72060	expressed protein		Responsive to oxidative stress (Luhua et al., 2008)	12,24	19,10	
255479_at	AT4G02380	late embryogenesis abundant family protein	AtLEA5/ AtSAG21	OE conferred resistance to oxidative stress (Mowla et al., 2006)	10,82	21,16	
247327_at	AT5G64120	putative peroxidase		cell wall peroxidase, produces superoxide (Rouet et al., 2006)	8,10	8,06	
259841_at	AT1G52200	expressed protein		OE conferred resistance to oxidative stress (Luhua et al., 2008)	7,60	9,96	
262119_s_at	AT1G02920 /// AT1G02930	putative glutathione-S-transferase	AtGSTF6/7	Stress-inducible; SA- and Ethylene-responsive expression (Wagner et al., 2002; Lieberherr et al., 2003)	7,38	14,15	
258941_at	AT3G09940	putative monodehydroascorbate reductase	AtMDAR3	Recovery of Asc from MonoDHA (Mittler et al., 2004)	6,91	6,92	
266267_at	AT2G29460	putative glutathione-S-transferase	AtGSTU4	No description available	5,91	32,23	5,68
260225_at	AT1G74590	putative glutathione-S-transferase	AtGSTU10	No description available	4,82	19,54	4,31
256245_at	AT3G12580	putative heat shock protein 70		No description available	2,80	3,26	
260581_at	AT2G47190	MYB transcription factor family	AtMYB2	Upregulated in response to H ₂ O ₂ (Gadjev et al., 2006)	2,16	2,48	
Group III genes - EDS1-dependent expressed genes, influenced by depleted SA							
265471_at	AT2G37130	peroxidase 21 (PER21) (P21) (PRXR5)		Upregulated in <i>vtc1</i> (Colville et al., 2008)		75,43	
246099_at	AT5G20230	plastocyanin-like domain-containing protein	AtBCB	Induced by Al- and ROS-treatment (Richards et al., 1998)		5,08	
251109_at	AT5G01600	ferritin 1	AtFER1	Required to maintain cellular redox homeostasis (Ravet et al., 2008)		3,94	
263831_at	AT2G40300	ferritin 4	AtFER4	Required to maintain cellular redox homeostasis (Ravet et al., 2008)		2,61	
251985_at	AT3G53220	thioredoxin family protein		Enzyme regulation by reducing disulfide bridges (Mittler et al., 2004)		2,43	
260706_at	AT1G32350	putative alternative oxidase	AtAOX1D	Stress induced transcript accumulation; Alternative respiration pathway in response to stress (Zsigmond et al., 2008)		2,28	
250633_at	AT5G07460	putative peptide methionine sulfoxide reductase	AtPMSR2	Repairs oxidatively damaged proteins; elevated oxidative stress in <i>pmsr2</i> (Bechtold et al., 2004)		-2,07	
248765_at	AT5G47650	MutT/nudix family protein	AtNUDT2	OE increases oxidative stress tolerance (Ogawa et al., 2008)		-2,21	
258419_at	AT3G16670	expressed protein		Responsive to oxidative stress (Luhua et al., 2008)		-2,66	
260745_at	AT1G78370	putative glutathione-S-transferase	AtGSTU20	No description available		-3,61	

Table 3.11: EDS1-dependent genes differentially regulated in response to oxidative stress

Listed genes are annotated as responsive to oxidative stress on TAIR and were categorized to function in different oxidative stress responses - by MIPS FunCat database, respectively.

When investigating gene lists for genes associated with cell death I found a number of cell death inducers/executors and cell death markers in all three groups (Table 3.3). In particular, I was interested in the identification of genes that may account for the

exacerbation of the cell death phenotype of *nudt7-1/sid2-1* compared to *nudt7-1*. Therefore I focused on genes differentially regulated between *nudt7-1* and *nudt7-1/sid2-1* in Group 2 and on genes in Group 3. In Group 2, I only found *FMO1* to be highly upregulated in *nudt7-1/sid2-1* compared to *nudt7-1*. *FMO1* was previously described as a cell death marker (Olszak et al., 2006). It was reported that *FMO1* transcripts are induced in mutants with deregulated PCD, such as *acd11* and *lsd1*, and during senescence. However, it remained unclear whether *FMO1* is also involved in cell death initiation or execution. In Group 3, two genes were identified that are tightly linked to execution of cell death. *Bax Inhibitor-1 (BI-1)*, an inhibitor of PCD, and the vacuolar processing enzyme gamma (γ -VPE), a positive regulator of PCD, were both upregulated. BI-1 is localized in the membrane of the endoplasmic reticulum (ER) (Watanabe et al., 2006) suggesting that PCD in *nudt7-1/sid2-1* results from ER stress. In addition, γ -VPE acts in the vacuole and shows caspase activity (Hara-Nishimura et al., 2005). The upregulation of both genes indicates that cell death in *nudt7-1/sid2-1* does not result from the cytotoxic effect of ROS overload but is a PCD.

Probe Set ID	AGI	Gene Title	Gene symbol	Description	Fold change <i>nudt7-1</i> vs <i>nudt7-1/eds1-2</i>	Fold change <i>nudt7-1/sid2-1</i> vs <i>nudt7-1/sid2-1/eds1-2</i>	Fold change <i>nudt7-1/sid2-1</i> vs <i>nudt7-1</i>
Group I genes - EDS1-dependent expressed genes, influenced by elevated SA							
254093_at	AT4G25110	caspase family protein	AtMC2	putative prodomain like mammalian "initiator" caspases; <i>LSD1</i> -like zinc finger domain (Vercammen et al.,2004; Epple et al.,2003)	8,40		
260735_at	AT1G17610	disease resistance protein-related		TIR-NBS gene lacking LRR domain (Meyers et al.,2003)	3,13		
Group II genes - EDS1-dependent but SA-independent expressed genes							
250435_at	AT5G10380	zinc-finger family protein	AtRING1	Plasmamembrane localized ubiquitin E3 ligase; positive regulator of cell death (Lin et al.,2008)	12,56	12,41	
266292_at	AT2G29350	alcohol dehydrogenase family protein	AtSAG13	strongly expressed in <i>acd11</i> (Brodersen et al.,2002)	9,60	12,67	
254243_at	AT4G23210	protein kinase family protein	AtCRK13	OE induces HR-associated cell death and SA-dependent resistance (Acharya et al.,2007)	7,61	10,20	
252572_at	AT3G45290	seven transmembrane MLO family protein	AtMLO3		7,27	4,00	
256012_at	AT1G19250	flavin-containing monooxygenase family protein	AtFMO1	Positive regulator of <i>EDS1</i> -dependent but SA-independent resistance (Bartsch et al.,2006)	5,69	76,12	13,67
247493_at	AT5G61900	calcium-dependent, phospholipid binding family protein	AtBON1	Loss-of-function in combination with <i>bon2</i> or <i>bon3</i> leads to extensive cell death. Suppressed by <i>pad4</i> or <i>eds1</i> (Yang et al.,2006)	4,89	7,37	
245038_at	AT2G26560	putative patatin	AtPLP2	Expression in response to pathogens depends on JA or ethylene; potentiates cell death but reduces efficiency of HR (La Camera et al.,2005)	4,64	23,40	
Group III genes - EDS1-dependent expressed genes, influenced by depleted SA							
252265_at	AT3G49620	2-oxoacid-dependent oxidase	AtDIN1	Accumulates in the dark and in senescing leaves. Strongly upregulated in response to various ROS (Fujiki et al.,2001; Gadjev et al.,2006)		34,20	
248829_at	AT5G47130	Bax-inhibitor-1 family	AtBI-1	Negative regulator of PCD induced by ER stress (Watanabe et al.,2008)		5,30	
253358_at	AT4G32940	vacuolar processing enzyme gamma	γ -VPE	Induces cell death by breakdown of vacuole. Exhibits caspase-1 activity (Kuroyanagi et al.,2005)		3,80	
251895_at	AT3G54420	Class IV chitinase	AtEP3	Involved in initial events of HR (de A. Gerhardt et al.,1997)		2,46	
248943_s_at	AT5G45440 /// AT5G45490	disease resistance protein-related		Meyers et al.,2003		-2,12	
252983_at	AT4G37980	mannitol dehydrogenase	AtELI3-1	RPM1-dependent transcript accumulation after pathogen infection (Kiedrowski et al.,1992)		-2,16	

Table 3.12: EDS1-dependent genes associated with cell death signalling

Listed genes are annotated as cell death-associated on TAIR and were categorized to function in cell death signalling by MIPS FunCat database, respectively.

4. Discussion

Arabidopsis plants lacking *NUDT7* display a phenotype characteristic of mutants with a deregulated defence pathway. This phenotype comprises enhanced resistance, stunted growth, elevated SA levels and spontaneous leaf cell death (Jambunathan and Mahalingam, 2006; Bartsch et al., 2006; Ge et al., 2007). The fact that cell death in *nudt7* is restricted to single cells and does not spread suggests an effect on regulation of the initiation of cell death rather than propagation of cell death. Further analysis revealed that the *nudt7* phenotype requires *EDSI* and it was concluded that *NUDT7* is involved in the negative regulation of *EDSI*-mediated defence signalling (Bartsch et al., 2006). *EDSI* represents a key signalling node in plants, mediating biotic and abiotic stress responses (Wiermer et al., 2005). Although the importance of *EDSI* signalling is well described, the underlying regulatory mechanisms are poorly understood. Thus, identification of *NUDT7* as a negative regulator of the *EDSI* pathway opened the possibility to gain insight into how plants regulate stress responses. I performed a closer characterization of *NUDT7* in terms of its genetic relationship to *EDSI* and *NUDT7* localization and dynamics in response to pathogens. I concluded that *EDSI* and *NUDT7* are part of a tight stress inducible programme but that their proteins do not interact with each other. Investigations into the possible role of *EDSI* and *NUDT7* in MTI revealed that neither is important for pre-invasive resistance. Rather, *EDSI* and *NUDT7* operate at a post-invasive level of plant resistance to host-adapted pathogens. *NUDT7* was found to limit *EDSI*-dependent ROS signalling causing growth retardation, cell death initiation and H₂O₂ accumulation. Oxidative stress-induced growth retardation and initiation of cell death, but not H₂O₂ accumulation, are independent of SA accumulation. Furthermore, *EDSI*-dependent ROS signalling requires *AtRbohD* for cell death initiation and H₂O₂ accumulation in *nudt7-1*. I concluded from these experiments that distinct *EDSI* signalling events are involved i) in cell death initiation in *nudt7-1* compared to cell death propagation in *lsd1* and ii) in cell death initiation and growth retardation in response to oxidative stress. Data obtained in this study will be discussed in the context of understanding how plants fine-tune stress responses to protect against invading pathogens but also conserve energy and tissue viability for growth and reproduction.

4.1. EDS1 and NUDT7 are part of a plant stress-inducible genetic programme

The expression pattern of *EDS1* and *NUDT7* revealed a tight co-regulation of both genes after induction of various stresses (Figure 3.3A) suggesting that they are part of a plant stress-inducible genetic programme. This finding is in agreement with previous reports showing that *NUDT7* and *EDS1* are upregulated in response to various stresses (Feys et al., 2001; Jambunathan and Mahalingam, 2006; Ge et al., 2007; Adams-Philipps et al., 2008) and studies describing a requirement for *EDS1* in abiotic stress responses (Chini et al., 2004; Mateo et al., 2004; Ochsenbein et al., 2006; Mühlenbock et al., 2008).

The results presented in Figure 3.3B and 3.3C suggest that *EDS1* does not strongly affect *NUDT7* transcript regulation but promotes NUDT7 protein accumulation. This was a rather unexpected finding, since the dependence of the *nudt7* phenotype on *EDS1* and the co-regulation of *EDS1* and *NUDT7* in responses to various stresses pointed to a strong transcriptional relationship. An indirect interaction between *EDS1* and *NUDT7* was further supported by the fact that *NUDT7* was transcriptionally upregulated after *Pst avrRPS4* and *Pst avrRPM1* infection (Figure 3.5A and 3.5B). This finding is consistent with microarray data showing upregulation of *NUDT7* after inoculation with *Pst avrRPS4* and *Pst avrRPM1* (Bartsch et al., 2006). Induction of *NUDT7* was shown to be *EDS1*- and *PAD4*-dependent after *Pst avrRPS4* but not after *Pst avrRPM1* infection.

The dynamics of NUDT7 protein accumulation in response to avirulent pathogens may be subjected to further regulations (Figure 3.5B). While *NUDT7* transcript and protein levels increased and declined similarly in response to *Pst avrRPS4* inoculation, NUDT7 protein seemed to be stabilized after infection with *Pst avrRPM1*.

Post-transcriptional regulation of *Arabidopsis* signalling pathway components has been described in ethylene signalling (Guo and Ecker, 2003; Potuschak et al., 2003; Gagne et al., 2004). It was shown that the SCF^{EBF1/2} (SKP1 Cullin F-box^{EIN3 Binding F-box1/2}) E3 ligase complex constitutively degrades EIN3, a key transcriptional regulator of ethylene signalling, thereby suppressing the ethylene response. Ethylene perception leads to stabilization of EIN3 and presumably reduces SCF^{EBF1/2} activity. Similar

observations have been reported for light signalling (Osterlund et al., 2000; Saijo et al., 2003; Seo et al., 2003). In darkness, the ubiquitin E3 ligase COP1 (Constitutive Photomorphogenesis 1) localizes to the nucleus and targets photomorphogenesis-mediating transcription factors such as HY5 (Long Hypocotyl 5) to degradation. Upon exposure to light, COP1 translocates to the cytosol and allows the HY5 pool to build up and to induce light signaling. However, these examples describe the post-transcriptional regulation of positive modulators of ethylene and light signaling, respectively. To our knowledge, post-transcriptional stabilization of a negative pathway regulator has not been reported in *Arabidopsis*. Although post-transcriptional regulation of negative pathway regulators has been described in auxin and JA signaling, repressors of these pathways are degraded upon signal perception (Quint and Gray, 2006; Katsir et al., 2008). Auxin signaling is negatively regulated by Aux/IAA (Auxin/Indole-3-Acetic Acid) proteins that heterodimerize with ARF (Auxin Response Factors) transcription factors thereby suppressing auxin-inducible gene expression (Quint and Gray, 2006). Perception of auxin by the SCF component TIR1 (Transport Inhibitor Response 1) increases the affinity of TIR1 for Aux/IAA proteins resulting in increased ubiquitination and turnover of Aux/IAs (Dharmasiri et al., 2005). The functions of SCF^{TIR1}, Aux/IAA and ARF transcription factors are analogues to core components of JA signaling. JA signaling is negatively regulated by JAZ proteins that suppress the activity of transcription factors mediating JA responses (Katsir et al., 2008). JA signals trigger the SCF^{COI1} (Coronatine Insensitive 1) complex that targets JAZ proteins for proteasomal degradation thereby liberating transcription factors that induce jasmonate-dependent transcriptional changes.

Thus, induced post-transcriptional accumulation of NUDT7 and other negative components of stress and cell death relay may represent an important mechanism for balancing the extent of abiotic and biotic stress responses. Testing whether an increase of NUDT7 protein in *eds1-2* upon paraquat treatment (Figure 3.12A) correlates with gene expression changes at the transcriptional level will inform us of the mode of NUDT7 regulation.

A comprehensive study analyzing 24 *Arabidopsis nudix hydrolase* genes predicted a cytosolic localization for 9 members while 15 nudix hydrolases were suggested to localize to different subcellular compartments (Ogawa et al., 2005). NUDT7 was predicted to be cytosolic. By performing microsomal and nuclear fractionation studies I was able to verify the cytosolic localization of NUDT7 (Figure 3.6A and 3.6B;

Supplemental Figure 2). In addition, the localization of NUDT7 did not change after pathogen challenge or chemical oxidative stress treatment. These results suggest that NUDT7 is restricted to the cytosol and suggest that NUDT7 exerts its function in this cellular compartment. Attempts to identify an *in vivo* activity of NUDT7 so far failed (Ge et al., 2007). Only two cytosolic *Arabidopsis* nudix hydrolases have been characterized *in vivo*, NUDT1 (an 8-oxo-GTP pyrophosphohydrolase) and NUDT2 (an ADP-ribose pyrophosphatase) (Yoshimura et al., 2007; Ogawa et al., 2009). Notably, both NUDT1 and NUDT2 are involved in oxidative stress protection. In particular, over expression of NUDT2 resulted in depleted ADP-ribose levels and increased tolerance to paraquat treatment (Ogawa et al., 2009).

Oxidative stress conditions lead to increased accumulation of highly reactive ADP-ribose in mammalian cells and can cause non-enzymatic mono-ADP-ribosylation of proteins accompanied by an immediate toxic effect (Deng and Barbieri, 2008; Ying, 2008). A major enzyme, generating free mono-ADP-ribose from poly-ADP-ribose, is PARG (poly (ADP-ribose) glycohydrolase) and *in planta* studies revealed that inhibition of poly-ADP-ribosylation correlated with enhanced stress tolerance and reduced stress-induced cell death (De Block et al., 2005). Furthermore, PARG-derived ADP-ribose was shown in mammalian cells to activate a plasma-membrane bound cation channel, TRPM2 (transient receptor potential melastatin 2), leading to Ca^{2+} influxes and cell death (Perraud et al., 2001; Fonfria et al., 2004; Yang et al., 2006). Notably, TRPM2 possesses a nudix motif that is essential for ADP-ribose binding and Ca^{2+} gating in response to oxidative stress (Perraud et al., 2005). Considering that NUDT7 possesses *in vitro* ADP-ribose pyrophosphatase activity (Ogawa et al., 2005) and an *Arabidopsis* PARG was expressed to high levels in healthy *nudt7-1* plants (Adams-Phillips et al., 2008), it is conceivable that NUDT7 modulates cytosolic mono-ADP-ribose levels. The decreased oxidative stress tolerance of *nudt7-1* mutants and the deregulated cell death phenotype described in my work (Figure 3.11) are consistent with a physiological ADP-ribose pyrophosphatase activity of NUDT7.

4.2. The EDS1 is not important for MAMP-triggered immunity

Transcript levels of *NUDT7* and *EDS1* increase upon MAMP treatment (Zipfel et al., 2004; Ge et al., 2007; Phillips-Adams et al., 2008). In addition, *nudt7-1* plants are hyper resistant to virulent pathogens that presumably induce MTI (Bartsch et al., 2006; Jambunathan and Mahalingam, 2006; Ge et al., 2007). The increased resistance of *nudt7-1* was shown to be *EDS1*-dependent (Bartsch et al., 2006). These data prompted me to investigate whether *EDS1* and *NUDT7* are components of MAMP-triggered signalling. My results demonstrated that MAMP-induced signalling events are not altered in *nudt7-1* and *eds1-2* compared to WT (Figure 3.9 A-C, data not shown). I therefore concluded that neither *NUDT7* nor *EDS1* are involved in MAMP signalling. This is consistent with recent studies (Peck et al., 2001; Zipfel et al., 2004; Tsuda et al., 2008) in which flagellin perception led to rapid phosphorylation events that were independent of SA and *EDS1* (Peck et al., 2001). Moreover, Zipfel et al. (2004) showed that pre-treatment of *Arabidopsis* with flg22 induces resistance to spray-inoculated *Pst* DC3000. Although *EDS1* was upregulated upon flg22 treatment, *eds1* mutants retained flg22-induced resistance. Recently it was reported that MAMP perception induced *SID2*- and partially *PAD4*-dependent SA accumulation and subsequent SA-mediated signalling, which contributed to resistance against virulent *Pst* (Tsuda et al., 2008). Intimate interaction of MAMP-triggered and SA-mediated signalling resulted in transcriptional activation of several SA-inducible genes. Thus, induction of *EDS1* and *NUDT7* in response to MAMPs might result from MAMP-triggered SA signalling.

Older, soil-grown *nudt7-1* plants exhibit constitutive *EDS1*-mediated signalling. This led to the assumption that defence is primed in *nudt7-1* and therefore could also involve primed MTI. Infection studies with virulent *Pst* DC3000 and attenuated virulent *Pst* Δ *avrPto/avrPtoB* strains resulted in similar differences in bacterial growth between *nudt7-1* and WT (Figure 3.9D). Therefore, I concluded that resistance in *nudt7-1* is unlikely to be caused by a primed MTI system but rather by enhanced post-invasive basal resistance that depends on *EDS1*. This conclusion is supported by data from Lipka et al. (2005) showing that *EDS1* was required for post-invasive resistance to non-adapted powdery mildew. Entry rates of *Erysiphe pisi* were not

altered in *eds1* relative to those of WT whereas epiphytic fungal growth in *eds1* substantially increased once pre-invasive resistance was breached.

Collectively, these data suggest that MTI operates independently of *EDSI* signalling and that other components are required to induce the *EDSI* pathway causing the *nudt7-1* phenotype.

4.3. Relationship of *EDSI* and *NUDT7* to ROS accumulation and signalling

The finding that a hyper-responsiveness to environmental elicitors did not account for deregulated resistance leading to the *nudt7-1* phenotype (Figure 3.9) prompted me to seek for other triggers. Many constitutive defence mutants show accumulation of H₂O₂ and O₂^{•-} (Lorrain et al., 2003). Induction of oxidative stress, for example in the *lsd1* and *flu* mutants, resulted in lesion formation and retarded growth (Jabs et al., 1996; Op den Camp et al., 2003). Notably, *EDSI* was shown in several studies to be required to mediate oxidative stress responses (Rusterucci et al., 2001; Mateo et al., 2004; Ochsenbein et al., 2006; Mühlenbock et al., 2008). These data suggest that growth retardation and spontaneous leaf cell death in *nudt7-1* could be caused by *EDSI*-mediated oxidative stress signalling. H₂O₂ staining indeed revealed high accumulation of this ROS in *nudt7-1* leaves compared to WT (Figure 3.10). Other studies reported contradictory results on ROS accumulation in *nudt7* mutants. Jambunathan and Mahalingam (2006) reported elevated levels of ROS in *nudt7* while Ge et al. (2007) argued against increased ROS levels in *nudt7* mutants. This might be due to different enzyme-based ROS detection protocols. Also, different growth conditions of plants are likely to result in different phenotypes. Indeed, growth of *nudt7-1* plants on commercial medium (jiffy-7 soil) attenuated growth retardation, cell death initiation and ROS accumulation in my study (Figure 3.10). It is probable that certain additives present in the MPIZ-soil but not in the jiffy soil trigger *Arabidopsis* resistance pathways.

Paraquat application on jiffy-soil-grown *nudt7-1* and *nudt7-1/sid2-1* plants resulted in severe growth retardation, more frequent initiation, but not spread, of cell death and high accumulation of H₂O₂ in *nudt7-1* (Figure 3.11). This phenotype was fully dependent on *EDSI* and, except H₂O₂ accumulation, largely independent of SA.

Earlier studies revealing a requirement for *EDS1* in promoting ROS signals were mainly based on investigations of SA-dependent RCD in *lsd1* (Rusterucci et al., 2001; Mateo et al., 2004; Mühlenbock et al., 2007, 2008). However, Bartsch et al. (2006) suggested that *EDS1* is also involved in SA-independent cell death induction, which is reinforced by my work. I could demonstrate that cell death in *nudt7-1* and *nudt7-1/sid2-1* is SA-independent but *EDS1*-dependent and can be exacerbated by chloroplastic ROS signals. These data imply that there are distinct mechanisms and requirements for SA-independent cell death induction compared to SA-dependent propagation of cell death. This further implies that *EDS1* is able to mediate different cell death signals (Figure 4.1). The complexity of such signalling events is demonstrated by investigations on the NADPH oxidase *AtRbohD*. *AtRbohD* provides the major source of ROS upon pathogen challenge and has been implicated in the negative regulation of SA-inducible RCD in *lsd1* (Torres et al., 2002, 2005). *Nudt7-1/rbohD* mutants exhibited similar quantities of cell death as *nudt7-1* on both soil systems tested indicating that *AtRbohD*-generated ROS does not influence cell death initiation in *nudt7-1* (Figure 3.7C and 3.11C). However, paraquat-induced cell death in *nudt7-1* was largely suppressed in *nudt7-1/rbohD* (Figure 3.11C), suggesting that *AtRbohD* is required to relay oxidative stress signals leading to exacerbated cell death initiation in *nudt7-1*. This finding is supported by a recent study showing that *AtRbohD* is required to process ROS signals from the chloroplast (Joo et al., 2005). O₃ fumigation induces a chloroplastic oxidative burst in guard cells as well as lesioning in adjacent cells. It was suggested that chloroplast-derived ROS signals activate *AtRbohD* and *AtRbohF* that in turn induce cytoplasmic ROS production in neighbouring cells thereby contributing to cell death. The fact that *AtRbohD* contributes to cell death induction (data herein; Torres et al., 2002; Joo et al., 2005) but restricts RCD (Torres et al., 2005) reinforces the hypothesis that distinct signalling events induce and propagate cell death, respectively (Figure 4.1).

Elucidation of such signalling events becomes even more complicated by the finding that EDS1 protein levels in the *nudt7-1/rbohD* mutant resembled the levels in *nudt7-1* plants (Figure 3.12C). Also, EDS1 protein levels similarly increased in *nudt7-1* and *nudt7-1/rbohD* after paraquat treatment. From my study, it remains unclear whether *EDS1* acts upstream or downstream of *AtRbohD*. *EDS1* could either activate *AtRbohD* leading to cell death induction or *EDS1* could be part of cell death execution as the result of *AtRbohD* activation by chloroplastic ROS. Alternatively, *EDS1* and *AtRbohD*

could form a propagative loop, in which *EDSI* perceives and potentiates ROS signals that are processed by *AtRbohD* and lead to *EDSI*-dependent cell death initiation in neighbouring cells (Figure 4.1).

Studies on *nudt7-1/rbohD* also led to the conclusion that *EDSI* mediates distinct signalling events causing oxidative stress induced cell death initiation and growth retardation. Growth retardation in response to paraquat treatment was fully dependent on *EDSI* (Figure 3.11B). *Nudt7-1/rbohD* mutants retained oxidative stress-induced growth retardation while *EDSI*-dependent cell death initiation was suppressed in these mutants compared to *nudt7-1* (Figure 3.11B and C).

Although there are reports implicating *EDSI* signalling events in $^1\text{O}_2$ -induced growth retardation and lesion formation (Ochsenbein et al., 2006), distinct *EDSI* mediated responses resulting in these phenotypes have not been distinguished. By contrast, the study from Ochsenbein et al. (2006) and my work suggest that *EDSI* might integrate different ROS signals to affect plant growth.

4.4. SA limits *EDSI*-dependent cell death initiation

The level of cell death in jiffy-soil-grown *nudt7-1* and *nudt7-1/sid2-1* plants was similar irrespective of oxidative stress treatment (Figure 3.11C) suggesting that cell death initiation is mediated by intrinsic *EDSI*-signalling independent of SA. SA-independent initiation of cell death has been described for a number of SA accumulating constitutive defence mutants. The *cpr5* (*constitutive expression of PR genes 5*), *hrl1* (*hypersensitive response-like 1*), *cet2* (*constitutive expressor of TH11.2 2*) and *cet4* mutants all display spontaneous lesioning that is not abolished by SA depletion (Bowling et al., 1997; Hilpert et al., 2001; Devadas et al., 2002; Nibbe et al., 2002). Instead, hormonal crosstalk including SA, JA and ethylene signalling was shown to contribute to lesion formation in these mutants (Clarke et al., 2000; Hilpert et al., 2001; Devadas et al., 2002; Nibbe et al., 2002). Recently, it was reported that *EDSI* promotes ethylene-dependent cell death initiation suggesting that *EDSI* triggers distinct hormone signalling pathways (Mühlenbock et al., 2008). The impact of JA and ethylene signalling on cell death initiation of *nudt7-1* and *nudt7-1/sid2-1* has not been investigated yet. Crosses between *nudt7-1*, *nudt7-1/sid2-1* and mutants impaired in JA/ethylene signalling will be performed to test whether JA/ethylene signalling impairs cell death initiation of *nudt7-1* and *nudt7-1/sid2-1*.

Application of two soil systems to grow *nudt7-1* and *nudt7-1/sid2-1* plants led to contradictory results on the regulatory role of SA on cell death initiation in these mutants. SA accumulation routed via PAD4 and SID2 antagonizes spontaneous leaf cell death in soil-grown *nudt7-1* plants (Figure 3.7). By contrast, cell death exacerbation in *nudt7-1* and *nudt7-1/sid2-1* upon oxidative stress induction was SA-independent (Figure 3.11B). Therefore I hypothesize that paraquat-induced ROS signalling overrides a potential dampening regulatory role of SA in *EDSI*-dependent cell death initiation (Figure 4.1). SA is produced in the chloroplasts (Strawn et al., 2007) and was shown to be essential for acclimation processes in response to high light and for regulation of the cellular redox homeostasis to prevent photo-oxidative damage (Mateo et al., 2006). Paraquat in turn induces light dependent $O_2^{\bullet-}$ production in the PS I in the chloroplast (Babbs et al., 1989). Hence, inducing continuous oxidative stress by paraquat treatment might overcome the photo-protective role of SA and result in exacerbated cell death in *nudt7-1* and *nudt7-1/sid2-1*.

Importantly the results presented in Figure 3.11 demonstrate that paraquat-induced ROS overload did not trigger cell death and growth retardation in *nudt7-1 per se* but was the result of defined *EDSI*-mediated signalling. This is consistent with former studies suggesting that paraquat and 1O_2 triggered cell death result from the activation of a genetic programme and is not caused by oxidative physiochemical damage (Chen and Dickman, 2004; Lee et al., 2007).

4.5. H_2O_2 is an important component of paraquat-induced initiation of cell death

Several studies described distinct signalling roles for $O_2^{\bullet-}$ and H_2O_2 (Gadjev et al., 2006; Laloi et al., 2006, 2007), and both ROS have been implicated in cell death induction (Jabs et al., 1996; Torres et al., 2002; Dat et al., 2003). In this work, I concluded a major signalling role for H_2O_2 in cell death initiation based on the results obtained with the *nudt7-1/rbohD* mutant. Several studies suggest a crucial role for AtRbohD-generated apoplastic H_2O_2 as intercellular signal causing intracellular H_2O_2 accumulation (Torres et al., 2002; Kwak et al., 2003; Joo et al., 2005), as discussed above. Whether *AtRbohD* is also required for cell death initiation in *nudt7-1/sid2-1* mutants will require further analysis. Similar quantities of dead cells in *nudt7-1* and

nudt7-1/sid2-1 upon oxidative stress induction argue for an involvement of AtRbohD-generated H_2O_2 in cell death initiation in *nudt7-1/sid2-1*.

Strong H_2O_2 staining in response to oxidative stress treatment was shown to be SA-dependent (Figure 3.11D). I concluded that SA tends to promote the accumulation of H_2O_2 . This is supported by several studies describing a feed forward loop by which SA and H_2O_2 promote their production and inhibit scavenging, respectively (Chen et al., 1993; Leon et al., 1995; Klessig et al., 2000). The relative impact of SA and *AtRbohD* on oxidative stress-induced H_2O_2 accumulation in *nudt7-1* does not become clear by my study. Quantification of SA in *nudt7-1* and *nudt7-1/rbohD* upon paraquat treatment will be required for further conclusions on this issue.

Alternatively, $O_2^{\bullet-}$ could also act as signal independently of H_2O_2 . Microarray data revealed that in soil-grown *nudt7-1/sid2-1* plants up to 30 $O_2^{\bullet-}$ marker genes are upregulated that are not affected in *nudt7-1* (Supplemental Table 3b). It is remarkable that the first five $O_2^{\bullet-}$ marker genes are within the ten most upregulated genes in *nudt7-1/sid2-1*, which indicates enhanced $O_2^{\bullet-}$ stress. Investigations whether these genes are similarly upregulated in *nudt7-1* and *nudt7-1/sid2-1* plants after paraquat treatment could help to elucidate if $O_2^{\bullet-}$ serves as signal molecule and is required for *EDS1*-dependent cell death initiation in *nudt7-1* and *nudt7-1/sid2-1*. Such an experiment will be supplemented by $O_2^{\bullet-}$ stainings of leaves from paraquat-treated plants.

4.6. Transcriptomics reveal altered redox homeostasis and constitutive defence signalling in *nudt7-1* and *nudt7-1/sid2-1*

I performed gene expression microarray analysis to identify additional components involved in *EDS1*-mediated signalling. The *EDS1*-dependent phenotypes of *nudt7-1* and *nudt7-1/sid2-1* offered the possibility to seek for genes that are particularly involved in oxidative stress signalling and cell death induction. Analysis of the performed gene expression microarrays exposed a large number of *EDS1*-dependent genes potentially affecting or involved in SA-mediated responses. I found that SA influences the expression of different ROS scavengers and ROS marker genes in *nudt7-1* and *nudt7-1/sid2-1* indicating that SA promotes H_2O_2 and antagonizes $O_2^{\bullet-}$ accumulation (Table 3.2, Supplemental table 3b). This finding is consistent with previous studies revealing SA mediated suppression and activation of different ROS

scavengers. Transcript levels of SOD, that dismutates $O_2^{\bullet-}$ to H_2O_2 , were shown to increase in response to SA (Rajjou et al., 2006) while H_2O_2 scavengers were found to be suppressed (Klessig and Durner, 1996; Chamnongpol et al., 1998). Moreover, gene expression profiling of *nudt7-1* and *nudt7-1/sid2-1* mutants supported the impact of SA on cell death initiation as shown in Figures 3.7 and 3.11 and discussed in section 4.4.

Comparison with the dataset from Bartsch et al. (2006) revealed a problematic issue (Bartsch et al., 2006). The microarray analysis from Bartsch et al. (2006) identified *EDS1*- and *PAD4*-dependent genes after infection of *Arabidopsis* with *Pst avrRPS4* and *Pst avrRPM1*. The expression of a number of genes correlated well between both data sets supporting the initial hypothesis that differentially regulated genes in *nudt7-1* and *nudt7-1/sid2-1* are expressed in an *EDS1*-dependent manner. The overlapping gene set comprises genes specifically induced by *Pst avrRPS4* and *Pst avrRPM1* but also genes suppressed by *eds1* and *pad4* in non-treated tissue. By contrast, these genes were found to be constitutively expressed in *nudt7-1* and *nudt7-1/sid2-1* suggesting a global induction of defence related genes. This finding implies that constitutive expression of such genes in *nudt7-1* and *nudt7-1/sid2-1* likely causes very indirect effects downstream of *EDS1*-induced transcriptional changes. Therefore, constitutive *EDS1*-signalling made it difficult to discriminate between genes acting in the *EDS1* pathway and genes that are activated as a result of *EDS1*-triggered responses. This complicated the further identification of *EDS1* pathway components by analyzing the constitutive defence mutants *nudt7-1* and *nudt7-1/sid2-1*.

Gene expression profiling is in progress to investigate whether genes that are differentially regulated in *nudt7-1* and *nudt7-1/sid2-1* are also affected by JA/ethylene signalling pathways (Penninckx et al., 1998; Schenk et al., 2000; Pre et al., 2008). Research on this could provide a deeper insight into whether disturbed SA – JA/ethylene crosstalk might be involved in growth retardation and cell death initiation in *nudt7-1* and *nudt7-1/sid2-1* (as discussed in section 4.4).

4.7. Positioning NUDT7 in the EDS1 pathway

Bartsch et al. (2006) revealed that the *eds1-2* mutation is epistatic to *nudt7-1*, positioning NUDT7 downstream of EDS1 in the signalling pathway. It remained elusive whether the antagonistic effect of SA on *nudt7-1* growth retardation and cell

death initiation was also dependent on *EDS1*. I was able to confirm that the negative effects of SA on the *nudt7-1* growth and cell death phenotype are *EDS1*-dependent by analysis of the *nudt7-1/sid2-1/eds1-2* triple mutant (Figure 3.7). I concluded that *EDS1* mediates two distinct signalling events that are both negatively regulated by *NUDT7* (Figure 4.1). *EDS1* induces the accumulation of SA leading to activation of defence responses (Feys et al., 2001) and, in addition, triggers a pathway that is negatively regulated by SA leading to the initiation of cell death and suppression of growth. Positioning *NUDT7* downstream of *EDS1* as a negative regulator is further supported by the fact that *EDS1* transcript and protein levels are increased in the *nudt7-1* mutant (Figure 3.3B and C). Despite the lack of information on the transcriptional level, the data showing that *EDS1* protein levels are reduced in *nudt7-1/sid2-1* compared to *nudt7-1* (Figure 3.12B) suggest that *NUDT7* acts upstream of a positive feedback loop by which *EDS1* promotes its own expression via SA.

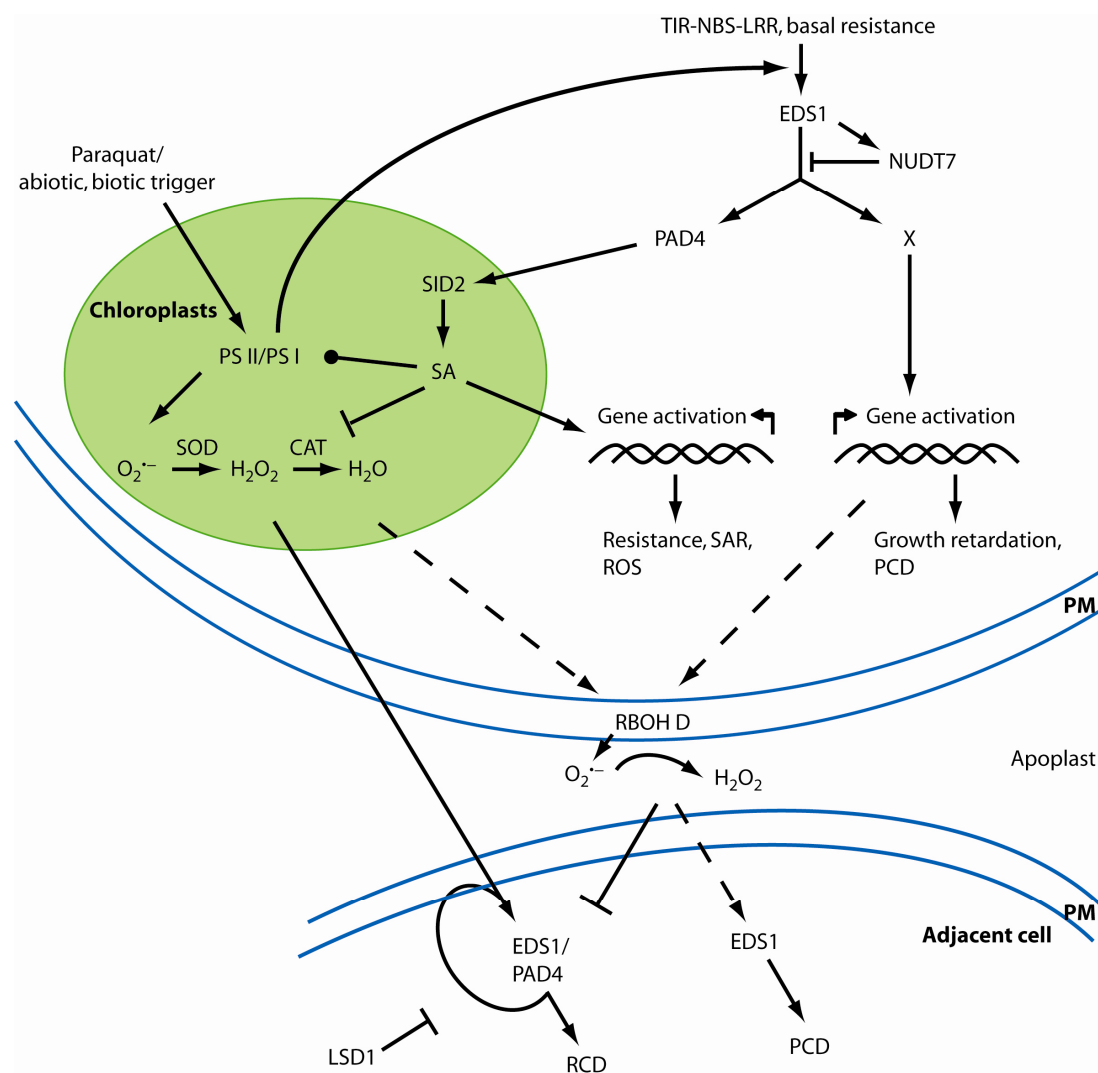


Figure 4.1: Model of *EDS1*-mediated signalling events upon oxidative stress induction

The model incorporates discussed results and hypotheses. Paraquat application activates *EDS1*-signalling which is deregulated in the *nutd7-1* mutant. Upon activation, *EDS1* triggers distinct signalling events (\rightarrow = positive regulation) leading to growth retardation, cell death and ROS accumulation. *EDS1* signalling could be negatively regulated by NUDT7 at the branch point of distinct *EDS1*-triggered pathways (\dashv = negative regulation). *EDS1* signal relay results in SA accumulation which is involved in several responses: SA was suggested to modulate photosynthesis (\bullet) and suppress CAT activity thereby potentially acting antagonistically on *EDS1* activation by ROS. SA and SA-dependent ROS generation might act in adjacent cells to trigger *EDS1/PAD4*-dependent runaway cell death (RCD). Programmed cell death (PCD) in *nutd7-1* is distinct from RCD and requires functional *AtRbohD*. Signals that activate *AtRbohD* could be derived from chloroplasts or from *EDS1* (dashed lines). *EDS1* could also act downstream of *AtRbohD* and be involved in cell death execution. For further details see text. PM = plasma membrane

4.8. Summary and perspectives

I have shown that the nudix hydrolase *NUDT7* negatively regulates distinct *EDS1*-mediated signalling branches governing growth retardation, SA-independent cell death initiation and SA-dependent ROS accumulation. *NUDT7* is part of a plant stress inducible genetic programme and largely post-transcriptionally regulated by *EDS1* in an indirect manner. Localization studies showed that *NUDT7* is restricted to the cytosol suggesting that it exerts its function in this compartment.

My work supports the view that MTI operates independently of the *EDS1* pathway and provides evidence that *NUDT7* is involved in the negative regulation of *EDS1*-mediated post-invasive resistance. Furthermore, the data presented reinforce a role of *EDS1* in oxidative stress signalling that underlies a negative regulatory effect of *NUDT7*. Exploring the roles of SA and the NADPH oxidase *AtRbohD* in *EDS1*-dependent ROS signalling emphasize the existence of distinct mechanisms of plant cell death initiation and cell death propagation.

The finding that *NUDT7* transcripts are responsive to numerous abiotic and biotic stresses suggests a broader role for *NUDT7* in regulation of plant stress responses. Identification of the *in vivo* substrate of *NUDT7* and elucidating how *NUDT7* is regulated at the transcriptional and post-transcriptional levels could help to evaluate how abiotic and biotic stress pathways are controlled.

A major challenge for future studies will be to dissect how distinct ROS signals are integrated in the *EDS1* pathway and transduced to cell death initiation and cell death propagation, respectively. Research on this theme could provide deeper insight into the poorly understood mechanisms of cell death control and its intersection with other stress and hormone response systems in plants. The fact that *EDS1* triggers SA-independent cell death prompts the question whether *EDS1*-dependent signalling engages other hormone pathways. Further analysis might help to understand mechanisms by which plants fine tune oxidative stress responses and defence signalling.

5. References

- Aarts, N., Metz, M., Holub, E., et al.** (1998). "Different requirements for EDS1 and NDR1 by disease resistance genes define at least two R gene-mediated signaling pathways in Arabidopsis." *Proceedings of the National Academy of Sciences of the United States of America* **95**(17): 10306-10311.
- Abramovitch, R. B. and Martin, G. B.** (2004). "Strategies used by bacterial pathogens to suppress plant defenses." *Current Opinion in Plant Biology* **7**(4): 356-364.
- Acharya, B. R., Raina, S., Maqbool, S. B., et al.** (2007). "Overexpression of CRK13, an Arabidopsis cysteine-rich receptor-like kinase, results in enhanced resistance to *Pseudomonas syringae*." *Plant Journal* **50**(3): 488-499.
- Adams-Phillips, L., Wan, J. R., Tan, X. P., et al.** (2008). "Discovery of ADP-ribosylation and other plant defense pathway elements through expression profiling of four different Arabidopsis-*Pseudomonas* R-avr interactions." *Molecular Plant-Microbe Interactions* **21**(5): 646-657.
- Alfano, J. R. and Collmer, A.** (2004). "Type III secretion system effector proteins: Double agents in bacterial disease and plant defense." *Annual Review of Phytopathology* **42**: 385-414.
- Alscher, R. G., Donahue, J. L. and Cramer, C. L.** (1997). "Reactive oxygen species and antioxidants: Relationships in green cells." *Physiologia Plantarum* **100**(2): 224-233.
- Apel, K. and Hirt, H.** (2004). "Reactive oxygen species: Metabolism, oxidative stress, and signal transduction." *Annual Review of Plant Biology* **55**: 373-399.
- Apostol, I., Heinstein, P. F. and Low, P. S.** (1989). "Rapid Stimulation of an Oxidative Burst During Elicitation of Cultured Plant-Cells - Role in Defense and Signal Transduction." *Plant Physiology* **90**(1): 109-116.
- Aro, E. M., Virgin, I. and Andersson, B.** (1993). "Photoinhibition of Photosystem-2 - Inactivation, Protein Damage and Turnover." *Biochimica Et Biophysica Acta* **1143**(2): 113-134.
- Asada, K.** (1999). "The water-water cycle in chloroplasts: Scavenging of active oxygens and dissipation of excess photons." *Annual Review of Plant Physiology and Plant Molecular Biology* **50**: 601-639.
- Asada, K.** (2000). "The water-water cycle as alternative photon and electron sinks." *Philosophical Transactions of the Royal Society of London Series B-Biological Sciences* **355**(1402): 1419-1430.
- Asai, T., Tena, G., Plotnikova, J., et al.** (2002). "MAP kinase signalling cascade in Arabidopsis innate immunity." *Nature* **415**(6875): 977-983.
- Aviv, D. H., Rusterucci, C., Holt, B. F., et al.** (2002). "Runaway cell death, but not basal disease resistance, in *Isd1* is SA- and NIM1/NPR1-dependent." *Plant Journal* **29**(3): 381-391.
- Axtell, M. J. and Staskawicz, B. J.** (2003). "Initiation of RPS2-specified disease resistance in Arabidopsis is coupled to the AvrRpt2-directed elimination of RIN4." *Cell* **112**(3): 369-377.
- Babbs, C. F., Pham, J. A. and Coolbaugh, R. C.** (1989). "Lethal Hydroxyl Radical Production in Paraquat-Treated Plants." *Plant Physiology* **90**(4): 1267-1270.
- Babior, B. M., Gilbert, D. L. and Colton, C. A.** (1999). "The production and use of reactive oxidants by phagocytes." *Reactive oxygen species in biological systems: An interdisciplinary approach*: 503-526.

- Barber, J.** (1998). "A multifaceted approach for elucidating the structure of photosystem II." *Photosynthesis: Mechanisms and Effects, Vols I-V*: 919-924.
- Bartsch, M., Gobbato, E., Bednarek, P., et al.** (2006). "Salicylic acid-independent ENHANCED DISEASE SUSCEPTIBILITY1 signaling in Arabidopsis immunity and cell death is regulated by the monooxygenase FMO1 and the nudix hydrolase NUDT7." *Plant Cell* **18**(4): 1038-1051.
- Bauer, Z., Gomez-Gomez, L., Boller, T., et al.** (2001). "Sensitivity of different ecotypes and mutants of Arabidopsis thaliana toward the bacterial elicitor flagellin correlates with the presence of receptor-binding sites." *Journal of Biological Chemistry* **276**(49): 45669-45676.
- Bechtold, U., Murphy, D. J. and Mullineaux, P. M.** (2004). "Arabidopsis peptide methionine sulfoxide reductase2 prevents cellular oxidative damage in long nights." *Plant Cell* **16**(4): 908-919.
- Bednarek, P., Pislewski-Bednarek, M., Svatos, A., et al.** (2009). "A glucosinolate metabolism pathway in living plant cells mediates broad-spectrum antifungal defense." *Science* **323**(5910): 101-6.
- Belkadir, Y., Subramaniam, R. and Dangl, J. L.** (2004). "Plant disease resistance protein signaling: NBS-LRR proteins and their partners." *Current Opinion in Plant Biology* **7**(4): 391-399.
- Bessman, M. J., Frick, D. N. and Ohandley, S. F.** (1996). "The MutT proteins or "nudix" hydrolases, a family of versatile, widely distributed, "housecleaning" enzymes." *Journal of Biological Chemistry* **271**(41): 25059-25062.
- Bittner-Eddy, P. D. and Beynon, J. L.** (2001). "The Arabidopsis downy mildew resistance gene, RPP13-Nd, functions independently of NDR1 and EDS1 and does not require the accumulation of salicylic acid." *Molecular Plant-Microbe Interactions* **14**(3): 416-421.
- Bolwell, G. P., Davies, D. R., Gerrish, C., et al.** (1998). "Comparative biochemistry of the oxidative burst produced by rose and French bean cells reveals two distinct mechanisms." *Plant Physiology* **116**(4): 1379-1385.
- Bonfoco, E., Krainc, D., Ankarcona, M., et al.** (1995). "Apoptosis and Necrosis - 2 Distinct Events Induced, Respectively, by Mild and Intense Insults with N-Methyl-D-Aspartate or Nitric-Oxide Superoxide in Cortical Cell-Cultures." *Proceedings of the National Academy of Sciences of the United States of America* **92**(16): 7162-7166.
- Bowling, S. A., Clarke, J. D., Liu, Y. D., et al.** (1997). "The cpr5 mutant of Arabidopsis expresses both NPR1-dependent and NPR1-independent resistance." *Plant Cell* **9**(9): 1573-1584.
- Bradley, D. J., Kjellbom, P. and Lamb, C. J.** (1992). "Elicitor-Induced and Wound-Induced Oxidative Cross-Linking of a Proline-Rich Plant-Cell Wall Protein - a Novel, Rapid Defense Response." *Cell* **70**(1): 21-30.
- Brodersen, P., Malinovsky, F. G., Hematy, K., et al.** (2005). "The role of salicylic acid in the induction of cell death in Arabidopsis acd11." *Plant Physiology* **138**(2): 1037-1045.
- Brodersen, P., Petersen, M., Nielsen, H. B., et al.** (2006). "Arabidopsis MAP kinase 4 regulates salicylic acid- and jasmonic acid/ethylene-dependent responses via EDS1 and PAD4." *Plant Journal* **47**(4): 532-546.
- Burch-Smith, T. M., Schiff, M., Caplan, J. L., et al.** (2007). "A novel role for the TIR domain in association with pathogen-derived elicitors." *PLoS Biology* **5**(3): doi:10.1371/journal.pbio.0050068.

- Cao, H., Bowling, S. A., Gordon, A. S., et al.** (1994). "Characterization of an Arabidopsis Mutant That Is Nonresponsive to Inducers of Systemic Acquired-Resistance." *Plant Cell* **6**(11): 1583-1592.
- Casper-Lindley, C., Dahlbeck, D., Clark, E. T., et al.** (2002). "Direct biochemical evidence for type III secretion-dependent translocation of the AvrBs2 effector protein into plant cells." *Proceedings of the National Academy of Sciences of the United States of America* **99**(12): 8336-8341.
- Chamnonpol, S., Willekens, H., Moeder, W., et al.** (1998). "Defense activation and enhanced pathogen tolerance induced by H₂O₂ in transgenic tobacco." *Proceedings of the National Academy of Sciences of the United States of America* **95**: 5818-5823.
- Chen, S. X. and Schopfer, P.** (1999). "Hydroxyl-radical production in physiological reactions - A novel function of peroxidase." *European Journal of Biochemistry* **260**(3): 726-735.
- Chen, Z. X., Silva, H. and Klessig, D. F.** (1993). "Active Oxygen Species in the Induction of Plant Systemic Acquired-Resistance by Salicylic-Acid." *Science* **262**(5141): 1883-1886.
- Chini, A., Grant, J. J., Seki, M., et al.** (2004). "Drought tolerance established by enhanced expression of the CC-NBS-LRR gene, ADR1, requires salicylic acid, EDS1 and ABI1." *Plant Journal* **38**(5): 810-822.
- Chisholm, S. T., Coaker, G., Day, B., et al.** (2006). "Host-microbe interactions: Shaping the evolution of the plant immune response." *Cell* **124**(4): 803-814.
- Clarke, J. D., Aarts, N., Feys, B. J., et al.** (2001). "Constitutive disease resistance requires EDS1 in the Arabidopsis mutants *cpr1* and *cpr6* and is partially EDS1-dependent in *cpr5*." *Plant Journal* **26**(4): 409-420.
- Clarke, J. D., Volko, S. M., Ledford, H., et al.** (2000). "Roles of salicylic acid, jasmonic acid, and ethylene in *cpr*-induced resistance in Arabidopsis." *Plant Cell* **12**(11): 2175-2190.
- Clough, S. J., Fengler, K. A., Yu, I. C., et al.** (2000). "The Arabidopsis *dnd1* "defense, no death" gene encodes a mutated cyclic nucleotide-gated ion channel." *Proceedings of the National Academy of Sciences of the United States of America* **97**(16): 9323-9328.
- Coaker, G., Falick, A. and Staskawicz, B.** (2005). "Activation of a phytopathogenic bacterial effector protein by a eukaryotic cyclophilin." *Science* **308**(5721): 548-550.
- Collins, N. C., Thordal-Christensen, H., Lipka, V., et al.** (2003). "SNARE-protein-mediated disease resistance at the plant cell wall." *Nature* **425**(6961): 973-7.
- Colville, L. and Smirnoff, N.** (2008). "Antioxidant status, peroxidase activity, and PR protein transcript levels in ascorbate-deficient Arabidopsis thaliana *vtc* mutants." *Journal of Experimental Botany* **59**(14): 3857-3868.
- Cunnac, S., Boucher, C. and Genin, S.** (2004). "Characterization of the cis-acting regulatory element controlling HrpB-mediated activation of the type III secretion system and effector genes in *Ralstonia solanacearum*." *Journal of Bacteriology* **186**(8): 2309-2318.
- Dangl, J. L. and Jones, J. D.** (2001). "Plant pathogens and integrated defence responses to infection." *Nature* **411**(6839): 826-33.
- Danon, A., Coll, N. S. and Apel, K.** (2006). "Cryptochrome-1-dependent execution of programmed cell death induced by singlet oxygen in Arabidopsis thaliana." *Proceedings of the National Academy of Sciences of the United States of America* **103**(45): 17036-17041.

- Dat, J. F., Pellinen, R., Beeckman, T., et al.** (2003). "Changes in hydrogen peroxide homeostasis trigger an active cell death process in tobacco." *Plant Journal* **33**(4): 621-632.
- Davletova, S., Rizhsky, L., Liang, H. J., et al.** (2005). "Cytosolic ascorbate peroxidase 1 is a central component of the reactive oxygen gene network of Arabidopsis." *Plant Cell* **17**(1): 268-281.
- De Block, M., Verduyn, C., De Brouwer, D., et al.** (2005). "Poly(ADP-ribose) polymerase in plants affects energy homeostasis, cell death and stress tolerance." *Plant Journal* **41**(1): 95-106.
- Delaney, T. P., Friedrich, L. and Ryals, J. A.** (1995). "Arabidopsis Signal-Transduction Mutant Defective in Chemically and Biologically Induced Disease Resistance." *Proceedings of the National Academy of Sciences of the United States of America* **92**(14): 6602-6606.
- Delaney, T. P., Uknes, S., Vernooij, B., et al.** (1994). "A Central Role of Salicylic-Acid in Plant-Disease Resistance." *Science* **266**(5188): 1247-1250.
- Delledonne, M., Zeier, J., Marocco, A., et al.** (2001). "Signal interactions between nitric oxide and reactive oxygen intermediates in the plant hypersensitive disease resistance response." *Proceedings of the National Academy of Sciences of the United States of America* **98**(23): 13454-13459.
- Deng, Q. and Barbieri, J. T.** (2008). "Molecular Mechanisms of the Cytotoxicity of ADP-Ribosylating Toxins." *Annual Review of Microbiology* **62**: 271-288.
- Deslandes, L., Olivier, J., Peeters, N., et al.** (2003). "Physical interaction between RRS1-R, a protein conferring resistance to bacterial wilt, and PopP2, a type III effector targeted to the plant nucleus." *Proceedings of the National Academy of Sciences of the United States of America* **100**(13): 8024-8029.
- Despres, C., Chubak, C., Rochon, A., et al.** (2003). "The Arabidopsis NPR1 disease resistance protein is a novel cofactor that confers redox regulation of DNA binding activity to the basic domain/leucine zipper transcription factor TGA1." *Plant Cell* **15**(9): 2181-2191.
- Devadas, S. K., Enyedi, A. and Raina, R.** (2002). "The Arabidopsis *hrl1* mutation reveals novel overlapping roles for salicylic acid, jasmonic acid and ethylene signalling in cell death and defence against pathogens." *Plant Journal* **30**(4): 467-480.
- Dharmasiri, N., Dharmasiri, S. and Estelle, M.** (2005). "The F-box protein TIR1 is an auxin receptor." *Nature* **435**(7041): 441-445.
- Dietrich, R. A., Richberg, M. H., Schmidt, R., et al.** (1997). "A novel zinc finger protein is encoded by the arabidopsis *LSD1* gene and functions as a negative regulator of plant cell death." *Cell* **88**(5): 685-694.
- Dodds, P. N., Lawrence, G. J., Catanzariti, A. M., et al.** (2006). "Direct protein interaction underlies gene-for-gene specificity and coevolution of the flax resistance genes and flax rust avirulence genes." *Proceedings of the National Academy of Sciences of the United States of America* **103**(23): 8888-8893.
- Doke, N. and Chai, H. B.** (1985). "Activation of Superoxide Generation and Enhancement of Resistance against Compatible Races of *Phytophthora-Infestans* in Potato Plants Treated with Digitonin." *Physiological Plant Pathology* **27**(3): 323-334.
- Draper, J.** (1997). "Salicylate, superoxide synthesis and cell suicide in plant defence." *Trends in Plant Science* **2**(5): 162-165.
- Durner, J. and Klessig, D. F.** (1996). "Salicylic acid is a modulator of tobacco and mammalian catalases." *Journal of Biological Chemistry* **271**(45): 28492-285.

- Durrant, J. R., Giorgi, L. B., Barber, J., et al.** (1990). "Characterization of Triplet-States in Isolated Photosystem-I Reaction Centers - Oxygen Quenching as a Mechanism for Photodamage." *Biochimica Et Biophysica Acta* **1017**(2): 167-175.
- Epple, P., Mack, A. A., Morris, V. R. F., et al.** (2003). "Antagonistic control of oxidative stress-induced cell death in Arabidopsis by two related, plant-specific zinc finger proteins." *Proceedings of the National Academy of Sciences of the United States of America* **100**(11): 6831-6836.
- Felix, G., Duran, J. D., Volko, S., et al.** (1999). "Plants have a sensitive perception system for the most conserved domain of bacterial flagellin." *Plant J* **18**(3): 265-76.
- Fernandez, A. P. and Strand, A.** (2008). "Retrograde signaling and plant stress: plastid signals initiate cellular stress responses." *Current Opinion in Plant Biology* **11**(5): 509-513.
- Feys, B. J., Moisan, L. J., Newman, M. A., et al.** (2001). "Direct interaction between the Arabidopsis disease resistance signaling proteins, EDS1 and PAD4." *Embo Journal* **20**(19): 5400-5411.
- Feys, B. J., Wiermer, M., Bhat, R. A., et al.** (2005). "Arabidopsis SENESCENCE-ASSOCIATED GENE101 stabilizes and signals within an ENHANCED DISEASE SUSCEPTIBILITY1 complex in plant innate immunity." *Plant Cell* **17**(9): 2601-2613.
- Fletcher, J., Bender, C., Budowle, B., et al.** (2006). "Plant pathogen forensics: capabilities, needs, and recommendations." *Microbiol Mol Biol Rev* **70**(2): 450-71.
- Fliegmann, J., Mithofer, A., Wanner, G., et al.** (2004). "An ancient enzyme domain hidden in the putative beta-glucan elicitor receptor of soybean may play an active part in the perception of pathogen-associated molecular patterns during broad host resistance." *J Biol Chem* **279**(2): 1132-40.
- Flor, H. H.** (1971). "Current Status of Gene-for-Gene Concept." *Annual Review of Phytopathology* **9**: 275-&.
- Fonfria, E., Marshall, I. C. B., Benham, C. D., et al.** (2004). "TRPM2 channel opening in response to oxidative stress is dependent on activation of poly(ADP-ribose) polymerase." *British Journal of Pharmacology* **143**(1): 186-192.
- Foyer, C. and Harbinson, J.** (1994). Oxygen metabolism and the regulation of photosynthetic electron transport. *Causes of Photooxidative Stress and Amelioration of Defense Systems in Plant*. C. Foyer and P. Mullineaux: 1-42.
- Foyer, C. H. and Noctor, G.** (2005). "Redox homeostasis and antioxidant signaling: A metabolic interface between stress perception and physiological responses." *Plant Cell* **17**(7): 1866-1875.
- Fryer, M. J., Oxborough, K., Mullineaux, P. M., et al.** (2002). "Imaging of photo-oxidative stress responses in leaves." *Journal of Experimental Botany* **53**(372): 1249-1254.
- Fujiki, Y., Yoshikawa, Y., Sato, T., et al.** (2001). "Dark-inducible genes from Arabidopsis thaliana are associated with leaf senescence and repressed by sugars." *Physiologia Plantarum* **111**(3): 345-352.
- Gadjev, I., Vanderauwera, S., Gechev, T. S., et al.** (2006). "Transcriptomic footprints disclose specificity of reactive oxygen species signaling in Arabidopsis." *Plant Physiology* **141**(2): 436-445.

- Gaffney, T., Friedrich, L., Vernooij, B., et al.** (1993). "Requirement of Salicylic-Acid for the Induction of Systemic Acquired-Resistance." *Science* **261**(5122): 754-756.
- Gagne, J. M., Smalle, J., Gingerich, D. J., et al.** (2004). "Arabidopsis EIN3-binding F-box 1 and 2 form ubiquitin-protein ligases that repress ethylene action and promote growth by directing EIN3 degradation." *Proceedings of the National Academy of Sciences of the United States of America* **101**(17): 6803-6808.
- Ge, X. C., Li, G. J., Wang, S. B., et al.** (2007). "AtNUDT7, a negative regulator of basal immunity in arabidopsis, modulates two distinct defense response pathways and is involved in maintaining redox homeostasis." *Plant Physiology* **145**(1): 204-215.
- Glazebrook, J., Rogers, E. E. and Ausubel, F. M.** (1996). "Isolation of Arabidopsis mutants with enhanced disease susceptibility by direct screening." *Genetics* **143**(2): 973-982.
- Glazebrook, J., Rogers, E. E. and Ausubel, F. M.** (1997). "Use of Arabidopsis for genetic dissection of plant defense responses." *Annual Review of Genetics* **31**: 547-569.
- Goehre, V., Spallek, T., Haeweker, H., et al.** (2008). "Plant Pattern-Recognition Receptor FLS2 Is Directed for Degradation by the Bacterial Ubiquitin Ligase AvrPtoB." *Current Biology* **18**(23): 1824-1832.
- Gomez-Gomez, L., Felix, G. and Boller, T.** (1999). "A single locus determines sensitivity to bacterial flagellin in Arabidopsis thaliana." *Plant Journal* **18**(3): 277-284.
- Gomez-Gomez, L. and Boller, T.** (2000). "FLS2: an LRR receptor-like kinase involved in the perception of the bacterial elicitor flagellin in Arabidopsis." *Mol Cell* **5**(6): 1003-11.
- Gomez-Gomez, L., Bauer, Z. and Boller, T.** (2001). "Both the extracellular leucine-rich repeat domain and the kinase activity of FSL2 are required for flagellin binding and signaling in Arabidopsis." *Plant Cell* **13**(5): 1155-63.
- Goodman, R. N. and Novacky, A. J.** The hypersensitive response in plants to pathogens, APS Press, St. Paul.
- Groom, Q. J., Torres, M. A., Fordham-Skelton, A. P., et al.** (1996). "rbohA a rice homologue of the mammalian gp91phox respiratory burst oxidase gene." *Plant Journal* **10**(3): 515-522.
- Guo, H. W. and Ecker, J. R.** (2003). "Plant responses to ethylene gas are mediated by SCF (EBF1/EBF2)-dependent proteolysis of EIN3 transcription factor." *Cell* **115**(6): 667-677.
- Halkier, B. A. and Gershenzon, J.** (2006). "Biology and biochemistry of glucosinolates." *Annu Rev Plant Biol* **57**: 303-33.
- Hammond-Kosack, K. E. and Parker, J. E.** (2003). "Deciphering plant-pathogen communication: fresh perspectives for molecular resistance breeding." *Curr Opin Biotechnol* **14**(2): 177-93.
- Hara-Nishimura, I., Hatsugai, N., Nakaune, S., et al.** (2005). "Vacuolar processing enzyme: an executor of plant cell death." *Current Opinion in Plant Biology* **8**(4): 404-408.
- Hauck, P., Thilmony, R. and He, S. Y.** (2003). "A Pseudomonas syringae type III effector suppresses cell wall-based extracellular defense in susceptible Arabidopsis plants." *Proceedings of the National Academy of Sciences of the United States of America* **100**(14): 8577-8582.

- Heath, M. C.** (2000). "Nonhost resistance and nonspecific plant defenses." *Curr Opin Plant Biol* **3**(4): 315-9.
- Hideg, E., Spetea, C. and Vass, I.** (1994). "Singlet Oxygen and Free-Radical Production During Acceptor-Induced and Donor-Side-Induced Photoinhibition - Studies with Spin-Trapping Epr Spectroscopy." *Biochimica Et Biophysica Acta-Bioenergetics* **1186**(3): 143-152.
- Hideg, E., Kalai, T., Hideg, K., et al.** (1998). "Photoinhibition of photosynthesis in vivo results in singlet oxygen production detection via nitroxide-induced fluorescence quenching in broad bean leaves." *Biochemistry* **37**(33): 11405-11411.
- Hideg, E., Barta, C., Kalai, T., et al.** (2002). "Detection of singlet oxygen and superoxide with fluorescent sensors in leaves under stress by photoinhibition or UV radiation." *Plant and Cell Physiology* **43**(10): 1154-1164.
- Hilpert, B., Bohlmann, H., op den Camp, R., et al.** (2001). "Isolation and characterization of signal transduction mutants of *Arabidopsis thaliana* that constitutively activate the octadecanoid pathway and form necrotic microlesions." *Plant Journal* **26**(4): 435-446.
- Jabs, T., Dietrich, R. A. and Dangl, J. L.** (1996). "Initiation of runaway cell death in an *Arabidopsis* mutant by extracellular superoxide." *Science* **273**(5283): 1853-1856.
- Jambunathan, N. and Mahalingam, R.** (2006). "Analysis of *Arabidopsis* Growth Factor Gene 1 (GFG1) encoding a nudix hydrolase during oxidative signaling." *Planta* **224**(1): 1-11.
- Janeway, C. A., et al.**, (2001). *Immunobiology* 5th ed.
- Jia, Y., Bryan, G. T., Farrall, L., et al.** (2000). "Direct interaction of resistance gene and avirulence gene products confers rice blast resistance." *Phytopathology* **90**(6 Supplement): S110.
- Jirage, D., Tootle, T. L., Reuber, T. L., et al.** (1999). "*Arabidopsis thaliana* PAD4 encodes a lipase-like gene that is important for salicylic acid signaling." *Proceedings of the National Academy of Sciences of the United States of America* **96**(23): 13583-13588.
- Jones, J. D. and Dangl, J. L.** (2006). "The plant immune system." *Nature* **444**(7117): 323-9.
- Jong de, A. J., Yakimova, E. T., Kapchina, V. M., et al.** (2002). "A critical role for ethylene in hydrogen peroxide release during programmed cell death in tomato suspension cells." *Planta* **214**(4): 537-545.
- Joo, J. H., Wang, S. Y., Chen, J. G., et al.** (2005). "Different signaling and cell death roles of heterotrimeric G protein alpha and beta subunits in the *Arabidopsis* oxidative stress response to ozone." *Plant Cell* **17**(3): 957-970.
- Kachroo, P., Yoshioka, K., Shah, J., et al.** (2000). "Resistance to turnip crinkle virus in *Arabidopsis* is regulated by two host genes and is salicylic acid dependent but NPR1, ethylene, and jasmonate independent." *Plant Cell* **12**(5): 677-690.
- Kachroo, P., Venugopal, S. C., Navarre, D. A., et al.** (2005). "Role of salicylic acid and fatty acid desaturation pathways in *ssi2*-mediated signaling." *Plant Physiology* **139**(4): 1717-1735.
- Kaku, H., Nishizawa, Y., Ishii-Minami, N., et al.** (2006). "Plant cells recognize chitin fragments for defense signaling through a plasma membrane receptor." *Proc Natl Acad Sci U S A* **103**(29): 11086-91.

- Katsir, L., Chung, H. S., Koo, A. J. K., et al.** (2008). "Jasmonate signaling: a conserved mechanism of hormone sensing." *Current Opinion in Plant Biology* **11**(4): 428-435.
- Kaminaka, H., Nake, C., Epple, P., et al.** (2006). "bZIP10-LSD1 antagonism modulates basal defense and cell death in Arabidopsis following infection." *Embo Journal* **25**(18): 4400-4411.
- Kiedrowski, S., Kawalleck, P., Hahlbrock, K., et al.** (1992). "Rapid Activation of a Novel Plant Defense Gene Is Strictly Dependent on the Arabidopsis-Rpm1 Disease Resistance Locus." *Embo Journal* **11**(13): 4677-4684.
- Kim, H. S., Desveaux, D., Singer, A. U., et al.** (2005). "The Pseudomonas syringae effector AvrRpt2 cleaves its C-terminally acylated target, RIN4, from Arabidopsis membranes to block RPM1 activation." *Proceedings of the National Academy of Sciences of the United States of America* **102**(18): 6496-6501.
- Kim, C. H., Meskauskiene, R., Apel, K., et al.** (2008). "No single way to understand singlet oxygen signalling in plants." *Embo Reports* **9**(5): 435-439.
- Klessig, D. F., Durner, J., Noad, R., et al.** (2000). "Nitric oxide and salicylic acid signaling in plant defense." *Proceedings of the National Academy of Sciences of the United States of America* **97**(16): 8849-+.
- Kloek, A. P., Verbsky, M. L., Sharma, S. B., et al.** (2001). "Resistance to Pseudomonas syringae conferred by an Arabidopsis thaliana coronatine-insensitive (coi1) mutation occurs through two distinct mechanisms." *Plant Journal* **26**(5): 509-522.
- Klotz, L. O.** (2002). "Oxidant-induced signaling: Effects of peroxynitrite and singlet oxygen." *Biological Chemistry* **383**(3-4): 443-456.
- Kobayashi, Y., Kobayashi, I., Funaki, Y., et al.** (1997). "Dynamic reorganization of microfilaments and microtubules is necessary for the expression of non-host resistance in barley coleoptile cells." *The Plant Journal* **11**(3): 525-537.
- Koch, M., Vorwerk, S., Masur, C., et al.** (2006). "A role for a flavin-containing mono-oxygenase in resistance against microbial pathogens in Arabidopsis." *Plant Journal* **47**(4): 629-639.
- Krieger-Liszak, A.** (2005). "Singlet oxygen production in photosynthesis." *Journal of Experimental Botany* **56**(411): 337-346.
- Kukavica, B., Mojovic, M., Vuccinic, Z., et al.** (2009). "Generation of hydroxyl radical in isolated pea root cell wall, and the role of cell wall-bound peroxidase, Mn-SOD and phenolics in their production." *Plant Cell Physiol.* **50**(2): 304-317.
- Kunkel, B. N. and Brooks, D. M.** (2002). "Cross talk between signaling pathways in pathogen defense." *Current Opinion in Plant Biology* **5**(4): 325-331.
- Kunze, G., Zipfel, C., Robatzek, S., et al.** (2004). "The N terminus of bacterial elongation factor Tu elicits innate immunity in Arabidopsis plants." *Plant Cell* **16**(12): 3496-507.
- Kuroyanagi, M., Yamada, K., Hatsugai, N., et al.** (2005). "Vacuolar processing enzyme is essential for mycotoxin-induced cell death in Arabidopsis thaliana." *Journal of Biological Chemistry* **280**(38): 32914-32920.
- Kwak, J. M., Mori, I. C., Pei, Z. M., et al.** (2003). "NADPH oxidase AtrbohD and AtrbohF genes function in ROS-dependent ABA signaling in Arabidopsis." *Embo Journal* **22**(11): 2623-2633.
- Kwon, C., Neu, C., Pajonk, S., et al.** (2008). "Co-option of a default secretory pathway for plant immune responses." *Nature* **451**(7180): 835-40.

- La Camera, S., Geoffroy, P., Samaha, H., et al.** (2005). "A pathogen-inducible patatin-like lipid acyl hydrolase facilitates fungal and bacterial host colonization in *Arabidopsis*." *Plant Journal* **44**(5): 810-825.
- Laloi, C., Apel, K. and Danon, A.** (2004). "Reactive oxygen signalling: the latest news." *Current Opinion in Plant Biology* **7**(3): 323-328.
- Laloi, C., Przybyla, D. and Apel, K.** (2006). "A genetic approach towards elucidating the biological activity of different reactive oxygen species in *Arabidopsis thaliana*." *Journal of Experimental Botany* **57**(8): 1719-1724.
- Laloi, C., Stachowiak, M., Pers-Kamczyc, E., et al.** (2007). "Cross-talk between singlet oxygen- and hydrogen peroxide-dependent signaling of stress responses in *Arabidopsis thaliana*." *Proceedings of the National Academy of Sciences of the United States of America* **104**(2): 672-677.
- Lamb, C. and Dixon, R. A.** (1997). "The oxidative burst in plant disease resistance." *Annual Review of Plant Physiology and Plant Molecular Biology* **48**: 251-275.
- Lawton, K. A., Potter, S. L., Uknes, S., et al.** (1994). "Acquired-Resistance Signal-Transduction in *Arabidopsis* Is Ethylene Independent." *Plant Cell* **6**(5): 581-588.
- Lee, K. P., Kim, C., Landgraf, F., et al.** (2007). "EXECUTER1- and EXECUTER2-dependent transfer of stress-related signals from the plastid to the nucleus of *Arabidopsis thaliana*." *Proceedings of the National Academy of Sciences of the United States of America* **104**(24): 10270-10275.
- Leon, J., Lawton, M. A. and Raskin, I.** (1995). "Hydrogen-Peroxide Stimulates Salicylic-Acid Biosynthesis in Tobacco." *Plant Physiology* **108**(4): 1673-1678.
- Levine, A., Tenhaken, R., Dixon, R., et al.** (1994). "H₂O₂ from the Oxidative Burst Orchestrates the Plant Hypersensitive Disease Resistance Response." *Cell* **79**(4): 583-593.
- Lieberherr, D., Wagner, U., Dubuis, P. H., et al.** (2003). "The rapid induction of glutathione S-transferases AtGSTF2 and AtGSTF6 by avirulent *Pseudomonas syringae* is the result of combined salicylic acid and ethylene signaling." *Plant and Cell Physiology* **44**(7): 750-757.
- Lin, S. S., Martin, R., Mongrand, S., et al.** (2008). "RING1 E3 ligase localizes to plasma membrane lipid rafts to trigger FB1-induced programmed cell death in *Arabidopsis*." *Plant Journal* **56**(4): 550-561.
- Lindeberg, M., Cartinhour, S., Myers, C. R., et al.** (2006). "Closing the circle on the discovery of genes encoding Hrp regulon members and type III secretion system effectors in the genomes of three model *Pseudomonas syringae* strains." *Molecular Plant-Microbe Interactions* **19**(11): 1151-1158.
- Lipka, V., Dittgen, J., Bednarek, P., et al.** (2005). "Pre- and postinvasion defenses both contribute to nonhost resistance in *Arabidopsis*." *Science* **310**(5751): 1180-3.
- Lorrain, S., Vaillau, F., Balaque, C., et al.** (2003). "Lesion mimic mutants: keys for deciphering cell death and defense pathways in plants?" *Trends in Plant Science* **8**(6): 263-271.
- Luhua, S., Ciftci-Yilmaz, S., Harper, J., et al.** (2008). "Enhanced tolerance to oxidative stress in transgenic *Arabidopsis* plants expressing proteins of unknown function." *Plant Physiology* **148**(1): 280-292.
- Mackey, D., Belkhadir, Y., Alonso, J. M., et al.** (2003). "*Arabidopsis* RIN4 is a target of the type III virulence effector AvrRpt2 and modulates RPS2-mediated resistance." *Cell* **112**(3): 379-389.

- Mackey, D., Holt, B. F., Wiig, A., et al.** (2002). "RIN4 interacts with *Pseudomonas syringae* type III effector molecules and is required for RPM1-mediated resistance in *Arabidopsis*." *Cell* **108**(6): 743-754.
- Mateo, A., Funck, D., Muhlenbock, P., et al.** (2006). "Controlled levels of salicylic acid are required for optimal photosynthesis and redox homeostasis." *Journal of Experimental Botany* **57**(8): 1795-1807.
- Mateo, A., Muhlenbock, P., Rusterucci, C., et al.** (2004). "Lesion simulating disease 1 - Is required for acclimation to conditions that promote excess excitation energy." *Plant Physiology* **136**(1): 2818-2830.
- Maxwell, D. P., Nickels, R. and McIntosh, L.** (2002). "Evidence of mitochondrial involvement in the transduction of signals required for the induction of genes associated with pathogen attack and senescence." *Plant Journal* **29**(3): 269-279.
- McDowell, J. M., Cuzick, A., Can, C., et al.** (2000). "Downy mildew (*Peronospora parasitica*) resistance genes in *Arabidopsis* vary in functional requirements for NDR1, EDS1, NPR1 and salicylic acid accumulation." *Plant Journal* **22**(6): 523-529.
- McLennan, A. G.** (2006). "The Nudix hydrolase superfamily." *Cellular and Molecular Life Sciences* **63**(2): 123-143.
- McLusky, S., Bennett, M. H., Beale, M. H., et al.** (1999). "Cell wall alterations and localized accumulation of feruloyl-3'-methoxytyramine in onion epidermis at sites of attempted penetration by *Botrytis allii* are associated with actin polarisation, peroxidase activity and suppression of flavonoid biosynthesis." *The Plant Journal* **17**(5): 523-534.
- Mehler, A. H.** (1951). "Studies on Reactions of Illuminated Chloroplasts .1. Mechanism of the Reduction of Oxygen and Other Hill Reagents." *Archives of Biochemistry and Biophysics* **33**(1): 65-77.
- Meskauskiene, R., Nater, M., Goslings, D., et al.** (2001). "FLU: A negative regulator of chlorophyll biosynthesis in *Arabidopsis thaliana*." *Proceedings of the National Academy of Sciences of the United States of America* **98**(22): 12826-12831.
- Meyers, B. C., Koziak, A., Griego, A., et al.** (2003). "Genome-wide analysis of NBS-LRR-encoding genes in *Arabidopsis*." *Plant Cell* **15**(4): 809-834.
- Mildvan, A. S., Xia, Z., Azurmendi, H. F., et al.** (2005). "Structures and mechanisms of Nudix hydrolases." *Archives of Biochemistry and Biophysics* **433**(1): 129-143.
- Miller, G., Suzuki, N., Rizhsky, L., et al.** (2007). "Double mutants deficient in cytosolic and thylakoid ascorbate peroxidase reveal a complex mode of interaction between reactive oxygen species, plant development, and response to abiotic stresses(1[W][OA])." *Plant Physiology* **144**(4): 1777-1785.
- Miller, G., Shulaev, V. and Mittler, R.** (2008). "Reactive oxygen signaling and abiotic stress." *Physiologia Plantarum* **133**(3): 481-489.
- Mishina, T. E. and Zeier, J.** (2006). "The *Arabidopsis* flavin-dependent monooxygenase FMO1 is an essential component of biologically induced systemic acquired resistance." *Plant Physiology* **141**(4): 1666-1675.
- Mittler, R., Lam, E., Shulaev, V., et al.** (1999). "Signals controlling the expression of cytosolic ascorbate peroxidase during pathogen-induced programmed cell death in tobacco." *Plant Molecular Biology* **39**(5): 1025-1035.
- Mittler, R., Vanderauwera, S., Gollery, M., et al.** (2004). "Reactive oxygen gene network of plants." *Trends in Plant Science* **9**(10): 490-498.

- Mou, Z., Fan, W. H. and Dong, X. N.** (2003). "Inducers of plant systemic acquired resistance regulate NPR1 function through redox changes." *Cell* **113**(7): 935-944.
- Mowla, S. B., Cuypers, A., Driscoll, S. P., et al.** (2006). "Yeast complementation reveals a role for an *Arabidopsis thaliana* late embryogenesis abundant (LEA)-like protein in oxidative stress tolerance." *Plant Journal* **48**(5): 743-756.
- Muehlenbock, P., Plaszczyca, M., Plaszczyca, M., et al.** (2007). "Lysigenous aerenchyma formation in *Arabidopsis* is controlled by LESION SIMULATING DISEASE1." *Plant Cell* **19**(11): doi:10.1105/tpc.106.048843.
- Muehlenbock, P., Szechynska-Hebda, M., Plaszczyca, M., et al.** (2008). "Chloroplast Signaling and LESION SIMULATING DISEASE1 Regulate Crosstalk between Light Acclimation and Immunity in *Arabidopsis*." *Plant Cell* **20**(9): 2339-2356.
- Mur, L. A. J., Kenton, P., Atzorn, R., et al.** (2006). "The outcomes of concentration-specific interactions between salicylate and jasmonate signaling include synergy, antagonism, and oxidative stress leading to cell death." *Plant Physiology* **140**(1): 249-262.
- Navarro, L., Zipfel, C., Rowland, O., et al.** (2004). "The transcriptional innate immune response to flg22. Interplay and overlap with Avr gene-dependent defense responses and bacterial pathogenesis." *Plant Physiol* **135**(2): 1113-28.
- Nawrath, C. and Metraux, J. P.** (1999). "Salicylic acid induction-deficient mutants of *Arabidopsis* express PR-2 and PR-5 and accumulate high levels of camalexin after pathogen inoculation." *Plant Cell* **11**(8): 1393-1404.
- Nawrath, C., Heck, S., Parinthewong, N., et al.** (2002). "EDS5, an essential component of salicylic acid-dependent signaling for disease resistance in *Arabidopsis*, is a member of the MATE transporter family." *Plant Cell* **14**(1): 275-286.
- Ndamukong, I., Al Abdallat, A., Thurow, C., et al.** (2007). "SA-inducible *Arabidopsis* glutaredoxin interacts with TGA factors and suppresses JA-responsive PDF1.2 transcription." *Plant Journal* **50**(1): 128-139.
- Nibbe, M., Hilpert, B., Wasternack, C., et al.** (2002). "Cell death and salicylate- and jasmonate-dependent stress responses in *Arabidopsis* are controlled by single *cet* genes." *Planta* **216**(1): 120-128.
- Nimchuk, Z., Eulgem, T., Holt, B. E., et al.** (2003). "Recognition and response in the plant immune system." *Annual Review of Genetics* **37**: 579-609.
- Nuhse, T. S., Peck, S. C., Hirt, H., et al.** (2000). "Microbial elicitors induce activation and dual phosphorylation of the *Arabidopsis thaliana* MAPK 6." *Journal of Biological Chemistry* **275**(11): 7521-7526.
- Nurnberger, T., Brunner, F., Kemmerling, B., et al.** (2004). "Innate immunity in plants and animals: striking similarities and obvious differences." *Immunol Rev* **198**: 249-66.
- Ochsenbein, C., Przybyla, D., Danon, A., et al.** (2006). "The role of EDS1 (enhanced disease susceptibility) during singlet oxygen-mediated stress responses of *Arabidopsis*." *Plant Journal* **47**(3): 445-456.
- Ogawa, T., Ueda, Y., Yoshimura, K., et al.** (2005). "Comprehensive analysis of cytosolic nudix hydrolases in *Arabidopsis thaliana*." *Journal of Biological Chemistry* **280**(26): 25277-25283.
- Ogawa, T., Ishikawa, K., Harada, K., et al.** (2009). "Overexpression of an ADP-ribose pyrophosphatase, AtNUDX2, confers enhanced tolerance to oxidative stress in *Arabidopsis* plants." *Plant Journal* **57**(2): 289-301.

- Olejniak, K., Plochocka, D., Grynberg, M., et al.** (2007). "Mutational analysis of the AtNUDT7 nudix hydrolase: Characterization of the critical residues in the Arabidopsis thaliana ADPRase." *Febs Journal* **274**: 202-202.
- Olszak, B., Malinovsky, F. G., Brodersen, P., et al.** (2006). "A putative flavin-containing mono-oxygenase as a marker for certain defense and cell death pathways." *Plant Science* **170**(3): 614-623.
- Op den Camp, R. G. L., Przybyla, D., Ochsenbein, C., et al.** (2003). "Rapid induction of distinct stress responses after the release of singlet oxygen in arabidopsis." *Plant Cell* **15**(10): 2320-2332.
- Ort, D. R. and Baker, N. R.** (2002). "A photoprotective role for O-2 as an alternative electron sink in photosynthesis?" *Current Opinion in Plant Biology* **5**(3): 193-198.
- Osterlund, M. T., Hardtke, C. S., Wei, N., et al.** (2000). "Targeted destabilization of HY5 during light-regulated development of Arabidopsis." *Nature* **405**(6785): 462-466.
- Overmyer, K., Brosche, M. and Kangasjarvi, J.** (2003). "Reactive oxygen species and hormonal control of cell death." *Trends in Plant Science* **8**(7): 335-342.
- Overmyer, K., Brosche, M., Pellinen, R., et al.** (2005). "Ozone-induced programmed cell death in the Arabidopsis radical-induced cell death1 mutant." *Plant Physiology* **137**(3): 1092-1104.
- Parker, J. E., Holub, E. B., Frost, L. N., et al.** (1996). "Characterization of eds1, a mutation in Arabidopsis suppressing resistance to Peronospora parasitica specified by several different RPP genes." *Plant Cell* **8**(11): 2033-2046.
- Peck, S. C., Nuhse, T. S., Hess, D., et al.** (2001). "Directed proteomics identifies a plant-specific protein rapidly phosphorylated in response to bacterial and fungal elicitors." *Plant Cell* **13**(6): 1467-1475.
- Penninckx, I., Thomma, B., Buchala, A., et al.** (1998). "Concomitant activation of jasmonate and ethylene response pathways is required for induction of a plant defensin gene in Arabidopsis." *Plant Cell* **10**(12): 2103-2113.
- Perraud, A. L., Fleig, A., Dunn, C. A., et al.** (2001). "ADP-ribose gating of the calcium-permeable LTRPC2 channel revealed by Nudix motif homology." *Nature* **411**(6837): 595-599.
- Pitzschke, A., Forzani, C. and Hirt, H.** (2006). "Reactive oxygen species signaling in plants." *Antioxidants & Redox Signaling* **8**(9-10): 1757-1764.
- Potuschak, T., Lechner, E., Parmentier, Y., et al.** (2003). "EIN3-dependent regulation of plant ethylene hormone signaling by two Arabidopsis F box proteins: EBF1 and EBF2." *Cell* **115**(6): 679-689.
- Pre, M., Atallah, M., Champion, A., et al.** (2008). "The AP2/ERF domain transcription factor ORA59 integrates jasmonic acid and ethylene signals in plant defense." *Plant Physiology* **147**(3): 1347-1357.
- Purvis, A. C.** (1997). "The role of adaptive enzymes in carbohydrate oxidation by stressed and senescing plant tissues." *Hortscience* **32**(7): 1165-1168.
- Quint, M. and Gray, W. M.** (2006). "Auxin signaling." *Current Opinion in Plant Biology* **9**(5): 448-453.
- Rajjou, L., Belghazi, M., Huguet, R., et al.** (2006). "Proteomic investigation of the effect of salicylic acid on Arabidopsis seed germination and establishment of early defense mechanisms." *Plant Physiology* **141**(3): 910-923.
- Rate, D. N., Cuenca, J. V., Bowman, G. R., et al.** (1999). "The gain-of-function Arabidopsis acd6 mutant reveals novel regulation and function of the salicylic

- acid signaling pathway in controlling cell death, defenses, and cell growth." *Plant Cell* **11**(9): 1695-1708.
- Rate, D. N. and Greenberg, J. T.** (2001). "The Arabidopsis aberrant growth and death2 mutant shows resistance to *Pseudomonas syringae* and reveals a role for NPR1 in suppressing hypersensitive cell death." *Plant Journal* **27**(3): 203-211.
- Ravet, K., Touraine, B., Boucherez, J., et al.** (2009). "Ferritins control interaction between iron homeostasis and oxidative stress in Arabidopsis." *Plant Journal* **57**(3): 400-412.
- Richards, K. D., Schott, E. J., Sharma, Y. K., et al.** (1998). "Aluminum induces oxidative stress genes in Arabidopsis thaliana." *Plant Physiology* **116**(1): 409-418.
- Ritter, C. and Dangl, J. L.** (1996). "Interference between two specific pathogen recognition events mediated by distinct plant disease resistance genes." *Plant Cell* **8**(2): 251-257.
- Robert-Seilantiz, A., Navarro, L., Bari, R., et al.** (2007). "Pathological hormone imbalances." *Current Opinion in Plant Biology* **10**: 372-379.
- Rouet, M. A., Mathieu, Y. and Lauriere, C.** (2006). "Characterization of active oxygen-producing proteins in response to hypo-osmolarity in tobacco and Arabidopsis cell suspensions: identification of a cell wall peroxidase." *Journal of Experimental Botany* **57**(6): 1323-1332.
- Rusterucci, C., Aviv, D. H., Holt, B. F., et al.** (2001). "The disease resistance signaling components EDS1 and PAD4 are essential regulators of the cell death pathway controlled by LSD1 in Arabidopsis." *Plant Cell* **13**(10): 2211-2224.
- Saijo, Y., Sullivan, J. A., Wang, H. Y., et al.** (2003). "The COP1-SPA1 interaction defines a critical step in phytochrome A-mediated regulation of HY5 activity." *Genes & Development* **17**(21): 2642-2647.
- Schenk, P. M., Kazan, K., Wilson, I., et al.** (2000). "Coordinated plant defense responses in Arabidopsis revealed by microarray analysis." *Proceedings of the National Academy of Sciences of the United States of America* **97**(21): 11655-11660.
- Schulze-Lefert, P.** (2004). "Knocking on the heaven's wall: pathogenesis of and resistance to biotrophic fungi at the cell wall." *Curr Opin Plant Biol* **7**(4): 377-83.
- Seo, H. S., Yang, J. Y., Ishikawa, M., et al.** (2003). "LAF1 ubiquitination by COP1 controls photomorphogenesis and is stimulated by SPA1." *Nature* **423**(6943): 995-999.
- Shao, F., Golstein, C., Ade, J., et al.** (2003). "Cleavage of Arabidopsis PBS1 by a bacterial type III effector." *Science* **301**(5637): 1230-1233.
- Shapiro, A. D. and Zhang, C.** (2001). "The role of NDR1 in avirulence gene-directed signaling and control of programmed cell death in Arabidopsis." *Plant Physiology* **127**(3): 1089-1101.
- Shen, Q. H., Saijo, Y., Mauch, S., et al.** (2007). "Nuclear activity of MLA immune receptors links isolate-specific and basal disease-resistance responses." *Science* **315**(5815): 1098-1103.
- Stein, M., Dittgen, J., Sanchez-Rodriguez, C., et al.** (2006). "Arabidopsis PEN3/PDR8, an ATP binding cassette transporter, contributes to nonhost resistance to inappropriate pathogens that enter by direct penetration." *Plant Cell* **18**(3): 731-46.
- Strawn, M. A., Marr, S. K., Inoue, K., et al.** (2007). "Arabidopsis isochorismate synthase functional in pathogen-induced salicylate biosynthesis exhibits

- properties consistent with a role in diverse stress responses." *Journal of Biological Chemistry* **282**(8): 5919-5933.
- Tada, Y., Spoel, S. H., Pajerowska-Mukhtar, K., et al.** (2008). "Plant immunity requires conformational changes of NPR1 via S-nitrosylation and thioredoxins." *Science* **321**(5891): 952-956.
- Tao, Y., Xie, Z., Chen, W., et al.** (2003). "Quantitative nature of Arabidopsis responses during compatible and incompatible interactions with the bacterial pathogen *Pseudomonas syringae*." *Plant Cell* **15**(2): 317-30.
- Ting, J. P. Y. and Williams, K. L.** (2005). "The CATERPILLER family: An ancient family of immune/apoptotic proteins." *Clinical Immunology* **115**(1): 33-37.
- Tiwari, B. S., Belenghi, B. and Levine, A.** (2002). "Oxidative stress increased respiration and generation of reactive oxygen species, resulting in ATP depletion, opening of mitochondrial permeability transition, and programmed cell death." *Plant Physiology* **128**(4): 1271-1281.
- Torres, M. A., Onouchi, H., Hamada, S., et al.** (1998). "Six Arabidopsis thaliana homologues of the human respiratory burst oxidase (gp91(phox))." *Plant Journal* **14**(3): 365-370.
- Torres, M. A., Dangl, J. L. and Jones, J. D. G.** (2002). "Arabidopsis gp91(phox) homologues AtrbohD and AtrbohF are required for accumulation of reactive oxygen intermediates in the plant defense response." *Proceedings of the National Academy of Sciences of the United States of America* **99**(1): 517-522.
- Torres, M. A., Jones, J. D. G. and Dangl, J. L.** (2005). "Pathogen-induced, NADPH oxidase-derived reactive oxygen intermediates suppress spread of cell death in Arabidopsis thaliana." *Nature Genetics* **37**(10): 1130-1134.
- Tsuda, K., Sato, M., Glazebrook, J., et al.** (2008). "Interplay between MAMP-triggered and SA-mediated defense responses." *Plant Journal* **53**(5): 763-775.
- Van Breusegem, F. and Dat, J. F.** (2006). "Reactive oxygen species in plant cell death." *Plant Physiology* **141**(2): 384-390.
- van der Biezen, E. A. and Jones, J. D. G.** (1998). "Plant disease-resistance proteins and the gene-for-gene concept." *Trends in Biochemical Sciences* **23**(12): 454-456.
- Van Mieghem, F. J. E., Nitschke, W., Mathis, P., et al.** (1989). "The Influence of the Quinone-Iron Electron Acceptor Complex on the Reaction Center Photochemistry of Photosystem II." *Biochimica et Biophysica Acta* **977**(2): 207-214.
- Van Wees, S. C. M. and Glazebrook, J.** (2003). "Loss of non-host resistance of Arabidopsis NahG to *Pseudomonas syringae* pv. phaseolicola is due to degradation products of salicylic acid." *Plant Journal* **33**(4): 733-742.
- Veraestrella, R., Blumwald, E. and Higgins, V. J.** (1992). "Effect of Specific Elicitors of *Cladosporium-Fulvum* on Tomato Suspension Cells - Evidence for the Involvement of Active Oxygen Species." *Plant Physiology* **99**(3): 1208-1215.
- Vercammen, D., van de Cotte, B., De Jaeger, G., et al.** (2004). "Type II metacaspases Atmc4 and Atmc9 of Arabidopsis thaliana cleave substrates after arginine and lysine." *Journal of Biological Chemistry* **279**(44): 45329-45336.
- Vranova, E., Inze, D. and Van Breusegem, F.** (2002). "Signal transduction during oxidative stress." *Journal of Experimental Botany* **53**(372): 1227-1236.
- Wagner, U., Edwards, R., Dixon, D. P., et al.** (2002). "Probing the diversity of the Arabidopsis glutathione S-transferase gene family." *Plant Molecular Biology* **49**(5): 515-532.

- Wagner, D., Przybyla, D., Camp, R. O. D., et al.** (2004). "The genetic basis of singlet oxygen-induced stress responses of *Arabidopsis thaliana*." *Science* **306**(5699): 1183-1185.
- Watanabe, N. and Lam, E.** (2006). "Arabidopsis Bax inhibitor-1 functions as an attenuator of biotic and abiotic types of cell death." *Plant Journal* **45**(6): 884-894.
- Whisson, S. C., Boevink, P. C., Moleleki, L., et al.** (2007). "A translocation signal for delivery of oomycete effector proteins into host plant cells." *Nature* **450**: 115-+.
- Wiermer, M.** (2005). Molecular and spatial characterisation of *Arabidopsis* EDS1 defence regulatory complexes. Max-Planck-Institute for Plant Breeding Research. Cologne, University of Cologne.
- Wiermer, M., Feys, B. J. and Parker, J. E.** (2005). "Plant immunity: the EDS1 regulatory node." *Current Opinion in Plant Biology* **8**(4): 383-389.
- Wildermuth, M. C.** (2006). "Variations on a theme: synthesis and modification of plant benzoic acids." *Current Opinion in Plant Biology* **9**(3): 288-296.
- Wildermuth, M. C., Dewdney, J., Wu, G., et al.** (2001). "Isochorismate synthase is required to synthesize salicylic acid for plant defence." *Nature* **414**(6863): 562-565.
- Wingler, A., Lea, P. J., Quick, W. P., et al.** (2000). "Photorespiration: metabolic pathways and their role in stress protection." *Philosophical Transactions of the Royal Society B-Biological Sciences* **355**(1402): 1517-1529.
- Wirthmueller, L., Zhang, Y., Jones, J. D. G., et al.** (2007). "Nuclear accumulation of the *Arabidopsis* immune receptor RPS4 is necessary for triggering EDS1-dependent defense." *Current Biology* **17**(23): 2023-2029.
- Witte, C. P., Noel, L. D., Gielbert, J., et al.** (2004). "Rapid one-step protein purification from plant material using the eight-amino acid StrepII epitope." *Plant Molecular Biology* **55**(1): 135-147.
- Wojtaszek, P.** (1997). "Oxidative burst: An early plant response to pathogen infection." *Biochemical Journal* **322**: 681-692.
- Xiao, S. Y., Ellwood, S., Calis, O., et al.** (2001). "Broad-spectrum mildew resistance in *Arabidopsis thaliana* mediated by RPW8." *Science* **291**(5501): 118-120.
- Yang, K. T., Chang, W. L., Yang, P. C., et al.** (2006). "Activation of the transient receptor potential M2 channel and poly(ADP-ribose) polymerase is involved in oxidative stress-induced cardiomyocyte death." *Cell Death and Differentiation* **13**(10): 1815-1826.
- Yang, S. H., Yang, H. J., Grisafi, P., et al.** (2006). "The BON/CPN gene family represses cell death and promotes cell growth in *Arabidopsis*." *Plant Journal* **45**(2): 166-179.
- Yao, N., Eisfelder, B. J., Marvin, J., et al.** (2004). "The mitochondrion - an organelle commonly involved in programmed cell death in *Arabidopsis thaliana*." *Plant Journal* **40**(4): 596-610.
- Yao, N. and Greenberg, J. T.** (2006). "*Arabidopsis* ACCELERATED CELL DEATH2 modulates programmed cell death." *Plant Cell* **18**(2): 397-411.
- Ying, W. H.** (2008). "NAD(+)/ NADH and NADP(+)/NADPH in cellular functions and cell death: Regulation and biological consequences." *Antioxidants & Redox Signaling* **10**(2): 179-206.
- Yoshimura, K., Ogawa, T., Ueda, Y., et al.** (2007). "AtNUDX1, an 8-oxo-7,8-dihydro-2'-deoxyguanosine 5'-triphosphate pyrophosphohydrolase, is responsible for eliminating oxidized nucleotides in *Arabidopsis*." *Plant and Cell Physiology* **48**: 1438-1449.

- Yoshioka, H., Numata, N., Nakajima, K., et al.** (2003). "Nicotiana benthamiana gp91(phox) homologs NbrbohA and NbrbohB participate in H₂O₂ accumulation and resistance to *Phytophthora infestans*." *Plant Cell* **15**(3): 706-718.
- Yu, X. H., Perdue, T. D., Heimer, Y. M., et al.** (2002). "Mitochondrial involvement in tracheary element programmed cell death." *Cell Death and Differentiation* **9**(2): 189-198.
- Zago, E., Morsa, S., Dat, J. F., et al.** (2006). "Nitric oxide- and hydrogen peroxide-responsive gene regulation during cell death induction in tobacco." *Plant Physiology* **141**(2): 404-411.
- Zhao, Y. F., Thilmony, R., Bender, C. L., et al.** (2003). "Virulence systems of *Pseudomonas syringae* pv. tomato promote bacterial speck disease in tomato by targeting the jasmonate signaling pathway." *Plant Journal* **36**(4): 485-499.
- Zhou, N., Tootle, T. L., Tsui, F., et al.** (1998). "PAD4 functions upstream from salicylic acid to control defense responses in *Arabidopsis*." *Plant Cell* **10**(6): 1021-1030.
- Zipfel, C., Robatzek, S., Navarro, L., et al.** (2004). "Bacterial disease resistance in *Arabidopsis* through flagellin perception." *Nature* **428**(6984): 764-7.
- Zipfel, C. and Felix, G.** (2005). "Plants and animals: a different taste for microbes?" *Curr Opin Plant Biol* **8**(4): 353-60.
- Zsigmond, L., Rigo, G., Szarka, A., et al.** (2008). "Arabidopsis PPR40 connects abiotic stress responses to mitochondrial electron transport." *Plant Physiology* **146**(4): 1721-1737.

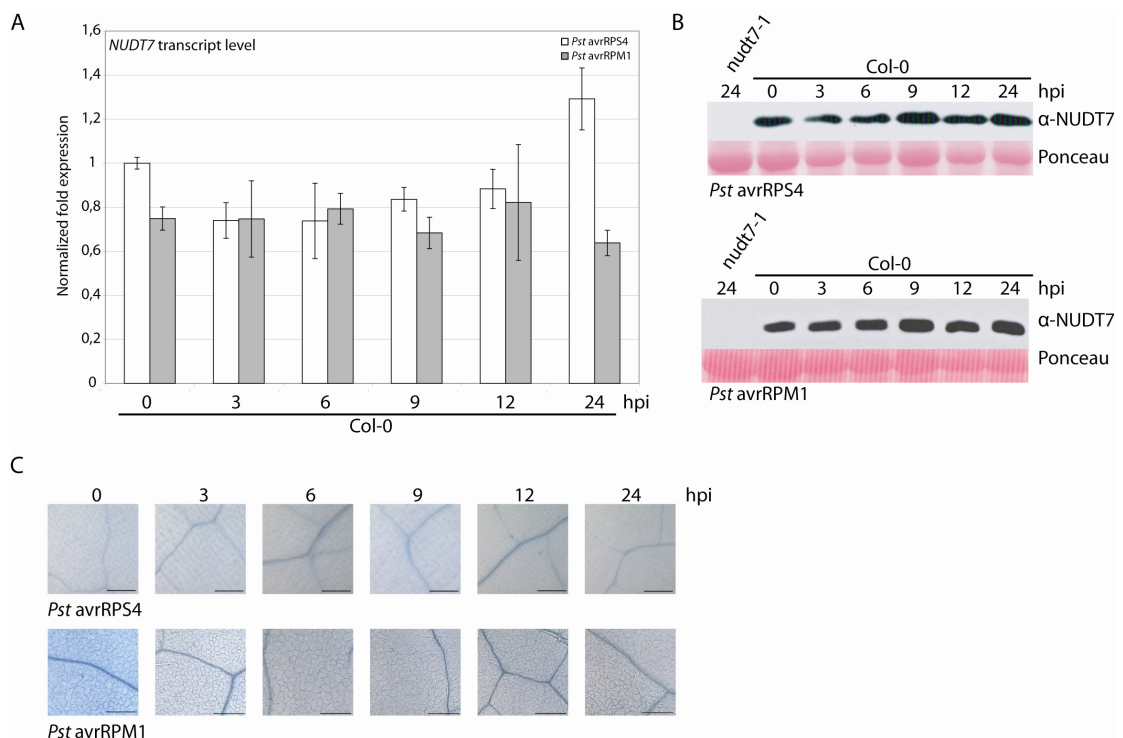
Supplemental data

Supplemental Figure 1: Control samples infiltrated with MgCl₂.

(A) 4-week-old plants were vacuum-infiltrated with 10mM MgCl₂. Leaf material was collected at the indicated time points and total RNA was extracted. Transcript levels were determined by quantitative real-time PCR using *UBC21* (*Ubiquitin Conjugating Enzyme 21*) as reference gene. Error bars represent standard deviation (SD). Controls shown here correspond to the infection assays shown in Figure 3.4.

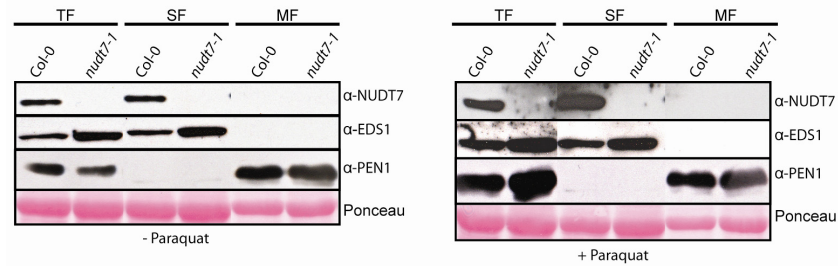
(B) Leaf material was harvested after indicated time points and total protein was extracted. NUDT7 protein was analysed on a Western blot with α -NUDT7 antibody. Ponceau staining served as loading control.

(C) 3-5 leaves were taken at indicated time points after inoculation and stained with trypan blue to detect plant cell death. Bars = 200 μ m.



Supplemental Figure 2: Microsomal fractionation of NUDT7 protein in healthy and paraquat treated plant tissue.

NUDT7 protein is exclusively soluble. Separation of healthy and paraquat-treated leaf tissue of indicated genotypes into soluble and microsomal fractions by ultracentrifugation. EDS1 and PEN1 antibodies served as soluble and microsomal markers, respectively. Paraquat application was performed as described in Figure 3.11A.



Supplemental Table 1: Gene lists of identified *EDS1*-dependent genes in *nudt7-1* and *nudt7-1/sid2-1*

GROUP I genes - *EDS1*-dependent expressed genes, influenced by elevated SA

Probe Set ID	AGI	Gene Title	Gene Symbol	Fold change <i>nudt7-1</i> vs <i>nudt7-1/eds1-2</i>
254975	at	AT4G10500	oxidoreductase, 2OG-Fe(II) oxygenase family protein	155.59166
249890	at	AT5G22570	WRKY family transcription factor	67.463425
263539	at	AT2G24850	aminotransferase, putative	57.18438
265161	at	AT1G30900	vacuolar sorting receptor, putative	27.282278
256431	s at	AT3G11010 /// AT5G27060	disease resistance family protein / LRR family protein	25.237722
262832	s at	AT1G14870 /// AT1G14880	expressed protein	22.483507
253181	at	AT4G35180	amino acid transporter family protein	19.147831
264434	at	AT1G10340	ankyrin repeat family protein	17.949308
265067	at	AT1G03850	glutaredoxin family protein	17.323801
249754	at	AT5G24530	oxidoreductase, 2OG-Fe(II) oxygenase family protein	16.99686
247293	at	AT5G64510	expressed protein	15.537856
261443	at	AT1G28480	glutaredoxin family protein	12.913411
254741	s at	AT4G13900 /// AT4G13920	pseudogene, similar to NL0D	12.168281
248970	at	AT5G45380	sodium:solute symporter family protein	11.899199
257623	at	AT3G26210	cytochrome P450 71B23, putative (CYP71B23)	10.188665
266782	at	AT2G29120	glutamate receptor family protein (GLR2.7)	9.826454
255406	at	AT4G03450	ankyrin repeat family protein	9.809719
251673	at	AT3G57240	beta-1,3-glucanase (BG3)	9.098922
252098	at	AT3G51330	aspartyl protease family protein	8.543597
254093	at	AT4G25110	latex-abundant family protein (AMC2) / caspase family protein	8.402632
252681	at	AT3G44350	no apical meristem (NAM) family protein	8.370337
259757	at	AT1G77510	protein disulfide isomerase, putative	8.298975
259065	at	AT3G07520	glutamate receptor family protein (GLR1.4)	8.235689
256596	at	AT3G28540	AAA-type ATPase family protein	8.226389
257763	s at	AT3G23110 /// AT3G23120	disease resistance family protein	8.013622
257139	at	AT3G28890	leucine-rich repeat family protein	7.4748297
260904	at	AT1G02450	NPR1/NIM1-interacting protein 1 (NIMIN-1)	7.472151
260068	at	AT1G73805	calmodulin-binding protein	7.3701954
252068	at	AT3G51440	strictosidine synthase family protein	7.1232033
260046	at	AT1G73800 /// AT1G73805	calmodulin-binding protein	7.0983357
254229	at	AT4G23610 /// AT4G23620	expressed protein	7.084939
257466	at	AT1G62840	expressed protein	7.0068216
253046	at	AT4G37370	cytochrome P450, putative	6.5963297
250302	at	AT5G11920	glycosyl hydrolase family 32 protein	6.4958987
267385	at	AT2G44380	DC1 domain-containing protein	6.2432256
257690	at	AT3G12830	auxin-responsive family protein	6.068427
248327	at	AT5G52750	heavy-metal-associated domain-containing protein	5.7639055
249743	at	AT5G24540	glycosyl hydrolase family 1 protein	5.5688396
256169	at	AT1G51800	leucine-rich repeat protein kinase, putative	5.275979
261692	at	AT1G08450	calreticulin 3 (CRT3)	5.1273503

246098	at	AT5G20400	oxidoreductase, 2OG-Fe(II) oxygenase family protein		5,119735
265993	at	AT2G24160	pseudogene, leucine rich repeat protein family		5,019295
255912	at	AT1G66960	lupeol synthase, putative / 2,3-oxidosqualene-triterpenoid cyclase, putative		4,9423046
254253	at	AT4G23320	protein kinase family protein		4,203093
251840	at	AT3G54960	thioredoxin family protein		4,1537275
259534	at	AT1G12290	disease resistance protein (CC-NBS-LRR class), putative		4,0247893
259489	at	AT1G15790	expressed protein		3,9911973
257473	at	AT1G33840	hypothetical protein		3,9187005
249581	at	AT5G37600	glutamine synthetase, putative		3,8499017
250764	at	AT5G05960	protease inhibitor/seed storage/lipid transfer protein (LTP) family protein		3,8053424
250604	at	AT5G07830	glycosyl hydrolase family 79 N-terminal domain-containing protein		3,7557356
257745	at	AT3G29240	expressed protein		3,7557232
251970	at	AT3G53150	UDP-glucuronosyl/UDP-glucosyl transferase family protein		3,708766
		AT5G38240	///		
249552	s at	AT5G38250	serine/threonine protein kinase, putative		3,6265843
258984	at	AT3G08970	DNAJ heat shock N-terminal domain-containing protein		3,5714397
262902	x at	AT1G59930	hypothetical protein		3,5106525
		AT1G67520	///		
264223	s at	AT3G16030	lectin protein kinase family protein		3,413283
265132	at	AT1G23830	expressed protein		3,372987
256252	at	AT3G11340	UDP-glucuronosyl/UDP-glucosyl transferase family protein		3,3227258
254245	at	AT4G23240	protein kinase family protein		3,209699
248263	at	AT5G53370	pectinesterase family protein		3,1861053
257101	at	AT3G25020	disease resistance family protein		3,1832132
260735	at	AT1G17610	disease resistance protein-related		3,1261053
267496	at	AT2G30550	lipase class 3 family protein		3,1038127
246524	at	AT5G15860	expressed protein		3,0927036
247448	at	AT5G62770	expressed protein		3,0046136
256962	at	AT3G13560	glycosyl hydrolase family 17 protein		2,9818132
255627	at	AT4G00955	expressed protein		2,9582276
250818	at	AT5G04930	phospholipid-transporting ATPase 1 / aminophospholipid flippase 1 / magnesium-ATPase 1 (ALA1)	ALA1	2,95518
		AT4G01750	///		
255564	s at	AT4G01770	expressed protein		2,8421776
250689	at	AT5G06610	expressed protein		2,838345
255319	at	AT4G04220	disease resistance family protein		2,6457455
260148	at	AT1G52800	oxidoreductase, 2OG-Fe(II) oxygenase family protein		2,417006
245611	at	AT4G14390	ankyrin repeat family protein		2,3640976
247618	at	AT5G60280	lectin protein kinase family protein		2,257037
		AT1G30410	///		
256308	s at	AT1G30420	ATP-binding cassette transport protein, putative		2,2280595
245375	at	AT4G17660	protein kinase, putative		2,1300125
252383	at	AT3G47780	ABC transporter family protein		2,1251478
249397	at	AT5G40230	nodulin-related		2,0112782
263431	at	AT2G22170	lipid-associated family protein		-2,3679373
262312	at	AT1G70830	Bet v I allergen family protein		-2,465771
		AT1G14230	///		
262661	s at	AT1G14250	nucleoside phosphatase family protein / GDA1/CD39 family protein		-2,52905
265277	at	AT2G28410	expressed protein		-2,5332708
		AT1G19550	///		
261149	s at	AT1G19570	dehydroascorbate reductase, putative		-2,5683665
249732	at	AT5G24420	glucosamine/galactosamine-6-phosphate isomerase-related		-3,3847506
250565	at	AT5G08000	glycosyl hydrolase family protein 17		-3,4175005
254232	at	AT4G23600	coronatine-responsive tyrosine aminotransferase / tyrosine transaminase		-3,5543911
		AT1G31680	///		
246573	at	AT1G31690	copper amine oxidase family protein		-4,4254813
259878	at	AT1G76790	O-methyltransferase family 2 protein		-4,606544
252345	at	AT3G48640	expressed protein		-12,412946

GROUP II genes - EDSI-dependent but SA-independent expressed genes

Probe Set ID	AGI	Gene Title	Gene Symbol	Fold change <i>nudt7-1</i> vs <i>nudt7-1/eds1-2</i>	Fold change <i>nudt7-1/sid2-1</i> vs <i>nudt7-1/sid2-1/eds1-2</i>
251625	at	AT3G57260	glycosyl hydrolase family 17 protein	918,25	1038,21
252549	at	AT3G45860	receptor-like protein kinase, putative	522,31	360,72
252170	at	AT3G50480	broad-spectrum mildew resistance RPW8 family protein	373,41	429,46
266070	at	AT2G18660	expansin family protein (EXPR3)	230,75	679,69
		AT4G23140 /// AT4G23160	receptor-like protein kinase 5 (RLK5)	143,10	131,46
254265	s at	AT5G39670 /// AT5G39680	calcium-binding EF hand family protein	117,14	213,65
254387	at	AT4G21850	methionine sulfoxide reductase domain-containing protein / SelR domain-containing protein	77,87	90,35
267546	at	AT2G32680	disease resistance family protein	76,45	80,02
		AT4G21830 /// AT4G21840	methionine sulfoxide reductase domain-containing protein / SelR domain-containing protein	70,74	80,04
256933	s at	AT3G22600	protease inhibitor/seed storage/lipid transfer protein (LTP) family protein	62,02	95,76
264635	at	AT1G65500	expressed protein	56,46	60,34
254271	at	AT4G23150	protein kinase family protein	54,04	25,81
248322	at	AT5G52760	heavy-metal-associated domain-containing protein	44,70	301,11
259550	at	AT1G35230	arabinogalactan-protein (AGP5)	43,77	38,13
246405	at	AT1G57630	disease resistance protein (TIR class), putative	40,42	80,22
258203	at	AT3G13950	expressed protein	38,90	55,62
250445	at	AT5G10760	aspartyl protease family protein	36,23	93,29

259385 at	AT1G13470	expressed protein		35,95	37,70
266017 at	AT2G18690	expressed protein		33,10	57,11
255341 at	AT4G04500	protein kinase family protein		31,80	46,38
252921 at	AT4G39030	enhanced disease susceptibility 5 (EDS5) / salicylic acid induction deficient 1 (SID1)	EDS5/SID1	31,49	45,94
255941 at	AT1G20350	mitochondrial import inner membrane translocase subunit Tim17, putative		30,06	18,06
247314 at	AT5G64000	3'(2'),5'-bisphosphate nucleotidase, putative / inositol polyphosphate 1-phosphatase, putative		29,95	25,19
255630 at	AT4G00700	C2 domain-containing protein		27,97	23,19
248932 at	AT5G46050	proton-dependent oligopeptide transport (POT) family protein		27,70	29,15
246302 at	AT3G51860	cation exchanger, putative (CAX3)		27,24	40,02
252908 at	AT4G39670	expressed protein		25,88	48,03
259507 at	AT1G43910	AAA-type ATPase family protein		25,86	45,92
257100 at	AT3G25010	disease resistance family protein		25,83	17,56
260116 at	AT1G33960	avirulence-responsive protein / avirulence induced gene (AIG1)		24,26	51,37
252136 at	AT3G50770	calmodulin-related protein, putative		23,27	120,30
250286 at	AT5G13320	auxin-responsive GH3 family protein		23,10	46,39
252417 at	AT3G47480	calcium-binding EF hand family protein		22,41	66,75
257061 at	AT3G18250	expressed protein		21,00	49,61
265597 at	AT2G20142 /// AT2G20145	Toll-Interleukin-Resistance (TIR) domain-containing protein		20,70	27,75
254101 at	AT4G25000	alpha-amylase, putative / 1,4-alpha-D-glucan glucanohydrolase, putative		20,47	38,63
258277 at	AT3G26830	cytochrome P450 71B15, putative (CYP71B15)		18,25	51,69
252131 at	AT3G50930	AAA-type ATPase family protein		18,19	23,50
249896 at	AT5G22530	expressed protein		17,34	22,37
260919 at	AT1G21525	expressed protein		16,77	65,05
255340 at	AT4G04490	protein kinase family protein		16,38	15,32
246927 s at	AT5G25250 /// AT5G25260	expressed protein		16,31	38,40
259410 at	AT1G13340	expressed protein		15,50	22,82
262177 at	AT1G74710	isochorismate synthase 1 (ICS1) / isochorismate mutase	ICS1	13,58	35,65
262930 at	AT1G65690	harpin-induced protein-related / HIN1-related / harpin-responsive protein-related		13,16	14,46
264648 at	AT1G09080	luminal binding protein 3 (BiP-3) (BP3)	BiP-3/BP3	13,01	8,50
250435 at	AT5G10380	zinc finger (C3HC4-type RING finger) family protein		12,56	12,41
256337 at	AT1G72060	expressed protein		12,24	19,10
249889 at	AT5G22540	expressed protein		11,57	7,69
267300 at	AT2G30140	UDP-glucuronosyl/UDP-glucosyl transferase family protein		11,41	5,84
253776 at	AT4G28390	ADP, ATP carrier protein, mitochondrial, putative / ADP/ATP translocase, putative / adenine nucleotide translocator, putative		11,30	13,24
255479 at	AT4G02380	late embryogenesis abundant 3 family protein / LEA3 family protein		10,82	21,16
263536 at	AT2G25000	WRKY family transcription factor		10,57	8,58
247071 at	AT5G66640	LIM domain-containing protein-related		10,53	7,44
254252 at	AT4G23310	receptor-like protein kinase, putative		10,41	7,44
252060 at	AT3G52430	phytoalexin-deficient 4 protein (PAD4)	pad4	10,22	19,14
248551 at	AT5G50200	expressed protein		10,16	13,79
265723 at	AT2G32140	disease resistance protein (TIR class), putative		10,08	18,07
248321 at	AT5G52740	heavy-metal-associated domain-containing protein		9,93	19,73
266292 at	AT2G29350	tropinone reductase, putative / tropine dehydrogenase, putative		9,60	12,67
261450 s at	AT1G21110 /// AT1G21120	O-methyltransferase, putative		9,40	19,57
253268 s at	AT4G34131 /// AT4G34135	UDP-glucuronosyl/UDP-glucosyl transferase family protein		8,98	8,75
250994 at	AT5G02490	heat shock cognate 70 kDa protein 2 (HSC70-2) (HSP70-2)		8,96	11,33
254660 at	AT4G18250	receptor serine/threonine kinase, putative		8,85	9,05
249867 at	AT5G23020	2-isopropylmalate synthase 2 (IMS2)	IMS2	8,58	3,32
265853 at	AT2G42360	zinc finger (C3HC4-type RING finger) family protein		8,42	7,52
261934 at	AT1G22400	UDP-glucuronosyl/UDP-glucosyl transferase family protein		8,32	18,93
258362 at	AT3G14280	expressed protein		8,23	7,08
260005 at	AT1G67920	expressed protein		8,22	9,65
255596 at	AT4G01720	WRKY family transcription factor		8,16	8,50
247327 at	AT5G64120	peroxidase, putative		8,10	8,06
260551 at	AT2G43510	trypsin inhibitor, putative		7,73	16,19
259502 at	AT1G15670	kelch repeat-containing F-box family protein		7,70	10,17
254243 at	AT4G23210	protein kinase family protein		7,61	10,20
259841 at	AT1G52200	expressed protein		7,60	9,96
247594 at	AT5G60800	heavy-metal-associated domain-containing protein		7,45	8,20
262119 s at	AT1G02920 /// AT1G02930	glutathione S-transferase, putative		7,38	14,15
252572 at	AT3G45290	seven transmembrane MLO family protein / MLO-like protein 3 (MLO3)		7,27	4,00
251054 at	AT5G01540	lectin protein kinase, putative		7,24	5,75
251884 at	AT3G54150	embryo-abundant protein-related		7,21	14,30
247740 at	AT5G58940	protein kinase family protein		7,21	3,36
249481 at	AT5G38900	DSBA oxidoreductase family protein		7,18	12,32
265658 at	AT2G13810	aminotransferase class I and II family protein		7,14	18,08
264590 at	AT2G17710	expressed protein		7,07	10,99
246368 at	AT1G51890	leucine-rich repeat protein kinase, putative		7,05	4,18
260015 at	AT1G67980	caffeoyl-CoA 3-O-methyltransferase, putative		7,01	29,34
264400 at	AT1G61800	glucose-6-phosphate/phosphate translocator, putative		6,91	13,83
258941 at	AT3G09940	monodehydroascorbate reductase, putative		6,91	6,92
256366 at	AT1G66880	serine/threonine protein kinase family protein		6,82	10,53
257185 at	AT3G13100	ABC transporter family protein		6,77	6,10
256940 at	AT3G30720	expressed protein		6,74	7,75
260648 at	AT1G08050	zinc finger (C3HC4-type RING finger) family protein		6,60	4,13
256877 at	AT3G26470	expressed protein		6,44	31,40
259852 at	AT1G72280	endoplasmic reticulum oxidoreductin 1 (ERO1) family protein		6,43	4,41
262542 at	AT1G34180	no apical meristem (NAM) family protein		6,36	5,82
249346 at	AT5G40780	lysine and histidine specific transporter, putative		6,35	8,59
248083 at	AT5G55420	expressed protein		6,24	11,86
248298 at	AT5G53110	expressed protein		6,19	4,76
255259 at	AT4G05020	NADH dehydrogenase-related		6,06	3,18
254247 at	AT4G23260	protein kinase family protein		6,04	6,02
261005 at	AT1G26420	FAD-binding domain-containing protein		6,02	8,98
251422 at	AT3G60540	sec61beta family protein		5,97	6,64
266267 at	AT2G29460	glutathione S-transferase, putative		5,91	32,23

249188	at	AT5G42830	transferase family protein		5,86	4,82
261021	at	AT1G26380	FAD-binding domain-containing protein		5,83	20,96
256874	at	AT3G26320	cytochrome P450 71B36, putative (CYP71B36)		5,73	7,39
256012	at	AT1G19250	flavin-containing monooxygenase family protein / FMO family protein		5,69	76,12
265189	at	AT1G23840	expressed protein		5,66	5,20
261986	s at	AT1G33720 /// AT1G33730	cytochrome P450, putative		5,64	8,02
260179	at	AT1G70690	kinase-related		5,64	4,59
259033	at	AT3G09410	pectinacetyltransferase family protein		5,45	12,03
263401	at	AT2G04070	MATE efflux family protein		5,43	3,19
260239	at	AT1G74360	leucine-rich repeat transmembrane protein kinase, putative		5,40	4,47
267483	at	AT2G02810	UDP-galactose/UDP-glucose transporter		5,38	6,33
261449	at	AT1G21120	O-methyltransferase, putative		5,31	5,92
246260	at	AT1G31820	amino acid permease family protein		5,29	9,60
251400	at	AT3G60420	expressed protein		5,27	9,93
249096	at	AT5G43910	pkB-type carbohydrate kinase family protein		5,19	6,70
259937	s at	AT1G71330 /// AT3G13080	ABC transporter family protein		5,00	4,00
254833	s at	AT4G12280 /// AT4G12290	copper amine oxidase family protein		4,97	7,24
247493	at	AT5G61900	copine BONZAI1 (BON1)	BON1	4,89	7,37
260225	at	AT1G74590	glutathione S-transferase, putative		4,82	19,54
252421	at	AT3G47540	chitinase, putative		4,78	5,45
255243	at	AT4G05590	expressed protein		4,66	4,14
245038	at	AT2G26560	patatin, putative		4,64	23,40
257591	at	AT3G24900	disease resistance family protein / LRR family protein		4,63	2,91
262085	at	AT1G56060	expressed protein		4,60	8,14
266167	at	AT2G38860	proteaseI (pipI)-like protein (YLS5)		4,57	9,66
267567	at	AT2G30770	cytochrome P450 71A13, putative (CYP71A13)		4,43	5,13
259559	at	AT1G21240	wall-associated kinase, putative	WAK3	4,39	6,15
258259	s at	AT3G26820 /// AT3G26840	esterase/lipase/thioesterase family protein		4,34	7,20
266474	at	AT2G31110	expressed protein		4,30	3,52
252977	at	AT4G38560	expressed protein		4,23	5,06
251790	at	AT3G55470	C2 domain-containing protein		4,21	9,84
251769	at	AT3G55950	protein kinase family protein		4,13	5,41
249377	at	AT5G40690	expressed protein		4,10	5,10
256576	at	AT3G28210	zinc finger (AN1-like) family protein		3,82	2,98
256969	at	AT3G21080	ABC transporter-related		3,74	6,07
251633	at	AT3G57460	expressed protein		3,69	4,27
256883	at	AT3G26440	expressed protein		3,67	5,11
248333	at	AT5G52390	photoassimilate-responsive protein, putative		3,64	38,91
254409	at	AT4G21400	protein kinase family protein		3,55	5,33
254573	at	AT4G19420	pectinacetyltransferase family protein		3,50	5,88
254178	at	AT4G23880	expressed protein		3,50	3,16
246842	at	AT5G26731	expressed protein		3,49	4,27
245788	at	AT1G32120	expressed protein		3,34	3,03
256451	s at	AT1G75170 /// AT5G04780	SEC14 cytosolic factor family protein / phosphoglyceride transfer family protein		3,21	4,62
256989	at	AT3G28580	AAA-type ATPase family protein		3,20	4,46
255430	at	AT4G03320	chloroplast protein import component-related		3,07	5,03
254735	at	AT4G13810	disease resistance family protein / LRR family protein		3,03	2,89
256245	at	AT3G12580	heat shock protein 70, putative / HSP70, putative		2,80	3,26
261216	at	AT1G33030	O-methyltransferase family 2 protein		2,79	11,64
248060	at	AT5G55560	protein kinase family protein		2,75	3,67
252309	at	AT3G49340	cysteine proteinase, putative		2,64	26,66
261476	at	AT1G14480	ankyrin repeat family protein		2,62	2,99
252827	at	AT4G39950	cytochrome P450 79B2, putative (CYP79B2)		2,53	3,98
254723	at	AT4G13510	ammonium transporter 1, member 1 (AMT1.1)	AMT1.1	2,51	3,15
264574	at	AT1G05300	metal transporter, putative (ZIP5)		2,46	3,12
249494	at	AT5G39050	transferase family protein		2,43	2,95
249988	at	AT5G18310	expressed protein		2,42	2,99
257939	at	AT3G19930	sugar transport protein (STP4)	STP4	2,34	2,16
254524	at	AT4G20000	VQ motif-containing protein		2,25	3,53
256376	s at	AT1G66690 /// AT1G66700	S-adenosyl-L-methionine:carboxyl methyltransferase family protein		2,24	6,95
248916	at	AT5G45840	leucine-rich repeat transmembrane protein kinase, putative		2,22	7,14
249770	at	AT5G24110	WRKY family transcription factor		2,20	2,12
260581	at	AT2G47190	myb family transcription factor (MYB2)		2,16	2,48
262703	at	AT1G16510	auxin-responsive family protein		2,00	2,91
254791	at	AT4G12910	serine carboxypeptidase S10 family protein		-2,27	-2,52
256441	at	AT3G10940	protein phosphatase-related		-2,34	-3,15
253331	at	AT4G33490	nucellin protein, putative		-2,38	-4,30
262891	at	AT1G79460	ent-kaurene synthase / ent-kaurene synthetase B (KS) (GA2)	GA2	-2,42	-5,61
245657	at	AT1G56720	protein kinase family protein		-2,67	-2,96
251856	at	AT3G54720	glutamate carboxypeptidase, putative (AMP1)		-2,89	-3,04
253254	at	AT4G34650	farnesyl-diphosphate farnesyltransferase 2 / squalene synthase 2 (SQS2)	SQS2	-2,89	-4,03
261826	at	AT1G11580	pectin methylesterase, putative		-3,15	-3,65
264987	at	AT1G27030	expressed protein		-3,20	-4,63
258901	at	AT3G05640	protein phosphatase 2C, putative / PP2C, putative		-3,82	-5,18
263574	at	AT2G16990	expressed protein		-4,19	-6,76
263497	at	AT2G42540	cold-responsive protein / cold-regulated protein (cor15a)	cor15a	-4,42	-5,57
257254	at	AT3G21950	S-adenosyl-L-methionine:carboxyl methyltransferase family protein		-4,53	-4,79
261428	at	AT1G18870	isochorismate synthase, putative / isochorismate mutase, putative		-4,71	-5,87
264741	at	AT1G62290	aspartyl protease family protein		-5,57	-7,28

GROUP III genes - *EDS1*-dependent expressed genes, influenced by depleted SA

Probe Set ID	AGI	Gene Title	Gene Symbol	Fold change <i>nudt7-1sid2-1</i> vs <i>nudt7-1/sid2-1/eds1-2</i>
257365	x at	AT2G26020	plant defensin-fusion protein, putative (PDF1.2b)	113.63386
263979	at	AT2G42840	protodermal factor 1 (PDF1)	93.09208
265471	at	AT2G37130	peroxidase 21 (PER21) (P21) (PRXR5)	(ATP2a) 75.42882
249052	at	AT5G44420	plant defensin protein, putative (PDF1.2a)	62.223446
267459	at	AT2G33850	expressed protein	61.612915
258675	at	AT3G08770	lipid transfer protein 6 (LTP6)	LTP6 52.615093
259009	at	AT3G09260	glycosyl hydrolase family 1 protein	50.05208
245393	at	AT4G16260	glycosyl hydrolase family 17 protein	49.800003
253753	at	AT4G29030	glycine-rich protein	47.666348
263783	at	AT2G46400	WRKY family transcription factor	44.11368
258100	at	AT3G23550	MATE efflux family protein	35.806293
258059	at	AT3G29035	no apical meristem (NAM) family protein	34.41309
252265	at	AT3G49620	2-oxoacid-dependent oxidase, putative (DIN11)	DIN11 34.204533
259925	at	AT1G75040	pathogenesis-related protein 5 (PR-5)	PR-5 27.620285
261459	at	AT1G21100	O-methyltransferase, putative	23.763609
254327	at	AT4G22490	protease inhibitor/seed storage/lipid transfer protein (LTP) family protein	22.966476
260881	at	AT1G21550	calcium-binding protein, putative	21.67051
245688	at	AT1G28290	pollen Ole e 1 allergen and extensin family protein	20.462524
249813	at	AT5G23940	transferase family protein	19.963556
245317	at	AT4G15610	integral membrane family protein	19.362165
245193	at	AT1G67810	Fe-S metabolism associated domain-containing protein	19.35344
248807	at	AT5G47500	pectinesterase family protein	19.304106
263565	at	AT2G15390	xyloglucan fucosyltransferase, putative (FUT4)	FUT4 16.961695
258791	at	AT3G04720	hevein-like protein (HEL)	HEL 15.132321
252993	at	AT4G38540	monooxygenase, putative (MO2)	MO2 14.954497
259850	at	AT1G72240	expressed protein	14.923575
246687	at	AT5G33370	GDSSL-motif lipase/hydrolase family protein	14.591388
247573	at	AT5G61160	transferase family protein	13.904214
254805	at	AT4G12480	protease inhibitor/seed storage/lipid transfer protein (LTP) family protein	13.797929
266223	at	AT2G28790	osmotin-like protein, putative	13.629877
260783	at	AT1G06160	ethylene-responsive factor, putative	13.6108675
264514	at	AT1G09500	cinnamyl-alcohol dehydrogenase family / CAD family	13.404583
249197	at	AT5G42380	calmodulin-related protein, putative	13.093036
258589	at	AT3G04290	GDSSL-motif lipase/hydrolase family protein	13.0818405
245401	at	AT4G17670	senescence-associated protein-related	12.651897
250575	at	AT5G08240	expressed protein	12.485031
260560	at	AT2G43590	chitinase, putative	11.88118
259382	s at	AT3G16420 /// AT3G16430	jacalin lectin family protein	11.650177
258682	at	AT3G08720	serine/threonine protein kinase (PK19)	11.014786
245976	at	AT5G13080	WRKY family transcription factor	10.692817
266415	at	AT2G38530	nonspecific lipid transfer protein 2 (LTP2)	LTP2 10.096741
245739	at	AT1G44110	cyclin, putative	9.871839
258376	at	AT3G17680	expressed protein	9.768558
259391	s at	AT1G06350 /// AT1G06360	fatty acid desaturase family protein	9.52829
267565	at	AT2G30750	cytochrome P450 71A12, putative (CYP71A12)	8.940427
260297	at	AT1G80280	hydrolase, alpha/beta fold family protein	8.874629
259655	at	AT1G55210	disease resistance response protein-related/ dirigent protein-related	8.758764
256125	at	AT1G18250	thaumatin, putative	8.741172
260948	at	AT1G06100	fatty acid desaturase family protein	8.687121
258480	at	AT3G02640	expressed protein	8.537933
262040	at	AT1G80080	leucine-rich repeat family protein	8.353576
263153	s at	AT1G54000 /// AT1G54010	myrosinase-associated protein, putative	8.319827
246214	at	AT4G36990	heat shock factor protein 4 (HSF4) / heat shock transcription factor 4 (HSTF4)	8.226794
264524	at	AT1G10070	branched-chain amino acid aminotransferase 2 / branched-chain amino acid transaminase 2 (BCAT2)	BCAT2 7.975753
247266	at	AT5G64570	glycosyl hydrolase family 3 protein	7.7230954
264261	at	AT1G09240	nicotianamine synthase, putative	7.6933303
246920	at	AT5G25090	plastocyanin-like domain-containing protein	7.503981
249942	at	AT5G22300	nitrilase 4 (NIT4)	NIT4 7.231743
254818	at	AT4G12470	protease inhibitor/seed storage/lipid transfer protein (LTP) family protein	7.213024
261927	at	AT1G22500	zinc finger (C3HC4-type RING finger) family protein	7.212768
251176	at	AT3G63380	calcium-transporting ATPase, plasma membrane-type, putative / Ca(2+)-ATPase, putative (ACA12)	ACA12 7.153207
257203	at	AT3G23730	xyloglucan:xyloglucosyl transferase, putative / xyloglucan endotransglycosylase, putative / endo-xyloglucan transferase, putative	7.117325
245349	at	AT4G16690	esterase/lipase/thioesterase family protein	7.1047072
248912	at	AT5G45670	GDSSL-motif lipase/hydrolase family protein	7.0539327
266655	at	AT2G25880	serine/threonine protein kinase, putative	6.813193
258395	at	AT3G15500	no apical meristem (NAM) family protein (NAC3)	6.5670695
258895	at	AT3G05600	epoxide hydrolase, putative	6.5499644
261394	at	AT1G79680	wall-associated kinase, putative	6.4141207
264377	at	AT2G25060	plastocyanin-like domain-containing protein	6.3888874
255433	at	AT4G03210	xyloglucan:xyloglucosyl transferase, putative / xyloglucan endotransglycosylase, putative / endo-xyloglucan transferase, putative	6.34995
263475	at	AT2G31945	expressed protein	6.3483076
260592	at	AT1G55850	cellulose synthase family protein	6.3039527
248100	at	AT5G55180	glycosyl hydrolase family 17 protein	6.1964536
249659	s at	AT5G36710 /// AT5G36800	expressed protein	6.187364
246505	at	AT5G16250	expressed protein	6.087555
259327	at	AT3G16460	jacalin lectin family protein	6.0272646
245181	at	AT5G12420	expressed protein	5.915852
248963	at	AT5G45700	NLI interacting factor (NIF) family protein	5.865953

247882 at	AT5G57785	expressed protein		5,8200994
257134 at	AT3G12870	expressed protein		5,7820983
264746 at	AT1G62300	WRKY family transcription factor		5,6205516
255460 at	AT4G02800	expressed protein		5,5989056
262229 at	AT1G68620	expressed protein		5,593891
256243 at	AT3G12500	basic endochitinase		5,5636654
262840 at	AT1G14900	high-mobility-group protein / HMG-I/Y protein		5,510773
265572 at	AT2G28210	carbonic anhydrase family protein		5,424906
248829 at	AT5G47130	Bax inhibitor-1 family / BI-1 family		5,3021135
257005 at	AT3G14190	expressed protein		5,245827
253754 at	AT4G29020	glycine-rich protein		5,240828
264802 at	AT1G08560	syntxin-related protein KNOLLE (KN) / syntxin 111 (SYP111)		5,2048078
264901 at	AT1G23090	sulfate transporter, putative		5,163023
257636 at	AT3G26200	cytochrome P450 71B22, putative (CYP71B22)		5,140558
246099 at	AT5G20230	plastocyanin-like domain-containing protein		5,0799804
245343 at	AT4G15830	expressed protein		5,035937
245885 at	AT5G09440	phosphate-responsive protein, putative		5,0250545
256832 at	AT3G22880	meiotic recombination protein, putative		5,0216208
263948 at	AT2G35980	harpin-induced family protein (YLS9) / HIN1 family protein / harpin-responsive family protein		4,972025
253340 s at	AT4G33260 /// AT4G33270	WD-40 repeat family protein	FZR	4,9477406
250054 at	AT5G17860	cation exchanger, putative (CAX7)		4,9462395
247819 at	AT5G58350	protein kinase family protein		4,836051
247429 at	AT5G62620	galactosyltransferase family protein		4,8341956
266613 at	AT2G14900	gibberellin-regulated family protein		4,80476
260840 at	AT1G29050	expressed protein		4,7627673
257206 at	AT3G16530	legume lectin family protein		4,7529316
251847 at	AT3G54640	tryptophan synthase, alpha subunit (TSA1)	TSA1	4,7093797
258813 at	AT3G04060	no apical meristem (NAM) family protein		4,682705
250891 at	AT5G04530	beta-ketoacyl-CoA synthase family protein		4,6549635
253636 at	AT4G30500	expressed protein		4,6416616
254384 at	AT4G21870	26.5 kDa class P-related heat shock protein (HSP26.5-P)	hsp26.5-P	4,6358023
264160 at	AT1G65450	transferase family protein		4,588639
251304 at	AT3G61990	O-methyltransferase family 3 protein		4,552665
257950 at	AT3G21780	UDP-glucuronosyl/UDP-glucosyl transferase family protein		4,5489597
260391 at	AT1G74020	strictosidine synthase family protein		4,5457845
266988 at	AT2G39310	jacalin lectin family protein		4,4917445
262819 at	AT1G11600	cytochrome P450, putative		4,4649425
264319 at	AT1G04110	subtilase family protein		4,4648404
263807 at	AT2G04400	indole-3-glycerol phosphate synthase (IGPS)	IGPS	4,447728
262543 at	AT1G34245	expressed protein		4,3635163
261366 at	AT1G53100	glycosyltransferase family 14 protein / core-2/1-branching enzyme family protein		4,333326
249060 at	AT5G44560	SNF7 family protein		4,2466583
257191 at	AT3G13175	expressed protein		4,1785545
264467 at	AT1G10140	expressed protein		4,1760783
264645 at	AT1G08940	phosphoglycerate/bisphosphoglycerate mutase family protein		4,1260204
246565 at	AT5G15530	biotin carboxyl carrier protein 2 (BCCP2)	BCCP2	4,1026106
245523 at	AT4G15910	drought-responsive protein / drought-induced protein (Di21)		4,0974784
260077 at	AT1G73620	thaumatin-like protein, putative / pathogenesis-related protein, putative		4,087135
263963 at	AT2G36080	DNA-binding protein, putative		4,085769
258201 at	AT3G13910	expressed protein		4,0403013
251065 at	AT5G01870	lipid transfer protein, putative		4,0344515
251109 at	AT5G01600	ferritin 1 (FER1)	FER1	3,9440389
265053 at	AT1G52000	jacalin lectin family protein		3,938255
266401 s at	AT2G38620 /// AT3G54180	cell division control protein, putative		3,9005573
264007 at	AT2G21140	hydroxyproline-rich glycoprotein family protein		3,8951776
245662 at	AT1G28190	expressed protein		3,8863041
246184 at	AT5G20950	glycosyl hydrolase family 3 protein		3,8574057
267349 at	AT2G40010	60S acidic ribosomal protein P0 (RPP0A)		3,82283
253285 at	AT4G34250	fatty acid elongase, putative	FAE1	3,8186395
255732 at	AT1G25450	very-long-chain fatty acid condensing enzyme, putative		3,8112886
259730 at	AT1G77660	MORN (Membrane Occupation and Recognition Nexus) repeat-containing protein / phosphatidylinositol-4-phosphate 5-kinase-related		3,8096619
253358 at	AT4G32940	vacuolar processing enzyme gamma / gamma-VPE		3,8034008
256981 at	AT3G13380	leucine-rich repeat family protein / protein kinase family protein		3,744521
258859 at	AT3G02120	hydroxyproline-rich glycoprotein family protein		3,7051547
262109 at	AT1G02730	cellulose synthase family protein		3,6751685
265117 at	AT1G62500	protease inhibitor/seed storage/lipid transfer protein (LTP) family protein		3,6592908
257318 at	AT2G07777	expressed protein		3,626681
257264 at	AT3G22060	receptor protein kinase-related		3,6034315
258487 at	AT3G02550	LOB domain protein 41 / lateral organ boundaries domain protein 41 (LBD41)	LBD41	3,6004925
254190 at	AT4G23885 /// AT4G23890	expressed protein		3,559391
261859 at	AT1G50490	ubiquitin-conjugating enzyme 20 (UBC20)	UBC20	3,5556233
253403 at	AT4G32830	protein kinase, putative		3,547329
250738 at	AT5G05730	anthranilate synthase, alpha subunit, component I-1 (ASA1)	ASA1	3,5162916
250437 at	AT5G10430	arabinogalactan-protein (AGP4)	AGP4	3,506925
253480 at	AT4G31840	plastocyanin-like domain-containing protein		3,5041928
247945 at	AT5G57140 /// AT5G57150	calcineurin-like phosphoesterase family protein		3,4681735
266581 at	AT2G46140	late embryogenesis abundant protein, putative / LEA protein, putative		3,456012
254333 at	AT4G22753	sterol desaturase family protein		3,38973
251982 at	AT3G53190	pectate lyase family protein		3,3690946
246831 at	AT5G26340	hexose transporter, putative		3,3312767
248320 at	AT5G52720	heavy-metal-associated domain-containing protein		3,3147497
260472 at	AT1G10990	expressed protein		3,3134885
251282 at	AT3G61630	AP2 domain-containing transcription factor, putative		3,3120866
262366 at	AT1G72890	disease resistance protein (TIR-NBS class), putative		3,2793896
249775 at	AT5G24160	squalene monooxygenase 1,2 / squalene epoxidase 1,2 (SQP1,2)	SQP1,2	3,2468727
265028 at	AT1G24530	transducin family protein / WD-40 repeat family protein		3,216285
249187 at	AT5G43060	cysteine proteinase, putative / thiol protease, putative		3,1417103
249125 at	AT5G43450	2-oxoglutarate-dependent dioxygenase, putative		3,1343665
259735 at	AT1G64405	expressed protein		3,1300576

249408	at	AT5G40330	myb family transcription factor		3,0985484
252050	at	AT3G52550	hypothetical protein		3,086277
258217	at	AT3G18000	phosphoethanolamine N-methyltransferase 1 / PEAMT1 (NMT1)	PEAMT1	3,0359042
250661	at	AT5G07030	aspartyl protease family protein		3,0114396
259618	at	AT1G48000	myb family transcription factor		3,0030928
248230	at	AT5G53830	VQ motif-containing protein		2,9863322
263404	s at	AT2G04090 /// AT2G04100	MATE efflux family protein		2,9506738
266996	at	AT2G34490	cytochrome P450 family protein		2,933073
267618	at	AT2G26760	cyclin, putative		2,9270887
258067	at	AT3G25980	mitotic spindle checkpoint protein, putative (MAD2)		2,9077404
259235	at	AT3G11600	expressed protein		2,894835
262939	s at	AT1G16300 /// AT1G79530	glyceraldehyde 3-phosphate dehydrogenase, cytosolic, putative / NAD-dependent glyceraldehyde-3-phosphate dehydrogenase, putative		2,8880095
253163	at	AT4G35750	Rho-GTPase-activating protein-related		2,873761
246247	at	AT4G36640	SEC14 cytosolic factor family protein / phosphoglyceride transfer family protein		2,8714268
253357	at	AT4G33400	dem protein-related / defective embryo and meristems protein-related		2,8536534
258218	at	AT3G18000	phosphoethanolamine N-methyltransferase 1 / PEAMT1 (NMT1)	PEAMT1	2,8394563
263496	at	AT2G42570	expressed protein		2,836137
260546	at	AT2G43520	trypsin inhibitor, putative		2,812299
267402	at	AT2G26180	calmodulin-binding family protein		2,8075106
260897	at	AT1G29330	ER lumen protein retaining receptor (ERD2) / HDEL receptor	ERD2	2,7851985
258962	at	AT3G10570	cytochrome P450, putative		2,7811532
258107	at	AT3G23560	MATE efflux family protein		2,7676818
260166	at	AT1G79840	homeobox-leucine zipper protein 10 (HB-10) / HD-ZIP transcription factor 10 / homeobox protein (GLABRA2)	GLABRA2	2,75716
247835	at	AT5G57910	expressed protein		2,749133
264588	at	AT2G17730	zinc finger (C3HC4-type RING finger) family protein		2,7475617
251284	at	AT3G61840	expressed protein		2,7343078
246133	at	AT5G20960	aldehyde oxidase 1 (AAO1)	AO1	2,7332864
251846	at	AT3G54560	histone H2A.F/Z		2,71942
264894	at	AT1G23040	hydroxyproline-rich glycoprotein family protein		2,714337
248118	at	AT5G50500	GDSL-motif lipase/hydrolase family protein		2,7005618
266352	at	AT2G01610	invertase/pectin methylesterase inhibitor family protein		2,6966934
260565	at	AT2G43800	formin homology 2 domain-containing protein / FH2 domain-containing protein		2,6896958
259429	at	AT1G01600	cytochrome P450, putative		2,6880546
253162	at	AT4G35630	phosphoserine aminotransferase, chloroplast (PSAT)	PSAT	2,6715658
262870	at	AT1G64710	alcohol dehydrogenase, putative	ADH	2,671544
251643	at	AT3G57550	guanylate kinase 2 (GK-2)		2,659305
249258	at	AT5G41650	lactoylglutathione lyase family protein / glyoxalase I family protein		2,6573257
262667	at	AT1G62810	copper amine oxidase, putative		2,6540356
260635	at	AT1G62420	expressed protein		2,6509051
251750	at	AT3G55710	UDP-glucuronosyl/UDP-glucosyl transferase family protein		2,6480224
264763	at	AT1G61450	expressed protein		2,6135952
263831	at	AT2G40300	ferritin, putative		2,6095965
250983	at	AT5G02780	In2-1 protein, putative	In2-1	2,584124
260060	at	AT1G73680	pathogen-responsive alpha-dioxygenase, putative		2,5831368
258803	at	AT3G04670	WRKY family transcription factor		2,5639384
260531	at	AT2G47240	long-chain-fatty-acid--CoA ligase family protein / long-chain acyl-CoA synthetase family protein		2,563174
257830	at	AT3G26690	MutT/nudix family protein		2,5562613
249839	at	AT5G23405	high mobility group (HMG1/2) family protein		2,5251014
258385	at	AT3G15510	no apical meristem (NAM) family protein (NAC2)		2,5207992
257193	at	AT3G13160	pentatricopeptide (PPR) repeat-containing protein		2,5180027
265116	at	AT1G62480	vacuolar calcium-binding protein-related		2,489088
255543	at	AT4G01870	tolB protein-related		2,4877338
246103	at	AT5G28640	SSXT protein-related / glycine-rich protein		2,487157
247864	s at	AT1G24807	anthranilate synthase beta subunit, putative	ASB	2,478941
258815	at	AT3G04000	short-chain dehydrogenase/reductase (SDR) family protein		2,464861
251895	at	AT3G54420	class IV chitinase (CHIV)		2,4605227
249184	at	AT5G43020	leucine-rich repeat transmembrane protein kinase, putative		2,4486358
252133	at	AT3G50900	expressed protein		2,4418738
257024	at	AT3G19100	calcium-dependent protein kinase, putative / CDPK, putative		2,4400597
256666	at	AT3G20670	histone H2A, putative		2,4302366
251985	at	AT3G53220	thioredoxin family protein		2,426719
264960	at	AT1G76930	proline-rich extensin-like family protein		2,406742
258707	at	AT3G09480	histone H2B, putative		2,3990126
257540	at	AT3G21520	expressed protein		2,3893268
259749	at	AT1G71100	ribose 5-phosphate isomerase-related		2,3703492
255410	at	AT4G03100	rac GTPase activating protein, putative		2,3489819
248896	at	AT5G46350	WRKY family transcription factor		2,3480818
267555	at	AT2G32765	small ubiquitin-like modifier 5 (SUMO)		2,3319046
259381	s at	AT3G16390	jacalin lectin family protein		2,3304365
258160	at	AT3G17820	glutamine synthetase (GS1)		2,3168323
250109	at	AT5G15230	gibberellin-regulated protein 4 (GASA4) / gibberellin-responsive protein 4		2,3050961
261785	at	AT1G08230	amino acid transporter family protein		2,3043194
258377	at	AT3G17690	cyclic nucleotide-binding transporter 2 / CNBT2 (CNGC19)		2,3032193
249794	at	AT5G23530	expressed protein		2,2911701
260706	at	AT1G32350	alternative oxidase, putative		2,2836225
257334	at				2,279476
246004	at	AT5G20630	germin-like protein (GER3)	GER3	2,2601826
257805	at	AT3G18830	mannitol transporter, putative		2,236081
254764	at	AT4G13250	short-chain dehydrogenase/reductase (SDR) family protein		2,2247248
247182	at	AT5G65410	zinc finger homeobox family protein / ZF-HD homeobox family protein		2,2115746
258075	at	AT3G25900	homocysteine S-methyltransferase 1 (HMT-1)	HMT-1	2,207048
250433	at	AT5G10400	histone H3		2,177905
254130	at	AT4G24540	MADS-box family protein		2,1709397
251811	at	AT3G54990	AP2 domain-containing transcription factor, putative		2,1569903
257879	at	AT3G17160	expressed protein		2,1462677
263264	at	AT2G38810	histone H2A, putative		2,140431
255942	at	AT1G22360	UDP-glucuronosyl/UDP-glucosyl transferase family protein		2,1388001
264517	at	AT1G10120	basic helix-loop-helix (bHLH) family protein		2,1253316
259384	at	AT3G16450	jacalin lectin family protein		2,114268
258530	at	AT3G06840	expressed protein		2,1132095

259061 at	AT3G07410	Ras-related GTP-binding family protein		2,100448
248510 at	AT5G50315	Mutator-like transposase family		2,093163
262605 at	AT1G15170	MATE efflux family protein		2,084784
260784 at	AT1G06180	myb family transcription factor		2,0759072
254233 at	AT4G23800	high mobility group (HMG1/2) family protein		2,0337257
250228 at	AT5G13840	WD-40 repeat family protein		2,0267239
262758 at	AT1G10780	F-box family protein		2,0222194
245576 at	AT4G14770	tesmin/TSO1-like CXC domain-containing protein		2,0136702
253073 at	AT4G37410	cytochrome P450, putative		2,0021665
245893 at	AT5G09270	expressed protein		2,0021086
250248 at	AT5G13740	sugar transporter family protein		-2,0067787
261256 at	AT1G05760	jacalin lectin family protein (RTM1)	RTM1	-2,015062
250633 at	AT5G07460	peptide methionine sulfoxide reductase, putative		-2,0725427
250366 at	AT5G11420	expressed protein		-2,0767264
265715 s at	AT1G13860 /// AT2G03480	dehydration-responsive protein-related		-2,07991
267060 at	AT2G32580	expressed protein		-2,0888693
252001 at	AT3G52750	chloroplast division protein, putative		-2,0894818
247552 at	AT5G60920	phytochelatin synthetase, putative / COBRA cell expansion protein COB, putative		-2,1074908
255645 at	AT4G00880	auxin-responsive family protein		-2,1137571
257008 at	AT3G14210	myosinase-associated protein, putative		-2,1171293
248943 s at	AT5G45440 /// AT5G45490	disease resistance protein-related		-2,1224864
263985 at	AT2G42750	DNAJ heat shock N-terminal domain-containing protein		-2,1343207
265824 at	AT2G35650	glycosyl transferase family 2 protein		-2,1409037
258977 s at	AT3G02020 /// AT5G14060	aspartate kinase, lysine-sensitive, putative		-2,1460583
246036 at	AT5G08370	alpha-galactosidase, putative / melibiase, putative / alpha-D-galactoside galactohydrolase, putative		-2,1462035
252983 at	AT4G37980	mannitol dehydrogenase, putative (ELI3-1)	ELI3-1	-2,1636715
260441 at	AT1G68260	thioesterase family protein		-2,1704702
261925 at	AT1G22540	proton-dependent oligopeptide transport (POT) family protein		-2,1736834
259188 at	AT3G01510	5'-AMP-activated protein kinase beta-1 subunit-related		-2,1796958
258015 at	AT3G19340	expressed protein		-2,1884162
245463 at	AT4G17030	expansin-related		-2,2031116
248765 at	AT5G47650	MutT/nudix family protein		-2,2101562
259180 at	AT3G01680	expressed protein		-2,2131503
255626 at	AT4G00780	mepirin and TRAF homology domain-containing protein / MATH domain-containing protein		-2,2229424
246487 at	AT5G16030	expressed protein		-2,2497022
260012 at	AT1G67865	expressed protein		-2,254838
251230 at	AT3G62750	glycosyl hydrolase family 1 protein		-2,26521
245307 at	AT4G16770	oxidoreductase, 2OG-Fe(II) oxygenase family protein		-2,2717423
248042 at	AT5G55960	expressed protein		-2,2849827
247747 at	AT5G59000	zinc finger (C3HC4-type RING finger) family protein		-2,3146422
261279 at	AT1G05850	chitinase-like protein 1 (CTL1)		-2,3325932
263709 at	AT1G09310	expressed protein		-2,3564086
262216 at	AT1G74780	nodulin family protein		-2,3937113
246281 at	AT4G36940	nicotinate phosphoribosyltransferase family protein / NAPRTase family protein		-2,4045968
257772 at	AT3G23080	expressed protein		-2,4067125
267367 at	AT2G44210	expressed protein		-2,4255192
254250 at	AT4G23290	protein kinase family protein		-2,43337
254563 at	AT4G19120	early-responsive to dehydration stress protein (ERD3)	ERD3	-2,4615073
255933 at	AT1G12750	rhomboid family protein		-2,4712815
245348 at	AT4G17770	glycosyl transferase family 20 protein / trehalose-phosphatase family protein		-2,4759212
254687 at	AT4G13770	cytochrome P450 family protein		-2,5091588
249688 at	AT5G36160	aminotransferase-related		-2,5391333
247162 at	AT5G65730	xyloglucan:xyloglucosyl transferase, putative / xyloglucan endotransglycosylase, putative / endo-xyloglucan transferase, putative		-2,564124
261221 at	AT1G19960	expressed protein		-2,57957
260007 at	AT1G67870	glycine-rich protein		-2,585389
254716 at	AT4G13560	late embryogenesis abundant domain-containing protein / LEA domain-containing protein		-2,6142042
256255 at	AT3G11280	myb family transcription factor		-2,6151307
258419 at	AT3G16670	expressed protein		-2,664353
248353 at	AT5G52320	cytochrome P450, putative		-2,6912122
267569 at	AT2G30790	photosystem II oxygen-evolving complex 23, putative	OEC23	-2,698875
247077 at	AT5G66420	expressed protein		-2,757152
260112 at	AT1G63310	expressed protein		-2,7583406
251181 at	AT3G62820	invertase/pectin methylesterase inhibitor family protein		-2,7790976
267170 at	AT2G37585	glycosyltransferase family 14 protein / core-2/I-branching enzyme family protein		-2,788725
266460 at	AT2G47930	hydroxyproline-rich glycoprotein family protein		-2,7990606
251360 at	AT3G61210	embryo-abundant protein-related		-2,8648355
262412 at	AT1G34760	14-3-3 protein GF14 omicron (GRF11)	GF14omicron	-2,8910055
266899 at	AT2G34620	mitochondrial transcription termination factor-related / mTERF-related		-2,8940377
266439 s at	AT2G43200	dehydration-responsive family protein		-2,9336007
263174 at	AT1G54040	kelch repeat-containing protein		-2,9744637
250337 at	AT5G11790	Ndr family protein		-3,0156941
257093 at	AT3G20570	plastocyanin-like domain-containing protein		-3,0373013
245743 at	AT1G51080	expressed protein		-3,0563338
252858 at	AT4G39770	trehalose-6-phosphate phosphatase, putative		-3,0832305
250753 at	AT5G05860	UDP-glucuronosyl/UDP-glucosyl transferase family protein		-3,1128771
262700 at	AT1G76020	expressed protein		-3,1220748
257044 at	AT3G19720	dynamain family protein		-3,2271602
249093 at	AT5G43880	expressed protein		-3,2491417
263495 at	AT2G42530	cold-responsive protein / cold-regulated protein (cor15b)	cor15b	-3,2664113
267538 at	AT2G41870	remorin family protein		-3,302061
252863 at	AT4G39800	inositol-3-phosphate synthase isozyme 1 / myo-inositol-1-phosphate synthase 1 / MI-1-P synthase 1 / IPS 1		-3,343508
259962 at	AT1G53690	DNA-directed RNA polymerases I, II, and III 7 kDa subunit, putative		-3,3945053
256461 s at	AT1G36280 /// AT4G18440	adenylosuccinate lyase, putative / adenylosuccinase, putative		-3,4212835
253650 at	AT4G30020	subtilase family protein		-3,4773629
262921 at	AT1G79430	myb family transcription factor-related		-3,5636942
257398 at	AT2G01990	expressed protein		-3,5708144

260745 at	AT1G78370	glutathione S-transferase, putative			-3,6100233
251402 at	AT3G60290	oxidoreductase, 2OG-Fe(II) oxygenase family protein			-3,618224
265828 at	AT2G14520	CBS domain-containing protein			-3,6421518
245088 at	AT2G39850	subtilase family protein			-3,6491795
257650 at	AT3G16800	protein phosphatase 2C, putative / PP2C, putative			-3,7871447
265884 at	AT2G42320	nucleolar protein gar2-related			-3,8955603
254662 at	AT4G18270	glycosyl transferase family 4 protein			-4,0610685
267644 s at	AT2G32870 /// AT2G32880	meprip and TRAF homology domain-containing protein / MATH domain-containing protein			-4,2324915
261309 at	AT1G48600	phosphoethanolamine N-methyltransferase 2, putative (NMT2)	NMT2		-4,296231
247794 at	AT5G58670	phosphoinositide-specific phospholipase C (PLC1)			-4,4009566
253040 at	AT4G37800	xyloglucan:xyloglucosyl transferase, putative / xyloglucan endotransglycosylase, putative / endo-xyloglucan transferase, putative			-4,622757
262232 at	AT1G68600	expressed protein			-4,8016524
261016 at	AT1G26560	glycosyl hydrolase family 1 protein			-4,9005904
250598 at	AT5G07690	myb family transcription factor (MYB29)			-5,5248113
252184 at	AT3G50660	steroid 22-alpha-hydroxylase (CYP90B1) (DWF4)	DWF4		-5,668479
249059 at	AT5G44530	subtilase family protein			-5,7320657
248270 at	AT5G53450	protein kinase family protein			-6,0523086
254371 at	AT4G21760	glycosyl hydrolase family 1 protein			-6,37771
265405 at	AT2G16750	protein kinase family protein			-6,4638696
258719 at	AT3G09540	pectate lyase family protein			-6,5114403
261684 at	AT1G47400	expressed protein			-16,97436
264511 at	AT1G09350	galactinol synthase, putative			-34,790356

Supplemental Table 2: EDS1-dependent genes differentially expressed between *nudt7-1* and *nudt7-1/sid2-1* in group 2

Probe Set ID	AGI	Gene Title	Gene Symbol	Fold change <i>nudt7-1</i> vs <i>nudt7-1/eds1-2</i>	Fold change <i>nudt7-1/sid2-1</i> vs <i>nudt7-1/sid2-1/eds1-2</i>	Fold change <i>nudt7-1/sid2-1</i> vs <i>nudt7-1</i>
256012_at	AT1G19250	flavin-containing monooxygenase family protein / FMO family protein		5.69	76.12	13,667996
248333_at	AT5G52390	photoassimilate-responsive protein, putative		3.64	38.91	10,705441
252309_at	AT3G49340	cysteine proteinase, putative		2.64	26.66	10,415017
266267_at	AT2G29460	glutathione S-transferase, putative		5.91	32.23	5,6796646
260015_at	AT1G67980	caffeoyl-CoA 3-O-methyltransferase, putative		7.01	29.34	5,0240355
252136_at	AT3G50770	calmodulin-related protein, putative		23.27	120.30	4,969678
256877_at	AT3G26470	expressed protein		6.44	31.40	4,9199743
260225_at	AT1G74590	glutathione S-transferase, putative		4.82	19.54	4,3093534
261216_at	AT1G33030	O-methyltransferase family 2 protein		2.79	11.64	4,2873034
261021_at	AT1G26380	FAD-binding domain-containing protein		5.83	20.96	3,6490214
256376 s_at	AT1G66690 /// AT1G66700	S-adenosyl-L-methionine:carboxyl methyltransferase family protein		2.24	6.95	3,3157592
261934_at	AT1G22400	UDP-glucuronosyl/UDP-glucosyl transferase family protein		8.32	18.93	2,9244804
248916_at	AT5G45840	leucine-rich repeat transmembrane protein kinase, putative		2.22	7.14	2,8002245
258277_at	AT3G26830	cytochrome P450 71B15, putative (CYP71B15)		18.25	51.69	2,7619095
259033_at	AT3G09410	pectinacetyltransferase family protein		5.45	12.03	2,7062626
265658_at	AT2G13810	aminotransferase class I and II family protein		7.14	18.08	2,5560515
264400_at	AT1G61800	glucose-6-phosphate/phosphate translocator, putative		6.91	13.83	2,4102075
248321_at	AT5G52740	heavy-metal-associated domain-containing protein		9.93	19.73	2,2125266
254573_at	AT4G19420	pectinacetyltransferase family protein		3.50	5.88	2,1285849
246405_at	AT1G57630	disease resistance protein (TIR class), putative		40.42	80.22	2,0027707
262891_at	AT1G79460	ent-kaurene synthase / ent-kaurene synthetase B (KS) (GA2)	GA2	-2.42	-5.61	-2,1278927
259385_at	AT1G13470	expressed protein		35.95	37.70	-2,161606
254265 s_at	AT4G23140 /// AT4G23160	receptor-like protein kinase 5 (RLK5)		143.10	131.46	-2,723742

Supplemental Table 3a: Expression of transcripts described to be specifically responsive to singlet oxygen (Gadjev et al., 2006) Green: transcript expression follows similar trend as previously described; red: transcript expression is opposite trend as previously described (Gadjev et al., 2006).

Probe Set ID	AGI	Gene Title	Fold change <i>nudt7-1</i> vs <i>nudt7-1/eds1-2</i>	Fold change <i>nudt7-1/sid2-1</i> vs <i>nudt7-1/sid2-1/eds1-2</i>	Fold change <i>nudt7-1/sid2-1</i> vs <i>nudt7-1</i>
Group I genes - EDS1-dependent expressed genes, influenced by elevated SA					
257139_at	AT3G28890	leucine-rich repeat family protein	7.4748297		
267385_at	AT2G44380	DC1 domain-containing protein	6.2432256		
259878_at	AT1G76790	O-methyltransferase family 2 protein	-4.606544		
Group II genes - EDS1-dependent but SA-independent expressed genes					
255941_at	AT1G20350	mitochondrial import inner membrane translocase subunit Tim17, putative	30.06	18.06	
247071_at	AT5G66640	LIM domain-containing protein-related	10.53	7.44	
262703_at	AT1G16510	auxin-responsive family protein	2.00	2.91	
258901_at	AT3G05640	protein phosphatase 2C, putative / PP2C, putative	-3.82	-5.18	
Group III genes - EDS1-dependent expressed genes, influenced by depleted SA					
245885_at	AT5G09440	phosphate-responsive protein, putative		5.0250545	
247429_at	AT5G62620	galactosyltransferase family protein		4.8341956	
250891_at	AT5G04530	beta-ketoacyl-CoA synthase family protein		4.6549635	
248230_at	AT5G53830	VQ motif-containing protein		2.9863322	
253162_at	AT4G35630	phosphoserine aminotransferase, chloroplast (PSAT)		2.6715658	
	AT3G16390 /// AT3G16400 ///				
259381_s_at	AT3G16410	jacalin lectin family protein		2.3304365	
248353_at	AT5G52320	cytochrome P450, putative		-2.6912122	

Supplemental Table 3b: Expression of transcripts described to be specifically responsive to superoxide (Gadjev et al., 2006)

Green: transcript expression follows similar trend as previously described; red: transcript expression is opposite trend as previously described (Gadjev et al., 2006).

Probe Set ID	AGI	Gene Title	Fold change <i>nudt7-1</i> vs <i>nudt7-1/eds1-2</i>	Fold change <i>nudt7-1/sid2-1</i> vs <i>nudt7-1/sid2-1/eds1-2</i>	Fold change <i>nudt7-1/sid2-1</i> vs <i>nudt7-1</i>
Group I genes - EDS1-dependent expressed genes, influenced by elevated SA					
254232_at	AT4G23600	coronatine-responsive tyrosine aminotransferase / tyrosine transaminase	-3.5543914		
246573_at	AT1G31680 /// AT1G31690	copper amine oxidase family protein	-4.4254819		
Group III genes - EDS1-dependent expressed genes, influenced by depleted SA					
263979_at	AT2G42840	protodermal factor 1 (PDF1)		93.09208	
267459_at	AT2G33850	expressed protein		61.612915	
258675_at	AT3G08770	lipid transfer protein 6 (LTP6)		52.615093	
259009_at	AT3G09260	glycosyl hydrolase family 1 protein		50.05208	
253753_at	AT4G29030	glycine-rich protein		47.666348	
261459_at	AT1G21100	O-methyltransferase, putative		23.763609	
254327_at	AT4G22490	protease inhibitor/seed storage/lipid transfer protein (LTP) family protein		22.966476	
245688_at	AT1G28290	pollen Ole e 1 allergen and extensin family protein		20.462524	
246687_at	AT5G33370	GDSL-motif lipase/hydrolase family protein		14.591388	
266223_at	AT2G28790	osmotin-like protein, putative		13.629877	
259382_s_at	AT3G16420 /// AT3G16430	jacalin lectin family protein		11.650177	
266415_at	AT2G38530	nonspecific lipid transfer protein 2 (LTP2)		10.096741	
258376_at	AT3G17680	expressed protein		9.768558	
256125_at	AT1G18250	thaumatin, putative		8.741172	
260948_at	AT1G06100	fatty acid desaturase family protein		8.687121	
258480_at	AT3G02640	expressed protein		8.537933	
258895_at	AT3G05600	epoxide hydrolase, putative		6.5499644	
259327_at	AT3G16460	jacalin lectin family protein		6.0272646	
247882_at	AT5G57785	expressed protein		5.8200994	
255460_at	AT4G02800	expressed protein		5.5989056	
262840_at	AT1G14900	high-mobility-group protein / HMG-I/Y protein		5.510773	
266988_at	AT2G39310	jacalin lectin family protein		4.4917445	
245523_at	AT4G15910	drought-responsive protein / drought-induced protein (Di21)		4.0974784	
264007_at	AT2G21140	hydroxyproline-rich glycoprotein family protein		3.8951776	
265117_at	AT1G62500	protease inhibitor/seed storage/lipid transfer protein (LTP) family protein		3.6592908	
250661_at	AT5G07030	aspartyl protease family protein		3.0114396	
257193_at	AT3G13160	pentatricopeptide (PPR) repeat-containing protein		2.5180027	
264960_at	AT1G76930	proline-rich extensin-like family protein		2.406742	
254233_at	AT4G23800	high mobility group (HMG1/2) family protein		2.0337257	
253073_at	AT4G37410	cytochrome P450, putative		2.0021665	

Supplemental Table 3c: Expression of transcripts described to be specifically responsive to hydrogen peroxide (Gadjev et al., 2006)

Green: transcript expression follows similar trend as previously described; red: transcript expression is opposite trend as previously described (Gadjev et al., 2006).

Probe Set ID	AGI	Gene Title	Fold change <i>nudt7-1</i> vs <i>nudt7-1/eds1-2</i>	Fold change <i>nudt7-1/sid2-1</i> vs <i>nudt7-1/sid2-1/eds1-2</i>	Fold change <i>nudt7-1/sid2-1</i> vs <i>nudt7-1</i>
Group I genes - EDS1-dependent expressed genes, influenced by elevated SA					
254975_at	AT4G10500	oxidoreductase, 2OG-Fe(II) oxygenase family protein	155,59166		
248970_at	AT5G45380	sodium:solute symporter family protein	11,899199		
266782_at	AT2G29120	glutamate receptor family protein (GLR2.7)	9,826454		
257763_s_at	AT3G23110 /// AT3G23120	disease resistance family protein	8,013622		
265993_at	AT2G24160	pseudogene, leucine rich repeat protein family	5,019295		
265132_at	AT1G23830	expressed protein	3,372987		
Group II genes - EDS1-dependent but SA-independent expressed genes					
267546_at	AT2G32680	disease resistance family protein	76,45	80,02	
248333_at	AT5G52390	photoassimilate-responsive protein, putative	3,64	38,91	10,705441
259385_at	AT1G13470	expressed protein	35,95	37,70	
254271_at	AT4G23150	protein kinase family protein	54,04	25,81	
248083_at	AT5G55420	Protease inhibitor/seed storage/LTP family protein [pseudogene]	6,24	11,86	
264590_at	AT2G17710	expressed protein	7,07	10,99	
256940_at	AT3G30720	expressed protein	6,74	7,75	
256969_at	AT3G21080	ABC transporter-related	3,74	6,07	
256883_at	AT3G26440	expressed protein	3,67	5,11	
260581_at	AT2G47190	myb family transcription factor (MYB2)	2,16	2,48	
263574_at	AT2G16990	expressed protein	-4,19	-6,76	
Group III genes - EDS1-dependent expressed genes, influenced by depleted SA					
257950_at	AT3G21780	UDP-glucuronosyl/UDP-glucosyl transferase family protein		4,5489597	
258803_at	AT3G04670	WRKY family transcription factor		2,5639384	
258707_at	AT3G09480	histone H2B, putative		2,3990126	
250433_at	AT5G10400	histone H3		2,177905	
253073_at	AT4G37410	cytochrome P450, putative		2,0021665	
254250_at	AT4G23290	protein kinase family protein		-2,43337	
254716_at	AT4G13560	late embryogenesis abundant domain-containing protein / LEA domain-containing protein		-2,6142042	
254371_at	AT4G21760	glycosyl hydrolase family 1 protein		-6,37771	

Danksagung

Ich möchte mich herzlich bei Dr. Jane Parker für ihre Unterstützung bei der Durchführung dieser Arbeit in ihrer Gruppe am MPIZ bedanken. Vielen Dank für die herzliche Betreuung und die vielen wertvollen Ratschläge.

Ebenso möchte ich meinem Doktorvater Herrn Prof. Dr. Paul Schulze-Lefert für die Möglichkeit zur Promotion am MPIZ danken.

Herrn Prof. Dr. Ulf Ingo Flügge und Herrn Prof. Dr. Martin Hülskamp danke ich für die freundliche Übernahme des Korreferates dieser Arbeit bzw. für die Übernahme des Prüfungsvorsitzes.

Ein Dankeschön geht Dr. Michael Bartsch, der mir sehr geholfen hat mich hier am MPIZ zu „akklimatisieren“ und dessen konstruktive Anregungen bei der Durchführung dieses Projektes sehr geholfen haben.

Ein großes Dankeschön geht an Dr. Corina Vlot, Dr. Sandra Noir und Dr. Johannes Stuttmann für das Korrekturlesen dieser Arbeit und die mentale Unterstützung.

Vielen Dank an alle ehemaligen und aktuellen JP-goup Mietglieder für die wundervolle Atmosphäre und ständige Hilfsbereitschaft. Vielen Dank Johannes, Jagreet, Corina, Koh, Katharina, Michael, Shige, Marcel, Servane, Shinpei, Guangjong, Jaqueline, Enrico, Steffen, Lennart, Ana, Robin, Dieter und Doris.

Am allermeisten möchte ich meiner Familie danken, die mich immer bei allem unterstützt hat und ohne die ich nicht da wäre wo ich bin. Vielen Dank für Alles!

Erklärung

Ich versichere, dass ich die von mir vorgelegte Dissertation selbständig angefertigt, die benutzten Quellen und Hilfsmittel vollständig angegeben und die Stellen der Arbeit - einschließlich Tabellen, Karten und Abbildungen -, die anderen Werken im Wortlaut oder dem Sinn nach entnommen sind, in jedem Einzelfall als Entlehnung kenntlich gemacht habe; dass diese Dissertation noch keiner anderen Fakultät oder Universität zur Prüfung vorgelegen hat; dass sie noch nicht veröffentlicht worden ist sowie, dass ich eine solche Veröffentlichung vor Abschluss des Promotionsverfahrens nicht vornehmen werde. Die Bestimmungen dieser Promotionsordnung sind mir bekannt. Die von mir vorgelegte Dissertation ist von Prof. Dr. Paul Schulze-Lefert betreut worden.

Köln, 09. März 2009

(Marco Straus)

